GEOCHEMICAL ASSESSMENT OF AN OLD UCHI TAILING DUMP IN KITWE, ZAMBIA

By

Stephen Muma

A Thesis submitted to the University of Zambia, School of Mines, in Fulfilment of the requirement for the Master of Science Degree in Integrated Water Resources Management

SCHOOL OF MINES, DEPARTMENT OF GEOLOGY,

INTEGRATED WATER RESOURCES MANAGEMENT CENTRE,

LUSAKA

2024.

COPYRIGHT

DECLARATION

This thesis has been written and submitted in accordance with the rules and regulations governing the award of the Master's degree programme in integrated water resource management at the University of Zambia. I further declare that the work submitted in this thesis is my original work and has not been presented for the award of any degree to any other university. Where other people’s work has been drawn upon, acknowledgement has been made.

Signature of author……………………………………………………………………..

Date……………………………………………………………………………………….

APPROVAL

This thesis of Stephen Muma has been approved as fulfilling the requirement for the award of the degree of Master of Science in Integrated Water Resource Management by the University of Zambia.

Internal Examiner 1

Name:

Signature ……………………… Date:………………………..

Internal Examiner 2

Name:

Signature ……………………… Date:………………………..

External Examiner

Name:

Signature ……………………… Date:………………………..

Chairperson-Board of Examiners

Name:

Signature ……………………… Date:………………………..

Supervisor

Name: Dr. Kawawa Banda

Signature ……………………… Date:………………………

ABSTRACT

This study investigates the characteristics of soil from an old Uchi Tailing Dump in Kitwe, Zambia, through field sampling and analysis. Soil samples were systematically collected using a grid sampling techniques to inform future environmentally responsible restoration strategies. Particle size distribution was assessed through sieve analysis while X-ray diffraction (XRD) provided insights into the soil's crystalline structure. Results from these techniques, along with elemental quantification using flame atomic absorption spectrometry, revealed a hierarchy of element concentrations in the Uchi Tailing Dump samples: Fe>Cu>Ca>Mn>Co>Zn, with pH ranging from 5.5 to 7.5. Notably, copper (0.56%) and cobalt (0.15%) levels were particularly high. Cuprite was identified as a significant source of copper while iron oxide contributed to elevated iron levels. XRD analysis highlighted quartz, kaolinite and dolomite as the predominant phases, with montmorillonite aiding in pH stability. The study also attributed high calcium content to calcite. Spatial distribution analysis revealed distinct patterns, with elevated copper in the northwest and increased cobalt in the northeast. Both topsoil and subsurface samples exhibited contamination, likely due to anthropogenic influences. The soil was predominantly fine sand (86% sand, 13% clay and 1.4% silt) with a gap-graded particle size distribution. The simulation results from PHREEQC revealed distinct saturation levels for various mineral phases within the tailings, with cupric ferrite ($CuFe_2O_4$) at 10.72, cuprite (Cu_2O) at 3.08, zincate ($ZnSO_4$: H_2O) at -9.54, gypsum ($CaSO_4$: $2H_2O$) at -4.85 and hematite (Fe_2O_3) at 13.10. The Geo-Accumulation Index (Igeo) confirmed contamination, particularly in copper (Igeo=5), cobalt (Igeo=2.5), iron (Igeo=0.5) and zinc (Igeo<0). Dust emissions, acid mine drainage, soil degradation and a reduction in biodiversity in the Uchi Stream are significant hazards associated with the Uchi Tailing Dump. In summary, the study underscores the significant pollution and environmental risks associated with the Uchi Tailing Dump, emphasizing the need for ongoing monitoring and remediation efforts to protect the ecosystem and community health in the area. In conclusion, this study highlights significant pollution and environmental risks at the Uchi Tailing Dump, emphasizing the necessity for continued monitoring and remediation efforts to safeguard the ecosystem and community health in the area.

DEDICATION

This Master Degree Programme is fondly dedicated to my Father Mr. Stephen Muma Senior, my dear Mother Charity Musonda Muma, my lovely wife Ruth Phiri Muma and my dearest daughter Michelle Tasheni Muma.

ACKNOWLEDGEMENTS

This Master's degree programme was conducted under the O.R. Tambo Africa Research Chairs Initiative (ORTARCHI) in Water Conservation: Enhancing catchment protection that facilitates water resources conservation through two thematic areas: multidisciplinary in nature and adopted through a holistic approach divided into two research areas: water quantity (including inter-basin transfers) and quality; and site-specific remediation technologies and land use change. I am immeasurably grateful to the O.R. Tambo (ORTARCHI) Research Chair Holder, Professor Imasiku A. Nyambe, who is also Coordinator, IWRM Centre, UNZA. I am also thankful to long-term successor O.R. Tambo (ORTARCHI) Dr. Kawawa Banda for career and professional guidance during my research at UNZA. I also wish to acknowledge and give thanks to Mrs. Ingrid M. Mukosa, Project Administrator O.R. Tambo (ORTARCHI) and the IWRM Centre at UNZA for helping with all administrative works and ensuring progress in my studies.

The generosity of the National Science and Technology Council (NSTC), Ministry of Water Development and Sanitation (MWDS) and Ministry of Mines in collaboration with UNZA's IWRM Centre cannot be overemphasized, for without them, I might not have had the opportunity to pursue this programme. A special thanks also goes to my supervisor, the Provincial Water Development Officer (PWDO) for Copperbelt, Mrs. Beatrice Kalonge Muyunda, for being extremely helpful.

I would like to extend special gratitude to my lovely wife, Ruth Phiri Muma, for her understanding and patience during the period of my study. I also wish to thank my dearest daughter, Michelle Tasheni Muma, for her loving support and endurance during the period of the study. Lastly, many more thanks go to my fellow IWRM student, Mrs. Justina Asa Kasabila, for guidance during research at UNZA. More thanks to all OR Tambo and UNZA students who helped me with my studies.

TABLE OF CONTENTS

LIST OF FIGURES

LIST OF TABLES

LIST OF APPENDICES

LIST OF EQUATIONS

LIST OF ACRONYMS AND ABBREVIATIONS

AAS	Atomic Absorption Spectroscopy
AMD	Acid Mine Drainage
ArcGIS	Software for Spatial Data Analysis
ARD	Acid Rock Drainage
BSAC	British South Africa Company
Covid-19	Coronavirus Disease of 2019
CSO	Central Statistical Office
GIS	Geographic Information System
GPS	Global Positioning System
GRZ	Government Republic of Zambia
IMF	International Monetary Fund
IWRM	Integrated Water Resources Management
KCM	Konkola Copper Mine
MCM	Mopani Copper Mine
MICP	Microbial Induced Calcite Precipitation
MWDS	Ministry of Water Development and Sanitation
NCCM	Nchanga Consolidated Copper Mines Limited
NFC	Non-ferrous Metals Mining of China
NGOs	Non-Governmental Organizations
NWASCO	National Water Supply and Sanitation Council

pH	Potential hydrogen
PHREEQC	PH REdox Equilibrium
PPM	Parts Per Million
RCML	Roan Copper Mines Limited
RST	Roan Selection Trust
TD26	Old Uchi Tailing Dump 26
TD27	New Uchi Tailing Dump 27
US EPA	United States Environmental Protection Agency
UNZA	University of Zambia
USD	United States dollar
USGS	United States Geological Survey
WARMA	Water Resources Management Authority
WHO	World Health Organization
XRD	X-ray Diffraction Analysis
ZAMREP	Zambia Mining and Environmental Remediation and Improvement Project.
ZCCM	Zambia Consolidated Copper Mines Limited
ZEMA	Zambia Environmental Management Agency
ZMD	Zambia Meteorological Department

CHAPTER ONE: INTRODUCTION

1.1 Background

Zambia has a rich history of mining, predominantly centred in the Copperbelt and North-Western provinces, known for their substantial copper and cobalt deposits (Kosgei & Mukuwa, 2020). The mining industry, a key economic driver for the country, has experienced significant growth over the decades. However, this growth has led to the generation of hazardous wastes, including tailings and overburden materials, which pose severe environmental and health risks (Sandell, 2020).

The pursuit of mineral resources due to rapid urbanisation and industrialisation, has resulted in elevated concentrations of heavy metals such as chromium (Cr), cadmium (Cd), mercury (Hg), lead (Pb), nickel (Ni), arsenic (As), zinc (Zn) and copper (Cu) in various environmental receptors, including water, air, soil and human populations. These metals present significant public health and environmental risks (Kribek et al., 2010). For instance, tailings can contaminate water bodies through leaching, adversely affecting aquatic ecosystems and making water unsafe for human consumption. Soil contamination can reduce agricultural productivity and cause the accumulation of metals in crops, posing risks to food safety. Airborne dust from tailings can lead to respiratory problems in humans and animals. Chronic exposure to heavy metals is associated with numerous health issues, including hypophosphatemia, heart disease, liver damage, various cancers, neurological disorders and central nervous system damage (Rahman, 2016). The bioaccumulation of these metals in the food chain further exacerbates their impact, leading to widespread ecological and health repercussions.

A significant challenge for the mining industry is the safe disposal of ore processing wastes or tailings. Tailings and waste rocks are the two most common mining wastes (Triantafyllidis et al., 2016). Tailings are the waste products from a mill, washery, or concentrator where the economically valuable metals or minerals have been extracted from the mined ore (Triantafyllidis et al., 2016). In contrast, waste rocks are generated during the excavation and mining of the ores (Nyambe & Kawamya, 2005). Historically, processing wastes were often dumped in nearby streams or creeks without consideration of their environmental impact (Kribek et al., 2010). In recent years, tailings are typically disposed of as slurry or paste in designated facilities, presenting unique environmental and physical challenges.

Mill tailings originating from sulphide ores are particularly problematic due to their high oxidation potential, which can lead to acid rock drainage (ARD) (Baieta et al, 2021). The flow of acidic water over sulphuric tailings increases the potential for metal leaching due to the fine-grained nature of the tailings material and the dissolution of heavy metal-bearing secondary phases at or near the surface (Vítková et al., 2010). Consequently, abandoned mine waste disposal sites containing sulphide minerals pose significant environmental threats, potentially contaminating surface and groundwater, soils and ecosystems (Sracek et al., 2012). Waste rock piles and mill tailings from mining activities, especially those containing sulphide minerals, are significant sources of acid mine drainage (AMD). The mining of minerals such as gold, copper, zinc and nickel is commonly associated with AMD problems, which can have severe health and ecological consequences (Vítková et al., 2011). AMD is formed when sulphide-bearing ores are exposed to oxygen and water, resulting in low-pH drainage water with high concentrations of sulphate, aluminium, iron and other toxic elements. This acidic water, characterised by high trace element concentrations, is detrimental to aquatic life (Sracek et al., 2012).

Geochemical models and simulations can be applied to understand the fate of pollutants in tailings, providing a valuable tool for reliable rehabilitation measures (Gelena, 2018). Advanced geotechnical remediation techniques can evaluate and exploit geochemical data to offer holistic solutions for environmental protection. Due to increased industrial, traffic and agricultural inputs, soil heavy metal concentrations in some industrialised areas have risen significantly, especially near mining and metallurgical industries. Total soil heavy metal concentration alone is not a reliable measure of bioavailability or potential environmental and health risks from soil contamination. Therefore, assessing the mobile and bioavailable forms of metals is vital. The partitioning of metals between the fractions bound to soil solids and the dissolved portion in soil solution reflects the metals' mobility and potential uptake by plants or soil biota, as well as their potential to leach into groundwater or surface water (Luo et al., 2006; Sillitoe et al., 2015).

Tailing dumps are embankments constructed from waste rocks to contain the tailings generated in a mine processing plant (Wallingford, 2019). These tailings often contain hazardous substances that can contaminate food chains, drinking water and the environment. The failure of tailing dumps can cause fatalities, irreversible ecological damage and significant economic losses. Soil characterisation is the first step toward risk assessment of these tailings, aiming for sustainable environmental protection. Accurate and comprehensive data collection during soil characterisation helps identify potential risks emanating from tailing dumps. Remediation of both water and soil resources is necessary to restore contaminated sites (Sracek et al., 2012). Thus, restoring mine wastelands is crucial to prevent further and future damages (Sracek et al., 2012).

Kitwe, a region characterised by intensive copper and cobalt mining activities spanning approximately three decades from 1930 to 1968, has experienced considerable economic growth due to its mining industry. However, alongside this economic prosperity, the mining activities have led to various environmental challenges, notably the accumulation of elevated concentrations of copper and cobalt in the tailings. These tailings, waste materials resulting from mining and processing activities, were typically deposited in the Uchi area.

Over time, the Uchi Tailing Dump has undergone oxidation due to prolonged exposure to air and water. Consequently, there is strong suspicion that local river and pore water have become contaminated by Acid Mine Drainage (AMD). This suspicion is supported by observable impacts on the local stream, known as Uchi Stream, where the number of aqueous species has significantly decreased, indicating potential contamination from the tailings (Dusengemungu et al., 2022).

Despite previous research efforts, gaps in understanding persist regarding the physicochemical properties of the Uchi Tailing Dump, particularly concerning specific locations within the dump, such as TD26 (old Uchi Tailing Dump) and TD27 (new Uchi Tailing Dump). Not only that, Uchi Tailing Dump was selected because it was historically used as a dumping site and due to rumours of its impact on the aquatic ecosystem, including a decline in fish populations in nearby water bodies. Additionally, the site was chosen to assess the efficiency of old mining methods by determining the percentage of materials they were able to extract. This study aimed to address these gaps by conducting a comprehensive investigation into the soil's physicochemical properties within the Uchi Tailing Dump. Through this investigation, the study seeks to provide meaningful insights into the environmental impacts and challenges posed by these tailings.

1.2 The Problem Statement

The mining industry stands as a cornerstone of Zambia's economy, having witnessed significant growth over several decades. With a mining legacy spanning over 90 years, mineral resources like copper (Cu) and cobalt (Co) have been intensively mined and smelted in the country (Sikamo et al., 2016). However, as the demand for metals, particularly copper, shows no signs of diminishing, there arises a critical need for the restoration of mine wastelands to mitigate environmental impacts and prevent potential threats to human health (Lindahl, 2014).

This study aims to address existing knowledge gaps concerning tailing dumps materials and the presence of heavy metals. Copper and cobalt, in particular, have been implicated in the pollution of water resources, agricultural plants and overall ecosystem health, including human well-being. Motivated by these concerns, the study focused on examining the tailings, which are mining wastes known to contain significant concentrations of such metals. To pave the way for future restoration efforts of tailing dumps, it is imperative to conduct a thorough assessment of their physical and chemical properties. Therefore, the initial step towards achieving this objective is to gain a comprehensive understanding of the contents of the tailing dumps in question.

Given that mining activities persist and their impacts are anticipated to endure, if not increase, it becomes crucial to investigate tailings characteristics for future restoration endeavours of the tailing dumps in Kitwe, Zambia. The overarching goal of this project is to address the issue of water stress in the Kafue River, which serves as a vital resource for various activities including hydroelectric power generation and agriculture. As part of this thematic area, ensuring the cleanliness of the areas affected by mining activities is paramount, particularly if inter-basin transfer initiatives are to be considered.

1.3 Research Objective

The overall objective of this study was to determine the geochemical characteristics of an old Uchi Tailing Dump, Kitwe, Zambia, with the following specific objectives:

(i) To assess the physical and chemical characteristics of the tailings within the tailing dump. This includes analysing parameters such as concentrations of various elements, mineralogy, particle size distribution, texture and pH;

(ii) To evaluate the mineral phases at the tailings using a modelling approach (PHREEQC). This helps to understand the speciation and distribution of species within the tailings; and

(iii) To evaluate the potential environmental risks and hazards associated with the Uchi Tailing Dump.

1.4 Research Questions

The study answers the following research questions:

(i) What are the physical and chemical characteristics of the tailings within and around the Uchi Tailing Dump in Kitwe, Zambia?

(ii) How do the computed saturation indices using geochemical modelling in PHREEQC help in understanding the speciation and distribution of aqueous species within the Uchi Tailing Dump and what implications do these indices have for potential mineral dissolution or precipitation and the release of contaminants into the surrounding environment? and

(iii) What are the levels of heavy metal concentrations and other toxic elements in the Uchi Tailing Dump and how do they pose potential environmental risks and hazards to the local ecosystem and human health? What are the specific contaminants of concern and what are their sources and pathways of dispersion?

1.5 Significance of the Study

This study addresses a knowledge gap pertaining to the physicochemical properties of soils within the Uchi Tailing Dump, located in Kitwe, Copperbelt Province, Zambia. As the first intensive research focusing on soil characteristics within the Uchi Tailing Dump globally, it illuminates previously unexplored aspects of this dump site. The Uchi Tailing Dump is a tailing dump of copper and cobalt wastes, yet there are no detailed geochemical and physicochemical analyses of its tailings. Consequently, this research not only enriches the evolving understanding of mining-polluted sites within the Copperbelt Province but also lays a foundational framework for future investigations, particularly regarding remediation strategies for tailing dumps across Zambia.

The findings of this study hold considerable significance, not only for academic pursuits but also for practical applications. They directly contribute to the doctoral thesis of the researcher, especially in the implementation of bioremediation techniques for the restoration of tailing dumps. Furthermore, the implications of this research extend beyond academia to various stakeholders, including mine companies and key players within the water sector such as the National Water Supply and Sanitation (NWASCO), Water Resources Management Authority (WARMA) and the Ministry of Water Development & Sanitation (MWDS). Regulatory bodies such as the Zambezi River Authority (ZRA) and Zambia Environmental Management Agency (ZEMA) also stand to benefit from enhanced insights into soil characteristics, as this knowledge informs effective water management strategies for both surface and groundwater resources. Ultimately, by contributing to the restoration of contaminated sites, this research endeavours to positively impact the well-being of the local community and safeguard environmental integrity.

CHAPTER TWO: LITERATURE REVIEW

2.0 General Remarks

This chapter offers an overview of Zambia's mining history and a review of earlier research on the effects of mining and mineral processing on soil, water and air at Uchi Tailing Dump in Kitwe, Copperbelt Province, Zambia. This chapter provides a summary of the geochemical characterisation of tailing dumps in Zambia, along with a review of previous studies conducted globally, in Zambia and specifically in the study area. The review highlights existing research on the characterisation and remediation of tailing dumps, emphasising gaps in knowledge that prompted the formulation and execution of this thesis. The contribution of the study to the body of knowledge is elaborated upon, emphasising its novel insights and advancements in understanding the physicochemical properties of tailing dumps, particularly in the study area of interest. Furthermore, the chapter discusses the lessons learned throughout the research process.

2.1 Mining in Zambia

Copper mining in Zambia dates back as far as early 1920s, when several mines were developed on the Copperbelt Province under the ownership of Anglo-American Corporation (ACC) and the Roan Selection Trust (RST mining group of companies) (Nyambe & Kawamya, 2005). The mines were later nationalised into two conglomerates, namely Nchanga Consolidated Copper Mines (NCCM) and Roan Copper Mines Limited (RCML) in 1969, with the government of the Republic of Zambia holding 51 percent of the shares (Lweya et al., 2015). Production peaked at 755,000 metric tonnes in 1970, making Zambia the world's eighth-largest copper producer (Nyambe & Kawamya, 2005). However, after the 1975s, global Cu prices and productivity began to fall, resulting in the 1982 merger of the two companies into a 100 percent nationalised Zambia consolidated copper mines (ZCCM). Thereafter, following the economic liberalisation policies introduced by the Republic of Zambia under the multiparty governance system in the 1990s, ZCCM was once again privatized, with about 75 percent of the shareholding held by large international multilateral mining companies and about 25 percent held by the government in 2000 (Elaw, 2010). At the time of privatisation, production capacity was at 250,000 metric tonnes and copper prices on the world stock market had declined to slightly below 1,800 USD per metric tonne as a result of increased global demand from emerging economies such as China and India.

This led to renewed investment in the mining sector and the development of new mines, particularly in the North-Western Province of Zambia. By 2010, the annual production stood at approximately 820,000 metric tonnes, contributing 5.2 percent of the global Cu production (USGS, 2015). An estimated total of over 30 million tonnes of Cu has been produced in Zambia ever since (Ettler et al., 2011). In the beginning of 2016, there was a reported drop in copper prices (IMF, 2019). This drop was from about 8,823 USD per metric tonne in 2011 to around 4,867 USD per metric tonne, marking one of the worst declines in the last five years. Despite this, again due to the impact of COVID-19 and climate change, copper production fell by 9% in 2021 (Africa Report, 2022). In 2020, Zambia experienced a remarkable 10.8% increase in copper production, reaching 882,061 metric tonnes, up from 796,430 metric tonnes the previous year. This achievement marked a significant milestone for Zambia, positioning it as Africa's second-largest copper producer. Looking forward, Zambia has set ambitious targets, aiming to surpass 900,000 metric tonnes of copper production in 2021 and ultimately exceed 1 million metric tonnes annually (USGS, 2015). This strategic vision underscores Zambia's commitment to expanding its copper industry and fostering economic growth. Moreover, with the global shift towards electric vehicles, which heavily rely on copper, the demand for the metal is expected to rise further, promising positive prospects for the mining sector. Despite the challenges posed by the COVID-19 pandemic in 2019, the outlook for Zambia's mining industry remains promising, driven by its resilient efforts and strategic initiatives (USGS, 2015).

2.1.1 Impacts of Mining

The mining industry, driven by rapid urbanisation and industrialisation, exerts significant impacts on environmental receptors such as people, water, air and soil (Mwandira, 2015). In Zambia, where mining serves as a key economic driver, particularly in regions abundant in copper deposits like the Copperbelt and North-Western Provinces, the expansion of mining activities has been notable (Sikamo et al., 2016). However, the extraction process generates substantial environmental challenges, notably through the production of mine tailings, which comprise fine-grained rock residues and process water containing dissolved metals and reagents (Kosgei & Mukuwa, 2020). These tailings, often stored on the surface or in underground voids, can cover vast areas and contain heavy metals like copper, iron, manganese, cobalt and zinc, posing significant environmental risks (Ngulube, 2016). Their disposal, typically done with minimal regard for environmental impact due to their lack of immediate financial value, underscores the urgency for enhanced regulation and sustainable management practices (Baghdasaryan, 2016). Consequently, the environmental effects of mining, including air and water pollution, soil degradation and health risks to nearby communities. Soil degradation occurs due to land disruption and contamination with heavy metals and chemicals, hampering agricultural productivity and biodiversity (Lindahl, 2014). Water pollution arises from runoff carrying toxins and sediments, contaminating water bodies and endangering aquatic ecosystems and human access to clean water sources (Sikamo et al., 2016). Air pollution results from dust and emissions generated during mining operations, leading to respiratory issues and environmental deterioration (Kosgei & Mukuwa, 2020). Moreover, nearby communities face health risks from exposure to pollutants, contributing to illnesses and long-term health complications.

2.1.2 Mine Tailings

Mine tailings, a by-product of mineral extraction and processing, consist of crushed rock and processing fluids from mills and washeries (Kossoff et al., 2014). During ore extraction, waste rock containing sulphides like pyrite and pyrrhotite is generated, which can lead to acid mine drainage upon weathering. The ratio of tailings to ore concentrate is often high, typically around 200:1 (Kossoff et al., 2014). In the context of Zambia, a key player in the global copper and cobalt market, the historical production of over a billion metric tonnes of ore underscores the magnitude of the mining industry's impact on the environment. Copper and cobalt, vital components of Zambia's mineral wealth, have driven extensive mining activities, particularly in regions like the Copperbelt (USGS, 2015). However, the closure of mines in 2009 has left behind significant environmental legacies, including the disposal of waste products such as tailings and refuse rocks.

Waste disposal practices, such as dumping tailings and refuse rocks, have raised environmental concerns, particularly in areas like the Uchi Tailing Dump in Zambia's Copperbelt region. Research conducted on TD26 at the Uchi Tailing Dump revealed high soil pollution, with a pollution load indicator of 0.329 (Dusengemungu et al., 2022). This indicates significant environmental degradation due to mining activities.

2.1.3 Copper and Cobalt

Copper mineralisation was first discovered at the turn of the century, but large-scale production only commenced in the 1930's with the start-up of Roan Antelope (Luanshya, 1931), followed rapidly by Nkana (1932), Mufulira (1933) and then Nchanga in 1939. Copper production exceeded 400, 000 tonnes per annum in the late 1950s and passed the 600, 000 tonnes per annum mark in the mid-1960s before beginning a progressive decline in 1976–77 and sinking to a 1996–97 low of 350, 000 tonnes per annum (Sikamo et al., 2016). The balance of mining-sector earnings came from sales of gold, silver and selenium, mostly as by-products of copper mining and from emerald sales.

At present, the sector contributes more than 70% of total export value, 10% of gross domestic product (GDP) and 28% of national revenue (Ribes, 2022). Significant mineral exploration started in the Zambian Copperbelt during the 1920s, when the British South African Company (BSAC) offered prospecting rights to large multinational companies. In 1957, Konkola Mine and Nchanga were brought into production as demand for metals rose in the post-World War II era. In 1969, the Zambian government nationalised the industry by acquiring a 51 percent stake in all mining utilities and reorganising them into Nchanga Consolidated Copper Mines Limited (NCCM) and Roan Copper Mines Limited (RCM). In 1979, this stake was further increased to 60.3 percent. In 1982, in an attempt to redress falling production trends, NCCM and RCM were merged into the Zambia Consolidated Copper Mines Limited (ZCCM), but this did not restore production in the sector. In 1995, a process for the purchase of mining and ore processing facilities was initiated (Lungu, 2008). At present, the two biggest copper mining companies in the Copperbelt are Mopani Copper Mines (MCM), with First Quantum and Glencore providing the major investment and Konkola Copper Mines (KCM). The KCM was purchased by Vedanta Resources (India) in 2006 (Ribes, 2022). Smaller companies operating in the surveyed part of the Copperbelt include Lubambe Copper Mine, Chibuluma Mines, Nonferrous Metal Mining of China (NFC) in Luanshya, Chambishi Copper Smelting Company, Sinohydro-Metal and Chambishi Metals. Ores are processed by flotation at Kitwe (the Nkana ore treatment plant), Chingola, Chililabombwe, Chambishi, Chibuluma and Mufulira ore treatment plants and for a long time, they were smelted and refined at the Mufulira, Kitwe, Chingola and Luanshya smelters (Lungu, 2008).

2.2 Geochemical Characterisation

The study of the chemistry of the Earth and the solar system's solid bodies, including the distribution, circulation and abundance of elements (and their ions and isotopes), molecules, minerals, rocks and fluids, is known as geochemistry (Rs & Limited, 2012). The objective of this section is to provide an overview of geochemistry, including its scope, significance and historical development. It highlights the interdisciplinary nature of geochemistry, which integrates chemistry and geology to study the distribution, circulation and abundance of elements, molecules, minerals, rocks and fluids within the Earth and the Solar System. Additionally, it aims to illustrate how geochemistry has contributed to our understanding of various processes, such as mantle convection, planetary formation and the origins of specific rock types like granite and basalt. The section also emphasizes key milestones in the establishment of geochemistry as a distinct scientific discipline, notably the pioneering work of Frank Wigglesworth Clarke and the establishment of major laboratories like the United States Geological Survey (USGS) in 1884. In the early 20th century, Max von Laue and William L. Bragg showed that X-ray scattering could be used to determine the structures of crystals. In the 1920s and 1930s, Victor Goldschmidt and associates at the University of Oslo applied these methods to many common minerals and formulated a set of rules for how elements are grouped. Geochemical characterisation is a fundamental and versatile tool that holds significant importance across numerous scientific and industrial domains (Gelena, 2018). Through this analytical approach, there is gain of important insight into minerals and soils, which aids in deciphering geological events and the history of specific regions. In mineral exploration and mining, geochemical techniques are indispensable, enabling geologists to identify anomalies in mineral concentrations that may indicate the presence of valuable ore deposits (Pettersson, 2002). This knowledge is important for making informed decisions about the viability of mining projects. Moreover, geochemical characterisation plays a vital role in environmental studies by assessing the impact of human activities on the environment, monitoring the presence and movement of pollutants and toxic elements and safeguarding water resources for human consumption and agricultural use.

Geochemical characterisation also plays a critical role in assessing health risks associated with exposure to certain elements and compounds, especially in areas with naturally elevated levels of toxic substances. Overall, this analytical approach provides indispensable data and knowledge that supports decision-making processes in scientific research, resource management, environmental protection and the preservation of human health and welfare.

2.3 Particle Size Distribution (PSD)

The analysis of particle-size distribution using the Unified Soil Classification System (USCS) (ASTM D 2487) is a common practice in geotechnical engineering (Astm D6913-04R2009, 2004). This involves determining particle-size diameters such as d10, d30, d50 and d60, corresponding to specific percentages (10%, 30%, 50% and 60%) of particles passing the cumulative particle-size distribution curve. These parameters are then used to calculate the coefficient of uniformity (CU) and coefficient of curvature (CC). The process begins by understanding the definitions of these particle sizes i.e. D10, D30 and D60. D10 represents the particle diameter where 10% of the soil is finer, D30 is where 30% is finer and D60 is where 60% is finer (Feng, 2008). A steeper slope on the left side of the curve indicates a higher proportion of finer particles like silt and clay while a gentler slope on the right side suggests a greater presence of coarser particles such as sand and gravel.

For performance testing, a simple equation is used:

Performance Test = [(Initial weight - Sum of Soil) / (Initial Weight)] * 100…………. Equation 2.

Equation 1: Performance Test equation for Particle Size Distribution Curve (Lemos et al., 2021)

If the result is less than 1%, the test is repeated. Percentage finer is calculated as 100 minus the cumulative percentage passing (Aluvihara and Kalpage, 2020). Sieve analysis, commonly employed for particle sizes larger than 0.075 mm, involves using a series of sieves with different mesh sizes to separate particles based on size. This method helps determine the fineness modulus, effective size and homogeneity coefficient of the soil sample (Required and Karakurt, 2021). The fineness modulus classifies the soil type while the effective size represents the sieve size through which 10% of the soil mass passes and the homogeneity coefficient describes the uniformity of particle sizes. The data from these analyses are used to construct a grain size distribution curve.

The coefficient of uniformity (CU) and coefficient of curvature (CC) are essential parameters in understanding particle size distribution. CU indicates the range of particle sizes within a material, with values less than 4 indicating a uniformly graded material, 4-6 suggesting a well-graded distribution and above 6 indicating a gap-graded material. CC assesses the shape of the particle size distribution curve, with values between 1 and 3 suggesting a well-graded material and values greater than 3 indicating a poorly graded material. A CC value below 1 signifies an asymmetrical distribution, often found in coarse-grained materials (Banahan and Byrne, 2019).

2.4 Mineralogical Characterisation

Mineral characterisation involves the study of minerals in terms of their size, habit, chemical composition, morphology, textural position and association (Månbro and Parian, 2023). There is an established and increasingly important need for this type of study applied to deposits of industrial minerals. This is due to increasing specification requirements for raw materials and mineral products to compete in the marketplace and the realisation that mineral characterisation can ensure optimisation of mineral processing, thus maximising profit (Saussaye et al., 2017). X-ray diffraction (XRD) is a powerful and non-destructive analytical tool widely used for characterizing crystalline materials (Thomas et al., 2022). X-ray diffraction (XRD) is a technique used to analyse the crystal structure of materials by measuring the diffraction of X-ray beams (Minz, 2013). The diffraction pattern obtained from a sample is used to identify the presence of different crystalline phases and determine their relative abundances. The XRD graph typically represents the intensity of diffracted X-rays as a function of the diffraction angle (2θ). The diffraction angle is related to the spacing between crystal planes in the material. When X-rays interact with the crystal lattice, they undergo constructive interference, resulting in diffraction peaks (Cook, 2000). The position and intensity of these peaks provide information about the crystal structure and phase composition.

The Olympus TERRA-538 Cobalt is an X-ray fluorescence (XRF) analyser that utilizes the principles of X-ray fluorescence spectroscopy in its operation (Månbro and Parian, 2023). The principle of science that the Olympus TERRA-538 Cobalt uses is X-ray fluorescence (XRF) spectroscopy. The XRF analyser emits X-rays onto the sample and when the X-rays interact with the atoms in the sample, they cause the atoms to become temporarily excited (Schlager and Karlsruhe, 2004). As the excited atoms return to their ground state, they emit characteristic X-ray fluorescence radiation. The analyser's detector measures the emitted X-rays and based on their characteristic energies, the instrument identifies and quantifies the elements present in the sample. The XRF technique is particularly useful for rapid and accurate elemental analysis of a wide range of materials, including metals, minerals, soils and environmental samples (Adebimpe and Fatoye, 2021). It is widely used in various fields, including geology, mining, environmental science and material analysis, due to its versatility, non-destructive nature and ability to provide real-time, on-site elemental analysis (Wang, 2016).

Ixchel and Luz (2021) demonstrated the use of XRD to identify and quantify crystalline phases in geological samples, highlighting its importance in mineralogical studies. Additionally, Sivakugan et al., (2000) utilized XRF analysis to determine elemental compositions in soil samples, emphasizing its role in environmental science for assessing soil quality and contamination levels. These studies collectively affirm the widespread acceptance and utility of XRD and XRF techniques across various scientific disciplines.

2.5 PHREEQC version 3-A Computer Programme

One such powerful geochemical modelling software in soil science is PHREEQC (PH REdox EQuilibrium in C), widely recognised for its capacity to analyse and predict chemical reactions within soil-water systems (Hart, 2002). Developed by the United States Geological Survey (USGS), PHREEQC version 3 is a computer programme designed to simulate chemical reactions and transport processes in natural or polluted water, laboratory experiments or industrial processes (Schro, 2005). It is a versatile geochemical programme applicable to various hydro-geochemical environments (Hart, 2002). PHREEQC was founded on the equilibrium chemistry of aqueous solutions interacting with minerals, gases, solid solutions, exchangers and sorption surfaces, hence its original acronym pH-REdox-Equilibrium (Robbins and Student, 2017). Over time, the programme has evolved to include the modelling of kinetic reactions and 1D (one-dimensional) transport (Hart, 2002). Users can specify rate equations in basic statements, interconnecting kinetic and equilibrium reactants. The one dimension (1D) transport algorithm in PHREEQC simulates dispersion, diffusion, solute movement in dual porosity media and multicomponent diffusion, where species have individual, temperature-dependent diffusion coefficients. Ion fluxes are adjusted to maintain charge balance during transport (Gelena, 2018). Moreover, PHREEQC boasts a powerful inverse modelling capability, enabling the identification of reactions that explain observed water compositions along a flow line or in the time course of an experiment.

In addition to PHREEQC, Geochemist's Workbench (GWB) stands as another notable tool for characterisation. However, PHREEQC distinguishes itself with its open-source nature, extensive user community and versatility in handling complex chemical reactions within soil-water systems. Its ability to simulate both equilibrium and kinetic reactions, coupled with its compatibility with various thermodynamic databases, provides a comprehensive platform for analysing and predicting geochemical processes. Moreover, PHREEQC's integration with other software packages and its continuous development and support further enhance its standing as a powerful tool in science research and analysis.

The programme's extensible chemical databases allow for the application of reaction, transport and inverse modelling capabilities to nearly any recognised chemical reaction influencing rainwater, soil water, groundwater and surface water quality (Triantafyllidis, Loupasakis and Tsangaratos, 2016). PHREEQC is not only a tool for modelling but also serves as a speciation programme, calculating saturation indices, distribution of aqueous species and the density and specific conductance of a specified solution composition. In addition to PHREEQC, MINTEQ is another notable computer programme for computing geochemical equilibria. Initially developed for incorporation into the Metals Exposure Analysis Modelling System (MEXAMS). MINTEQ is utilised for assessing the fate and migration of selected priority pollutant metals in aquatic systems (Triantafyllidis et al., 2016).

The application of PHREEQC analysis in soil science helped to examine a plethora of critical processes. These include the weathering of minerals, ion exchange reactions, redox transformations and the complex interactions between soil constituents and environmental factors.

2.6 Atomic Absorption Spectroscopy Principle

Atomic Absorption Spectroscopy (AAS) is an absorption spectroscopic method that utilizes the absorption of light by free atoms in a gaseous state to determine the quantitative composition of chemical components (Jehanabad, 2020). In this process, a solution containing metal salt (M+X–) is aspirated into a flame, forming a vapour containing atoms of the metal. Many of these gaseous metal atoms remain in the ground state and absorb the radiant energy of their specific wavelength (Saha et al., 2022). When light of the resonance wavelength is passed through the flame containing these analytic atoms, a portion of the light is absorbed. The extent of this absorption is directly proportional to the number of ground state atoms present in the flame (Boss and Fredeen, 2000) (Equation 1).

$$A = \log\frac{I_0}{I_t} = KLN_0$$

Where,

N_0 = concentration of atoms in the flame

L= path length through the flame

K = constant related to absorption coefficient

Equation 2: Beer-Lambert's law concept (Boss & Fredeen, 2000)

The principle behind AAS revolves around measuring the absorption of characteristic wavelengths of light by the atoms of the elements being analysed. The method involves several key components and steps. It starts with a light source, such as a hollow cathode lamp or electrodeless discharge lamp, emitting light covering a range of wavelengths (Pettersson et al., 2000). A Monochromator is then used to isolate the desired wavelength from this light source. Next, the sample, which can be in various forms such as liquids, solids or gases, is introduced into the path of the light beam. Depending on the sample's nature, methods like flame atomisation, graphite furnace or cold vapour generation are employed to atomise the sample, converting it into gaseous atoms. As these sample atoms pass through the light beam, they absorb specific wavelengths of light corresponding to their characteristic absorption lines (Bernhard Welz, 2010).

The intensity of the absorbed light is then measured by a detector, typically a photomultiplier tube or photodiode. This signal is converted into an electrical signal and sent to a computer or data acquisition system for analysis. To quantify the element of interest, a calibration curve is constructed using standards of known concentrations. The concentration of the element in the sample is subsequently determined by comparing the intensity of the absorption signal for the sample to the calibration curve (Ettler et al., 2012). When a metal atom is converted into a gas and light is passed from the sources, the ground state of the atom gets excited by absorbing the radiation of a particular wavelength. The absorbance is determined by Beer-Lambert's law; the logarithmic ratio of the intensity of incident light to the intensity of the absorbing species (Boss & Fredeen,

2000) (Equation 1). Beer-Lambert's law, also known as Beer's law, is a fundamental concept in analytical chemistry used for the quantification of solute concentration in a solution based on its ability to absorb light (Hart, 2002). This law establishes a direct relationship between the absorbance of light by a solution and the concentration of the solute within it, as well as the path length the light travels through the solution.

The Atomic Absorption Spectrophotometer was utilised for its sensitivity in detecting elemental levels, particularly in light of past studies indicating elevated levels of elements resulting from historical mining practices in the area. Given the known high concentrations of elements associated with older mining methods, the sensitivity of the Atomic Absorption Spectrophotometer was deemed sufficient for accurate measurement without the need for a more sensitive instrument such as Inductively Coupled Plasma (ICP). This strategic choice ensured efficient and effective analysis of elemental levels in the samples collected from the study area.

2.7 Spatial Distribution

Spatial distribution through interpolation is a key geo-statistical method used to estimate and visualize variable values, such as element concentrations in soil, at locations where no samples are taken (Duarte et al., 2020). This technique relies on the spatial relationships between sampled site to predict values at unsampled locations. The process involves using mathematical algorithms to fill in the gaps between sampled sites, creating a continuous surface of estimated values across the study area (Saha et al., 2022). In environmental studies, experts have extensively explored spatial distribution through interpolation to better understand and map various phenomena. Studies have also focused on applying interpolation techniques to predict soil properties, such as nutrient levels or pollutant concentrations, across landscapes. Different interpolation methods have been developed and studied in the context of geo-statistics and spatial analysis. Among the common methods are Inverse Distance Weighting (IDW), Kriging, Splines and Radial Basis Functions (Haldar and Tišljar, 2013). Each of these methods offers unique approaches to estimating values at unsampled locations based on known data points.

IDW is a straightforward method that assumes the influence of a sample point decreases with distance. In this method, closer sample sites have a greater impact on the estimated value at an unsampled location compared to points farther away (Duarte et al., 2020). It is relatively simple to implement, making it a popular choice for interpolation tasks. However, IDW may not capture complex spatial patterns as effectively as more advanced methods. On the other end of the spectrum, Kriging is a more complex interpolation method that considers the spatial autocorrelation of the data. It not only provides estimates of values at unsampled locations but also offers measures of uncertainty (Duarte et al., 2020). This feature is particularly valuable for decision-making processes where understanding the reliability of the estimates is important. Kriging is known to perform well when there is a strong spatial correlation in the data, leading to reliable estimates and uncertainty measures (Câmara et al., 2022).

Researchers have conducted comparative studies to understand the strengths and weaknesses of these interpolation methods in different scenarios. Studies have shown that Kriging excels when there is a strong spatial correlation present in the data, offering reliable estimates and deep uncertainty measures (USGS, 2015). Furthermore, advancements in geographic information systems (GIS) have enabled the integration of spatial interpolation with other data layers, such as land use, topography and satellite imagery. This integration allows for more accurate and comprehensive spatial modelling, aiding in tasks like land suitability assessment, environmental impact analysis and natural resource management (Trevor et al., 2019).

2.8 Ecological Classification Schemes

Ecological classification schemes are frameworks used to categorise and organise ecological systems based on various criteria such as climate, vegetation, soil and topography. These schemes are essential for understanding and managing ecosystems, biodiversity and natural resources (Chileshe et al., 2020). Among these schemes, the Geo-Accumulation Index holds particular significance. Unlike other indices such as Enrichment Factor or Contamination Factor, the Geo-Accumulation Index provides a robust quantitative measure of the accumulation of heavy metals or pollutants in soils and sediments, offering insights into anthropogenic impacts on the environment (Guimarães et al., 2011). Its structured approach facilitates the identification of areas requiring remediation and supports the development of effective environmental management strategies, making it a vital tool for this study.

The Geo-Accumulation Index (Igeo) serves as a numerical scale used in environmental studies to assess the degree of accumulation of specific elements or substances in soils or sediments compared to background levels (Guimarães et al., 2011). Introduced by Müller in 1969, it is widely utilized for evaluating environmental contamination and potential health risks associated with various elements in the environment. This index is particularly valuable for understanding the long-term accumulation of trace elements or pollutants in soils and sediments. It considers the background concentration of elements in the environment, important for distinguishing between natural and human-induced sources of contamination.

The Igeo scale provides a numeric value indicating the level of metal accumulation in soil. Positive Igeo values indicate enrichment, while zero or negative values suggest no enrichment or background levels, respectively (Table 1). This scale helps classify the pollution status of an area based on pollutant concentrations in the environment. It offers a systematic approach to assess environmental contamination levels and evaluate the impact of human activities on the environment. The results of assessments utilizing the Geo-Accumulation Index (Igeo) can guide the implementation of measures to protect the environment and ensure the safety of local ecosystems and human populations. This approach aids in mitigating potential environmental risks and hazards associated with sites like the Uchi Tailing Dump, promoting responsible waste management practices.

Table 1: The Geo-Accumulation index (Igeo) scale classifying the pollution status

Class	**Value**	**Soil Quality**
0	Igeo ≤ 0	Practically uncontaminated or no accumulation
1	0<Igeo < 1	Uncontaminated to moderately contaminated
2	1<Igeo < 2	Moderately contaminated
3	2<Igeo < 3	Moderately to heavily contaminated
4	3<Igeo < 4	Heavily contaminated
5	4<Igeo < 5	Heavily to very heavily contaminated
6	5Igeo < 0	Extremely contaminated

This table presents a summary of the Geo-Accumulation Index (Igeo) classification scale and corresponding soil quality categories based on Igeo values (Chileshe et al., 2020). The classification system ranges from 0 to 6, with each class indicating a different level of contamination. A value of 0 (Igeo ≤ 0) represents soils that are practically uncontaminated or show no accumulation of pollutants. Class 1 (0 < Igeo < 1) signifies soils that are uncontaminated to moderately contaminated. Class 2 (1 < Igeo < 2) indicates moderately contaminated soils while class 3 (2 < Igeo < 3) suggests soils that are moderately to heavily contaminated. Class 4 (3 < Igeo < 4) represents soils that are heavily contaminated and class 5 (4 < Igeo < 5) signifies soils that are heavily to very heavily contaminated. The highest class, class 6 (5 < Igeo < 0), indicates soils that are extremely contaminated (Guimarães et al., 2011).

2.9 Previous Studies

There are many earlier works of literature on geochemical characterisation, including local, regional and international works. Although there are numerous reviewed papers, only a few are listed below.

Initially, a geochemical investigation was conducted by Bohdan and colleagues (2014), on the pollution of soils with dust released from the tailing dump in the Rosh Pinah region of Namibia. The study's objective was to evaluate dust dispersion in a region and its effects on the environment using modelling. According to the findings, the main environmental danger in the town of Rosh Pinah appeared to be the dust that was blown out of the tailings dump and to a lesser extent, from the ore treatment plant. The study also discovered that air-borne dust particles suspended in the atmosphere had significant levels of zinc, lead, manganese and copper, but only trace amounts of arsenic and cadmium. They used low volume portable samplers to characterise the dust fallout from the tailing dump.

Secondly, a study on the distinction between lithogenic and anthropogenic sources of metals and sulphur in the soils in the central-northern region of the Zambian Copperbelt mining was conducted by Nyambe and colleagues (2010). To distinguish between lithogenic sources of metals and anthropogenic soil contamination brought on by the fallout of dust from mining operations, floatation ore treatment plants, tailing dumps, smelters and slag dumping grounds, the study presented samples of topsoil along with reference samples of subsurface soil from a depth of 80–90 cm. These samples were collected in the central–northern part of the Zambian Copperbelt. The findings presented that the topsoil were found to be significantly higher in sulphur, copper and cobalt relative to subsurface soil over a large part of the surveyed area and zinc, lead, arsenic and mercury contents showed a definite increase in the close neighbourhood of smelters and in the direction of prevailing winds. The study indicated the increase of chemical elemental composition in the topsoil to be due to anthropogenic activities. The study also used the factor analyses to characterise i.e., slag specific, bedrock specific, smelter specific, tailings specific and organic carbon specific. This study concluded that the chemical composition of the tailing's material plays a major role in characterisation.

Thirdly, a study was conducted by Mwandira (2014), on the creation of bioremediation techniques for water and soil contaminated with heavy metals in the Kabwe mine. In this project, lead-contaminated and leach plants in Kabwe were to be bio-cemented using Microbially Induced Calcium Carbonate Precipitation (MICP). In the study, the potential for stabilising mine waste and an assessment of the efficiency of microbially produced calcium carbonate precipitation was discussed (MICP). The study characterised the soil based on strength, slaking behaviour, water absorption and hydraulic conductivity. The study also looked at long term chemical stability of conducting mass leaching tests on the waste samples using U.S EPA method 1315 and also analysed the pH, conductivity and lead concentration. In this study the physical and chemical properties of the mine wastes of the abandoned Kabwe Mine were investigated. Another contribution to this study, was the isolation and identification of two indigenous ureolytic bacteria from the abandoned mine site namely O. profundus KBZ 1-3 and O. profundus KBZ 2-5. The use of MICP to cap mine wastes would eliminate both dust generation and water infiltration, restoring the contaminated site. Although many ureolytic bacteria have been isolated, continued isolation and identification of more novel species, especially those that are indigenous to the area, is indispensable.

Rahman (2016), also did a study on the bioremediation of hazardous metals for preserving ecosystems and human health. According to the report, drinking water was contaminated by heavy metal contaminants that were released into the ecosystem as waste by human activities, which affects millions of people and animals around the world. According to the study, chronic exposure to these heavy metals causes many fatal diseases, including diabetes, cancer, keratosis, gangrene and cardio-vascular ailments. Thus, it is crucial for human well-being that these toxins are removed from the land, water and environment. Lysinibacillus Sphaericus B1-CDA, Enterobacter cloacae B2-DHA and Lysinibacillus sp. BA2 were identified and investigated in this research together with chromium- and nickel-resistant bacteria. The results showed that the liquid medium's arsenic and chromium concentrations had been decreased to 50% and 81%, respectively. The adsorption values of BA2 after 6 hours of exposure to nickel were 238.04 mg of Ni (II) per gramme of dead biomass, showing that BA2 may lower the nickel content of the solution to 53.89%. According to the study's findings, these bacteria are important for eliminating hazardous metals from contaminated sources.

Adebimpe and Fatoye (2021), did a different investigation in which they characterised the tailings from the Itakpe Iron Ore Mine in Itakpe, Nigeria. This study made the case that understanding the properties of tailings is essential for managing and using them in the mining and construction sectors. Tailings from the Itakpe iron ore mine's waste dumps were gathered and subjected to laboratory analysis to ascertain their chemical and physical properties, including their permeability, porosity, specific gravity, particle size distribution, chemical composition and elemental bioavailability factor. Geochemical speciation with quantitative X-ray powder diffraction was used to evaluate the chemical and mineral composition of Itakpe iron ore tailings (Adebimpe & Fatoye, 2021). This study aimed to offer base line data necessary to assess metal mobility and bioavailability. The distribution of heavy metals such as Cu, Ni, Cd, Cr, Zn and Fe was determined using multi- step sequential extraction. The results obtained indicated that the permeability is 6.24 x 10-3 cm/sec, porosity is 35% and specific gravity is 3.58. The tailings were found to be well graded sand gravel. Significantly elevated concentrations of nickel and zinc were observed in the exchangeable and carbonate-bound fractions, indicating their mobility within the soil. Additionally, these metals were found to be bound to Fe-Mn oxides, even though in slightly mobile regions. Interestingly, a higher concentration of nickel was detected in the residual fraction, suggesting its relatively stable presence within the soil matrix. This result implies that nickel and zinc partially enter into the food chain. The concentration results for chromium and cadmium revealed that these metals have the potential to easily enter the food chain. This is due to their presence in the mobile region of the soil and their higher mobility percentages, indicating a greater likelihood of movement and uptake by plants or organisms within the ecosystem (Rahman, 2016).

2.9.1 Gap Analysis

The geochemical characterisation of the entire Uchi Tailing Dump region lacks comprehensive investigation in prior research, with no utilisation of computer software to forecast potential future outcomes or suggest corrective actions. This study aims to bridge these gaps by filling in missing data through geochemical characterisation and employing the PHREEQC computer programme to simulate possible processes/reactions happing at the site. However, while existing research has identified alarming levels of soil pollution in TD26 of the Uchi Tailing Dump, there remains a significant gap in understanding the physiochemical characteristics and environmental impact of adjacent areas like TD27. This underscores the need for further research to assess and address the environmental implications of mining waste disposal practices at Uchi Tailing Dump, Kitwe, Copperbelt Province of Zambia.

2.9.2 Limitations

During the analysis at the Uchi Tailing Dump, several limitations were encountered. Firstly, challenges arose with the availability of reagents required for analysing elements such as arsenic, restricting the comprehensive assessment of certain pollutants. Additionally, the presence of stray dogs posed a significant safety concern, necessitating police escorts when accessing deeper areas of the dumpsite. Despite encountering challenges such as the unavailability of reagents for analysing certain elements and the presence of stray dogs requiring police escorts, the diligent efforts of the research team ensured that representative samples were collected from the entire Uchi Tailing Dump area. Though the collection process may have taken longer than anticipated, the commitment to obtaining comprehensive data remained unwavering, ultimately contributing to a more thorough understanding of the environmental conditions and potential risks associated with the site.

CHAPTER THREE: DESCRIPTION OF THE STUDY AREA

3.0 General Remarks

This sub-section presents the location and description of Uchi Tailing Dump, Kitwe, Copperbelt Province, Zambia. It includes the regional setting, location, population, climate, hydrology, geomorphology, soils, vegetation, geology and ore mineralisation.

3.1 Regional Setting

Zambia is located in southern Africa, east of Angola, between 15000 S and 30000 E, with an area of 752 614 km^2, of which 740 724 km^2 are land and 11 890 km^2 are water. Zambia borders the Democratic Republic of Congo (DRC) in Kinshasa in the north, Tanzania in the northeast, Malawi and Mozambique in the east, Zimbabwe, Botswana and Namibia in the south and Angola in the west.

3.2 Location of Uchi Tailing Dump

In the Copperbelt Province of Zambia, Uchi Tailing Dump, which served as a dumpsite for Nkana Mine from 1931 to 2009, is situated at latitude 12° 49' 53" south and longitude 28° 13' 29" east of Kitwe (Figure 1). The map also distinguishes between two sampled sites, TD26 marked with green dots and TD27 marked with red dots, as well as sediments indicated by blue dots, within the Uchi Tailing Dump situated in Kitwe, Zambia (Figure 1C). These sampled sites represent specific locations where geological and mineralogical analyses have been conducted, offering important insights into the composition and characteristics of the tailing dump's materials. There are two sections of the Uchi Tailing Dump, with the old section (TD26) marked in green (Figure 2a) and the new section (TD27) (Figure 2b) highlighted in red (Figure 2). TD26 and TD27 are roughly 77 and 46.7 hectares in size, respectively. Kitwe is located in the Copperbelt Province and is made up of townships and suburban areas, including Parklands, Riverside, Buchi, Chimwemwe, Kwacha, Nkana East, Nkana West, Garneton, Ndeke, Miseshi, Wusakile, Mindolo, Chachacha and Race Course, to mention a few. The city is sometimes referred to as Kitwe-Nkana. Nkana is derived from the name of the senior Chief Nkana of the Lamba-speaking people of the Copperbelt Province. The Chief's area covers the towns of Kitwe, Mufulira, Kalulushi-Chibuluma and Chambishi. Kitwe is the third-largest city in terms of infrastructure development and the second-largest city in terms of size and population in Zambia. Kitwe is one of the most developed commercial and industrial areas in the nation, alongside Ndola and Lusaka. Uchi Tailing Dump is a reservoir in the Copperbelt. Uchi Tailings Dump is situated nearby Taonga's Place and south of Kitwe Tailing Dump.

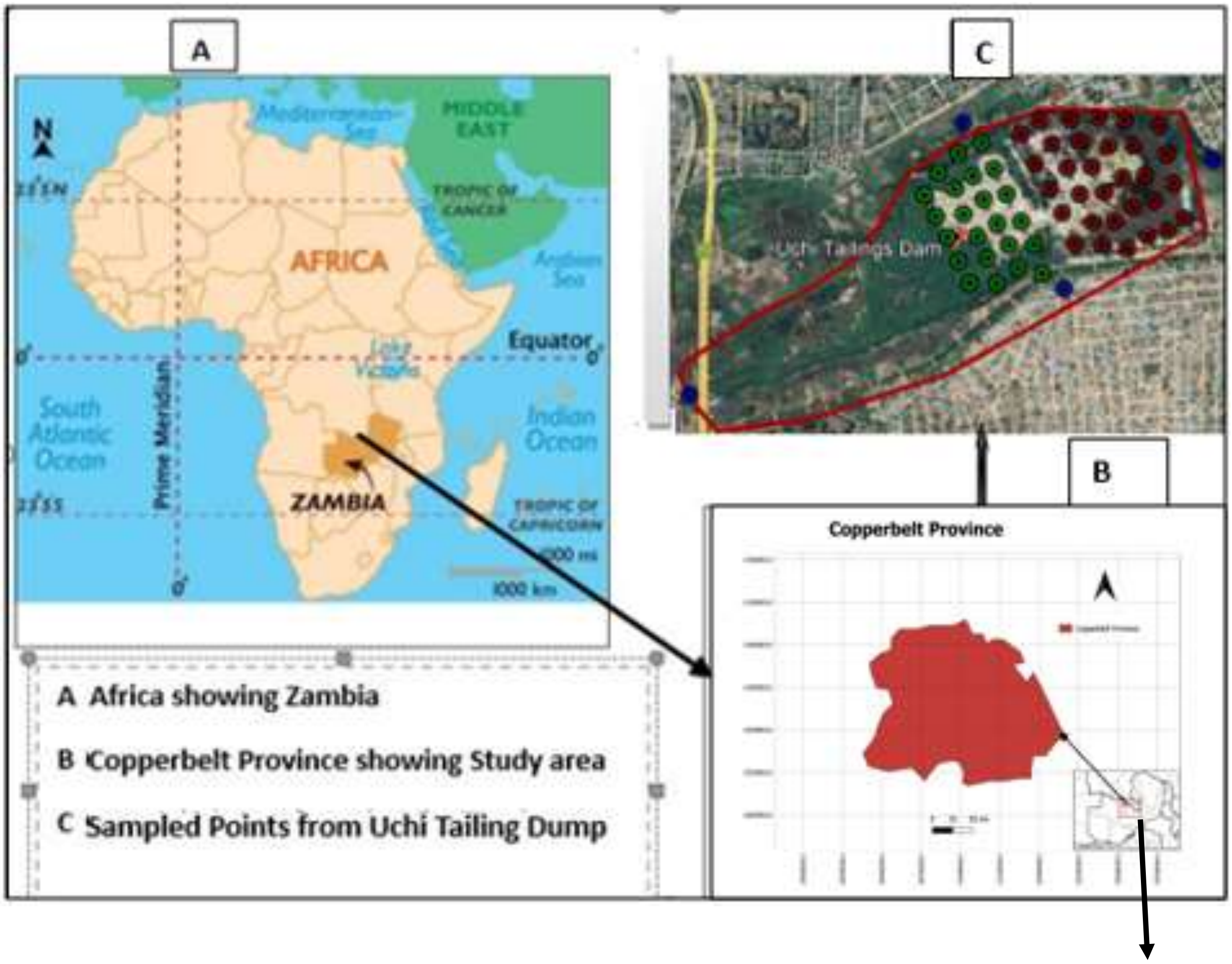

Figure 1: Map showing the location of Uchi Tailing Dump, Kitwe, Copperbelt Province, Zambia

Figure 2: Detailed map of TD26 and TD27 of Uchi Tailing Dump, Kitwe, Zambia

Figure 2a: Image captured by the Drone (DJI Mini 2) revealing TD26's vastness from an aerial perspective, Uchi Tailing Dump, Kitwe, Zambia

Figure 2b: Image captured by the Drone (DJI Mini 2) revealing TD27's vastness from an aerial perspective, Uchi Tailing Dump, Kitwe, Zambia

3.3 Population

The studied region belongs to the Zambian part of the Copperbelt Administrative Province of Zambia, which covers an area of about 31,000 km^2. Compared to Zambia as a whole, the Copperbelt Province is densely populated. The Zambia 2021 census showed the population of the Copperbelt Province to be 1.6 million, which constitutes 15% of the total Zambian population. Ndola (528,330 people) serves as the administrative centre. The largest centre of population is Kitwe, with a total population of 363,734 (Central Statistical Office, 2021).

3.4 Climate and Hydrology

The Zambian Copperbelt has three distinct seasons: the winter months of May to July are generally cool and dry, with a mean daily temperature of around 20ºC and rainfall below 150 mm; August to October is characterised by hot, dry conditions, with maximum temperatures around 36ºC and the wet season typically is from November to April, when over 90% of the region´s mean annual precipitation of 1,350 mm falls (Zambia Meteorological Department (ZMD), 2023) (Figure 3). The predominant wind direction is from the south-easterly quadrant (thus producing a net atmospheric contaminant plume to the north-west), with maximum speeds of about 30 m/s in the summer months and 22 m/s in the winter (Bailey, 2021). The scope of the project is the Kitwe Central Business District (CBD), bordered by Oxford, Chisokone, Obote and President Avenue.

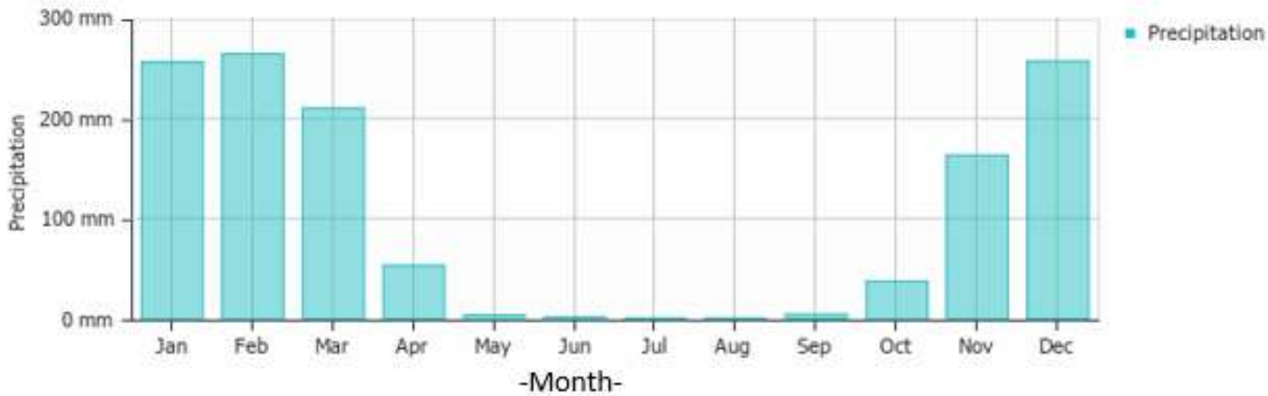

Figure 3: Average monthly rainfall in Kitwe, Copperbelt Province, Zambia (ZMD, 2023)

3.5 Geomorphology, Soils and Vegetation

The Kafue River and its tributaries cut a swath through the generally undulating terrain. Although river floodplains are typically narrow, they may become broader near the rivers. The Kafue River, which follows the Kafue anticline and flows first southeast and then south, regulates the drainage system in the Copperbelt region (Sracek et al., 2012). The Lubengele river, which drains the mining district of Chililabombwe and the Mufulira River, which drains the mining district of Mufulira, are the two most significant sinistral tributaries of the Kafue River (Pettersson, 2002). Mutupa, Mwekera and Kamfinsa rivers are other significant tributaries. The Mushishima and its tributaries, Mwambashi and Muntimpa, are the most significant dextral tributary rivers in the Chingola District. Several small rivers, including the Uchi, Mindolo, Kitwe and Busakile, drain the Kitwe region. The Kalulushi River drains the territory to the west of Kitwe. The tiny rivers Itawa, Twapia, Chibolele, Kansenshi, Moshiashi and Kafubu make up the river network in the Ndola region. These rivers run south from Ndola and combine to form the Kafubu River, one of the primary southern tributaries of the Kafue in this region. The majority of tributary rivers and streams begin as headwater wetlands known as Dambos.

The soils on the Zambian Copperbelt are divided into two categories: easily drained soils and dambo (waterlogged) soils (Mendelsohn, 2000). The freely draining soils of the Zambian Copperbelt can be divided into four different types, according to the World Reference Base for soil resources Working Group (WRB, 2014). These types are Haplic Ferrasol Eutric, Haplic Plinthosol Eutric, Haplic Ferrasol Xantic and Haplic Plinthosol Dystric (Ettler et al., 2014). Iron and aluminium oxides have an accumulation that gives Ferrasols their characteristic red and yellow hues (from which the name of the soil group is derived). Ferrasols are typically low in organic carbon and acidic (pH-KCl: 3.94–7.15) in the investigated area. The Copperbelt's freely draining soils can be categorised as belonging to the Ferrasol group (Acrid, orthic or rhodic Ferrasols) by World Reference Base for soil resources. Kaolinite, quartz and other elements make up plinthosols, which when repeatedly wet and dried causes them to irrevocably harden into Petroplinthite (WRB, 2014). Plinthosols are deficient in humus. A high-water table prevents tree growth in the dambo type of soils (poorly drained soils in wetlands), which are wet all the time or just sometimes. Swelling clays, or clays created by neoformation from rock weathering, make up a large component of these materials. They fall under the category of vertosols, according to the World Reference Base for soil resources Working Group. Typically, grassland, shrubland and forests made of miombo and acacia trees cover the soil.

Mupapa (Afzeia quanzensis), Mulobwa (Pterocarpus angiogenesis), Mubanga (Afrormosis angiogenesis), Musase (Albizia antunesiana) and Saninga are the plants that grow beneath the canopy (Faurea saligna). Suputu (Brachystegia spiciformis), Susamba (Branchiostegal boehmii), Mopane (Colophospermum mopane) and Acacia are the primary trees that provide tall canopies (Mendelsohn, 2005).

3.6 Stratigraphy of the Copperbelt

The Uchi Tailing Dump, located in the Copperbelt region, is sourced from a geological formation characterised by a unique stratigraphy typical of the area. The Copperbelt is renowned for its rich deposits of copper and cobalt, primarily found within sedimentary rock formations. The Lufubu schists and intrusive granitoids make up the Paleoproterozoic magmatic arc sequence that makes up the oldest pre-Katanga Basement Complex in Zambia's Copperbelt (Rainaud et al., 2005). The Paleoproterozoic Muva Supergroup's quartzites and metapelites are incongruously deposited above the Basement Complex. The Neoproterozoic Katanga Supergroup, which includes of metasediments typically split into the Roan Group and underlying Kundulungu Group, is unconformably overlain by the Nchanga pink microcline granite and adamellite, the youngest intrusion in the pre-Katanga Supergroup (Nyambe & Kawamya, 2005). The first rift cycle of the Katanga Supergroup formation lasted from 880 to 820 Ma when the Roan group was deposited (Rainaud et al., 2005). After uplift, the Kundulungu group of the Katanga Supergroup was likely deposited during the second rift basin development (Yantambwe and Cailteux, 2019).

The Lower Roan Formation, which is composed of conglomerates, argillaceous and carbonate shale, limestone and dolomite, is the bottom portion of the Katanga Supergroup, to which the copper and cobalt mineralisation is associated. Pyrite (FeS_2), chalcopyrite ($CuFeS_2$), bornite (Cu_5FeS_4), chalcocite (Cu_2S), digenite (Cu_9S_5), linnaeite (Co_3S_4) and carrolite $CuCo_2S_4$ are the main minerals in stratiform and Strat-bound Cu-Co deposits (Kossoff et al., 2014) The average ore grade is 3.0% for copper and 0.18 % for cobalt. Co ore has an average grade of 0.18 weight percent compared to Cu ore's 3 weight percent (Rainaud et al., 2005). Many genetic ideas have been proposed to explain the origin of Cu and Co in light of the high metal content (Sillitoe et al., 2015). There are three types of genetic models namely Sydiagenetic, Hydrothermal-epigenetic and Metamorphic.

CHAPTER FOUR: METHODOLOGY

4.0 General Remarks

This chapter outlines an overview of the methods and tools employed to characterise the Uchi Tailing Dump, incorporating geochemical methodologies that integrate both physical and chemical analyses. It begins by detailing the approach taken for the reconnaissance survey, followed by a description of the methods used to collect the data, which align with the specific objectives of this study.

4.1 Data Collection

Data collection at the Uchi Tailing Dump involved systematic sampling of both topsoil and subsurface samples from various locations within the dump area. Fieldwork was conducted during both rainy and dry seasons to capture potential seasonal variations. Sampling techniques included grid sampling to ensure representative coverage of the area. Samples were collected for analysis of chemical composition, mineralogical structure using X-ray diffraction (XRD), particle size distribution through sieve analysis, elemental quantification using techniques such as flame atomic absorption spectrometry and texture. Spatial analysis was conducted to identify patterns in contaminant distribution. Additionally, hydro-geochemical analysis and geochemical simulation using PHREEQC were employed to further understand the geochemical processes within the tailings.

4.1.1 Reconnaissance Survey and Desk Study

A month-long reconnaissance survey was conducted in collaboration with a team from the School of Mines in Colorado, United States of America (USA). This study was motivated by the necessity to fill the data gaps present in the current literature regarding the geochemical characterisation of the Uchi Tailing Dump. The first objective of this reconnaissance was to document the various activities and operations taking place at the Uchi Tailing Dump. This encompassed observing and recording activities involved, along with gaining an understanding of the individuals and entities involved in these operations. Additionally, the survey extended beyond the confines of the tailing dump itself. The survey sought to become intimately acquainted with the surrounding ecosystem. This encompassed a thorough examination of the area's environmental conditions, flora, fauna and any potential impacts resulting from mining activities on the local ecology. Such a holistic perspective was essential in understanding the broader implications of the Uchi Tailing Dump's presence in the region. Moreover, the dedicated efforts to delineate the precise boundaries of the property housing the Uchi Tailing Dump and identify its legal owner.

The desk study involved a review of extensive literature, including books, scholarly articles and reports, pertaining to the geochemical characterisation of tailing dumps not only in Kitwe and the broader Copperbelt Region in Zambia but also in other countries across Africa and beyond. This comprehensive analysis provided important data into the Uchi Tailing Dump. The findings from this thorough review significantly enriched the descriptive account of the study area within this thesis.

4.1.2 Field Methods for Soil Sampling

The first sampling of topsoil and subsurface soils was conducted in September 2022 at Uchi Tailing Dump, Kitwe, Zambia. Beginning on Monday, September 26, 2022, soil samples were collected utilising a sampling grid method that also took the various zonation's into account. Topsoil samples were taken from the Uchi Tailing Dump using a systematic grid sampling technique that was adapted from regional geochemical mapping done by the Forum for European Geological Surveys (FOREGS) Geochemistry working group and geochemical mapping done in 2007 in Zambia's Copperbelt Province (Kribek et al, 2007). This method which was widely been used worldwide is recommended for geochemical sampling sites. An auger, a shovel, a handheld shovel, a GPS and other tools were utilised to gather soil samples. The topsoil was collected in the field at a depth interval of 0-30cm using soil auger. From the northern to the southern portion of Uchi Tailing Dump, one fifty-two (152) samples in total were taken at 100-meter intervals. To include all necessary areas and provide a well-representative, meaningful sample, the interval of 100 m was chosen for the samples based on the scale and the area. Based on a survey and the overall size of the land, this 100-meter spacing was selected.

(a) Sample Locations

The map highlights two distinct sampled sites, TD26 in green and TD27 in red, within the Uchi Tailing Dump located in Kitwe, Zambia (Figure 4). These sampled sites represent specific locations where geological and mineralogical analyses have been conducted, offering important data into the composition and characteristics of the tailing dump's materials. The colour-coded differentiation of TD26 and TD27 aids in identifying and comparing variations in mineralisation, ore grades or other relevant factors between these two sampling sites. This information contributes to a more comprehensive understanding of the tailing dump's geological features and potential mineral resources in the Kitwe area of Zambia.

Figure 4: Map showing Soil Sampling sites at Uchi Tailing Dump, Kitwe, Copperbelt Province, Zambia

(b) Sediment Sampling and Characterisation

A total of eight (8) river bed sediments were collected by using sediment scoop from around the Uchi Tailing Dump stream, encompassing the north, east, west and south sides of the Dump to observe the extent of the tailings in the stream (Figure 5). This collection process was conducted to assess the dispersion and impact of tailings in the stream from various directions. The collected samples provided significant insights into the contamination levels, flow patterns and potential environmental consequences. The sediments were carefully sampled, labelled and stored in zip lock bags to prevent contamination and subsequent laboratory analyses provided detailed information about the composition of the tailings and their environmental implications for the stream and the surrounding ecosystem.

.

Figure 5: Map of river bed sediments in blue near and outside Uchi Tailing Dump in Kitwe, Zambia

The samples collected were taken to the University of Zambia, School of Mines for laboratory analysis (Figure 6A). The soil samples were subjected to air drying for a period of five days (Figure 6B). The air-dried soil samples were sieved by using a 200 µm sieve for size fractionation (Figure 6C). After that, one gram (1g) of soil was weighed using the mass balance (Figure 6D, E). This 1g of soil sample was transferred to the conical flask and digested with 20ml of the aqua regia solution (Figure 6G, H). The mixture was then heated until the appearance of nitrous fumes indicating complete digestion (Figure 6F). The samples were examined for copper (cu), cobalt (co), zinc (zn) and lead (pb) using an Atomic Absorption Spectrophotometer (AAS; Figure 6I).

Figure 6: (A) Field sampling at Uchi Tailing Dump, Kitwe, Zambia; (B) Air drying of Soil samples for 5 days; (C) Sieving 200 μm; (D) Mass balance (E) Measuring 1g of each sample; (F) Mixture

digestion; (G) Cooling for 5 minutes; (H) Filtering; and (I) AAS analysis at the Geochemistry Analytical Laboratory, University of Zambia, Lusaka, Zambia

(c) Vertical Profiling

Vertical profiling was conducted at the Uchi Tailing Dump, located in Kitwe, Copperbelt Province, Zambia (Figure 7). The sampling process involved excavating pits, typically at regular intervals, to capture the vertical variation of heavy metal concentrations (Figure 7a). This method involved taking samples at various depths within the soil profile to assess the distribution of contaminants (Figure 7b). At each depth, soil samples were carefully collected and analysed for elements such as copper (Cu), cobalt (Co), iron (Fe), zinc (Zn), calcium (Ca) and manganese (Mn).

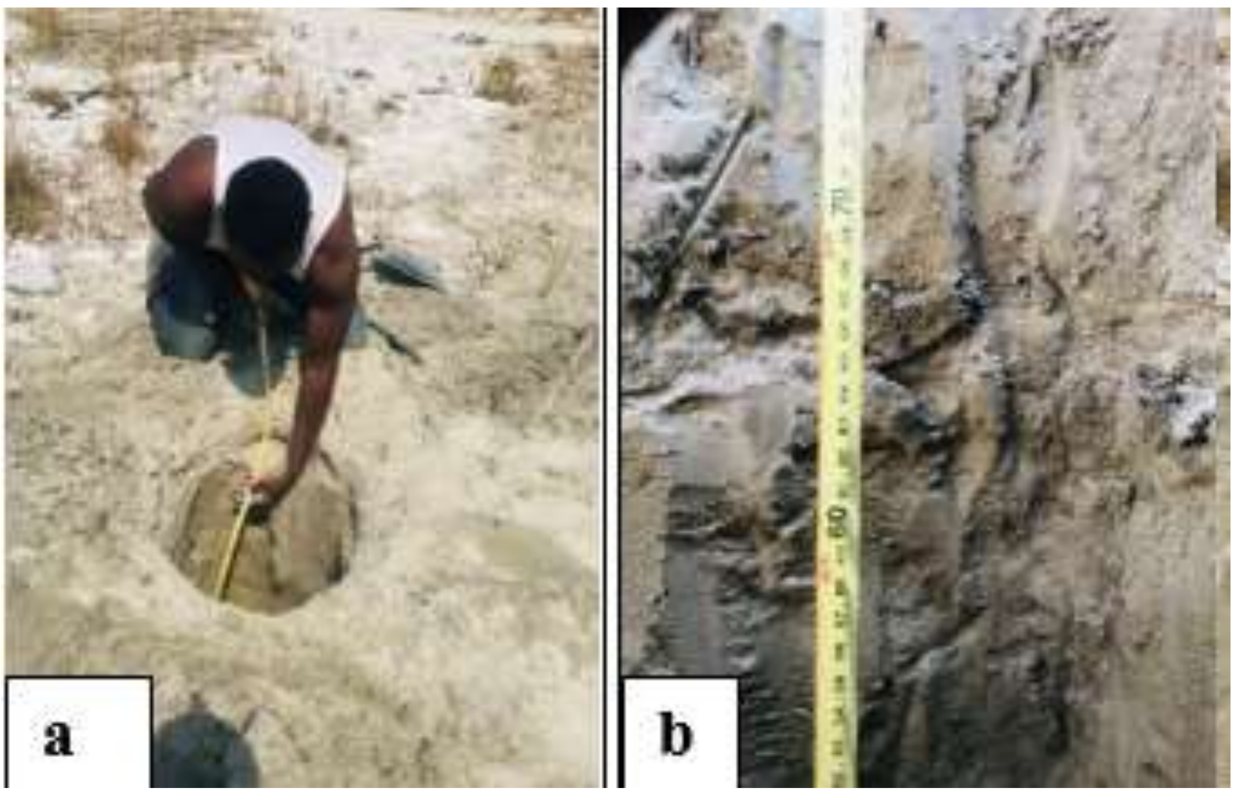

Figure 7: (a) and (b) Vertical profiling conducted at Uchi Tailing Dump in Kitwe, Copperbelt Province, Zambia

4.2 Analysis

Analysis at the Uchi Tailing Dump involved a comprehensive range of techniques to understand its characteristics and potential environmental impacts. Soil samples underwent chemical analysis to determine concentrations of copper, cobalt, iron, lead, calcium, manganese and zinc. X-ray diffraction (XRD) analysis was used to identify the predominant mineral phases. Particle size distribution analysis provided the soil's texture. Additionally, geochemical modelling using PHREEQC helped simulate mineral saturation levels. The Geo-Accumulation Index (Igeo) confirmed contamination levels, particularly in copper and cobalt efforts at the Uchi Tailing Dump.

4.2.1 Analytical Methods for the Chemical Analysis

The mine waste soil was analysed for potentially toxic elements of environmental concern, namely Cu, Co, Fe, Pb Ca, Mn and Zn. This analysis was conducted on a total of 152 soil samples using a flame/furnace Atomic Absorption Spectrophotometer (AAS: PerkinElmer Inc., Shelton, Connecticut, USA) equipped with Syngistix for AA software, version 4.0. The analysis took place at a geochemistry laboratory located at the University of Zambia (UNZA) in Lusaka, Zambia. The AAS was first calibrated using standards for each metal. Every metal to be tested was read by employing specific lamps and parameters according to the metal (Table 2). Approximately 1 gramme of soil samples was weighed and transferred to an Erlenmeyer flasks and 20 ml of Aqua Regia was added. The resulting suspension was heated on the hot plate until appearance of nitrous fumes. Following this, the mixture was allowed to cool for five minutes and the Erlenmeyer flask was rinsed with 10 ml of distilled water. Subsequently, 10 ml of HCl was added and the mixture was heated to dissolve any remaining residue. Using a 100 ml volumetric flask, the sample was then rinsed three times with distilled water. The washings were transferred to another flask for additional dilution with distilled water and homogenisation by shaking. The results were reported in ppm (Parts Per Million)/ mg/l and in mg/kg. Each sample was digested and analysed in duplicate to ensure consistency in the results.

Table 2: Shows Specifications for the Lamps used in Atomic Absorption Spectrophotometry (AAS) analysis for various metals at the University of Zambia laboratory, Lusaka, Zambia

Metal	Lamp Specifications				
	Band Width (nm)	Wavelength (nm)	Lamp Current (mA)	Detection limits (ppm)	Flame type
Cu	0.7	324.275	15-25	0.003	air
Co	0.2	240.730	15-25	0.005	air
Fe	0.2	248.330	12-25	0.002	air

Ca	0.2	279.480	12-25	0.010	air
Zn	0.7	283.310	10-25	0.010	air
Mn	0.7	213.860	8-25	0.002	air

4.2.2 A Study to Characterise the Hydro-Geochemistry and Transport Patterns of Elements at Uchi Tailing Dump

This section of hydrology focused on investigating the chemical properties and elemental transport patterns within Uchi area. It encompasses a range of activities and analysis aimed at understanding how elements move through the environment, particularly within water systems. The investigation includes:

(a) Mineralogical Characterisation

Mineralogical characterisation was conducted using the Olympus TERRA-538 tool, which employs X-ray fluorescence (XRF), to gain understanding into the crystallographic structure of the soil materials under investigation (Figure 8). Firstly, the XRF analyser was calibrated using known standards of cobalt-copper concentrations obtained from the Geology laboratory. This calibration involved analysing standard samples with known cobalt-copper concentrations to establish a calibration curve, enabling the conversion of X-ray intensity measurements into cobalt-copper concentrations. To prepare the soil samples, approximately 5-10 grammes of each were air-dried and ground into a fine powder to ensure homogeneity. These samples were then placed into sample cups for analysis. The TERRA-538 Cobalt XRF analyser was set up on a table and powered on. Each prepared soil sample was individually placed in the sample cup, which was then inserted into the XRF analyser. The machine was configured to analyse each sample for approximately one minute to obtain accurate measurements. During the analysis, X-rays were emitted onto the soil sample, causing the soil's elements, such as cobalt and copper, to emit secondary X-rays. The analyser detected and measured these secondary X-rays to determine the cobalt-copper concentration in each sample. The results, displaying the cobalt-copper concentrations, were directly shown on the XRF analyser's screen or stored for later analysis. These measurements were recorded for further investigation. After completing the analysis of all soil samples, the XRF analyser was cleaned thoroughly. This included wiping down the sample cup holder to ensure no sample residue remained, maintaining the instrument's integrity for future use.

Figure 8: Olympus TERRA-538 XRD, Lusaka, Zambia

(b) Thin Section Analysis

Thin section analysis was employed for the examination of samples from the Uchi Tailing Dump. This method involved the preparation of extremely thin slices or sections of specimen, typically around 30 micrometres (μm) in thickness, which were then mounted on glass slides. These thin sections were trans-parented and allowed to examine the mineralogical and textural characteristics of rocks under a microscope. The prepared thin section was placed under a petrographic microscope equipped with polarizing filters and specialized lighting. The mineral composition, textures and structures within the sample were observed in great detail. The use of polarized light helped reveal properties like birefringence, which provided information about mineral orientations and relationships.

4.2.3 The Spatial Distribution of Elements at Uchi Tailing Dump

The spatial distribution of elements in the Uchi area was analysed using advanced mathematical algorithms, specifically the Kriging method, which is a well-established geo-statistical technique utilised within the Geographic Information Systems (GIS) software on the computer. The study began by analysing variograms to understand the differences between each sampling point, providing information into the variability across the area. Following this, variogram analysis was conducted to look deeper into the spatial autocorrelation structure of the variables, revealing how they were related in terms of their spatial patterns. Thereafter, variogram model was employed to guide the interpolation process using Kriging, a method that filled data gaps between sampled sites with more accurate estimates. Leveraging Geographic Information System (GIS) applications, weights were calculated based on both the distances between points and their spatial correlations, adding precision to the interpolation. Subsequently, values were interpolated at unmeasured locations, creating a comprehensive spatial representation of the distribution of elements within the Uchi area. Finally, the resulting maps were analysed to identify hotspots, trends and patterns of element concentrations.

4.2.4 Particle-Size Distribution (Gradation) of Soils Using Sieve Analysis

The soil samples collected from the field were carefully chosen to accurately represent the soil's characteristics. These soil samples from Uchi Tailing Dump were later transported to the University of Zambia laboratory, Lusaka. Upon arrival, the moisture content in each sample was measured to ensure consistency during subsequent testing. The particle size distribution analysis was conducted using a series of sieves with varying mesh sizes (Figure 9A). The sieves were arranged in ascending order of opening sizes, with larger openings (lower numbers) on top and smaller openings (higher numbers) at the bottom. The stack included sieves with openings of 4.75mm, 2mm, 1.18mm, 0.43mm, 0.212mm and 0.075mm, with a #200 sieve at the bottom with a 75 µm opening size. A pan was attached securely to the bottom sieve to collect soil particles passing through the finest sieve. The soil samples underwent thorough drying in an oven for 24 hours at a temperature of 105°C (Figure 9B), ensuring complete removal of moisture and consistent results during the sieving process. Subsequently, the dried soil samples were subjected to sieving using a mechanical sieve shaker (Figure 9C) located at the University of Zambia laboratory in Lusaka. The shaking duration was set for 10 minutes to ensure equilibrium, where the amount of soil retained on each sieve reached a constant value. After the shaking process, each sieve and the pan were carefully removed from the stack. The soil retained on each sieve and the soil collected in the pan were weighed accurately to the nearest gramme. These weights represented the amount of soil particles of different sizes retained by each sieve during the shaking process. Finally, all the sieves were carefully cleaned to remove any residues from previous tests that could potentially impact the accuracy of the results. This process followed the IS 460-1962 technique standard, allowing for reliable and consistent analysis of the particle size distribution in the soil samples.

Percentage retained on any sieve = (weight of soil retained / total weight) x 100
Cumulative percentage retained = sum of percentages retained on any sieve on all coarser sieves.

Percentage finer than any sieve retained.	= 100 percent minus cumulative Size, N Percentage

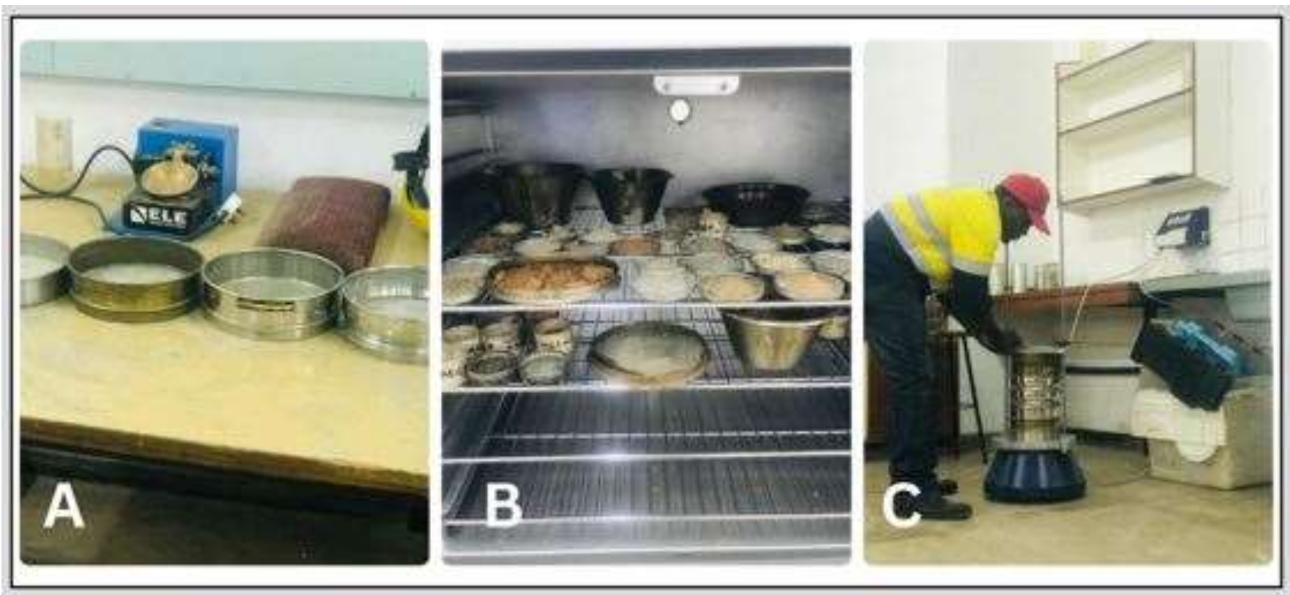

Figure 9: (A) Different Sieves sizes, Geology lab, Lusaka, Zambia; (B) Oven drying for 24 hrs at 105 ^{o}C; (C) Sieve shaker at the University of Zambia, Lusaka, Zambia

4.2.5 Soil Texture

In this study, soil texture was determined using a combination of qualitative and quantitative methods, including the texture by feel method and the Mason Jar Test (Satterfield, 2009). The soil classification based on textural analysis using the USDA triangle (2017) was conducted to determine the soil type of the samples (Chen et al., 2020) (Figure 10). The USDA triangle, as depicted in Figure 10, is a graphical representation that classifies soils based on their proportions of sand, silt and clay. After conducting the sieve analysis and determining the percentage of particles in each size range, the data were plotted on the USDA triangle to identify the soil type.

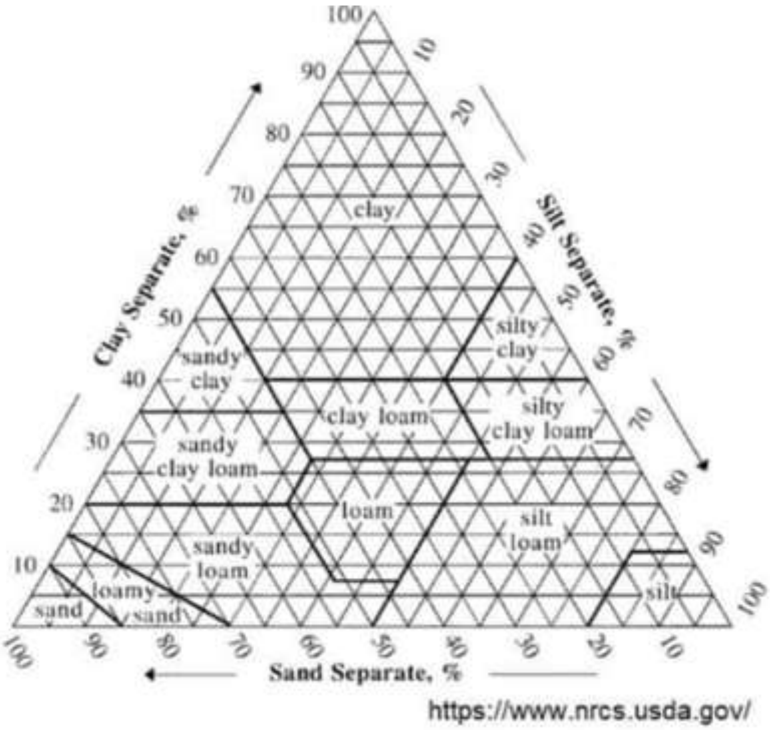

Figure 10: Soil Classification textural USDA triangle (2017), Lusaka, Zambia (Chen et al., 2020)

The Mason Jar Test for soil texture analysis began with the gathering of Mason glass jars, essential for soil particle settling (Figure 11A). Before conducting the Mason Jar Test for soil texture analysis, several materials were gathered, including a glass jar, a ruler, a black marker and granular dishwashing detergent. Prior to starting the test, the soil samples underwent a brief oven-drying process for 2 minutes at a controlled temperature to ensure proper drying and removal of excess moisture (Figure 11B). The initial step involved preparing the soil by sieving it over a bucket to break up particles and remove larger rocks, roots and organic matter, ensuring a more accurate analysis. To begin the test, a glass jar was selected and filled halfway with well-sifted soil. The finely sifted soil was carefully placed into the jar, filling it to approximately one-third of its capacity. The soil was then mixed with water and a small amount of dish soap. Subsequently, the test commenced with the vigorous shaking of the soil-water mixture in the Mason jars, a crucial step performed at the Geology laboratory in Lusaka, Zambia. After allowing the soil/water mixture to settle undisturbed for 48-72 hours, the sand, silt and clay particles separated and formed distinct horizons within the jar (Figure 11C). The proportions of each soil particle size fraction were then determined based on the heights of their respective layers within the settled mixture. The following steps were carried out to measure the layers:

1. After one minute of settling, the height of the sand layer was marked on the side of the jar using a black marker;
2. After two hours, the height of the silt layer was marked; and
3. Finally, after 2-3 days when the water became clear, indicating complete settling, the height of the clay layer was marked

Finally, USDA soil texture triangle was employed to determine the soil type based on the proportions of sand, silt and clay obtained. The pyramid from the USDA link aided in identifying the specific soil type based on the textural class determined by proportions of these three soil components (Schnably and Virginia, 2003).

Figure 11: (A) Gathering mason glass jars; (B) Oven drying for 2 minutes; (C) Allowing for settling of soils after vigorous shaking from Geology laboratory, Lusaka, Zambia

4.2.6 Geochemical Modelling

Computer simulations of speciation and saturation indices for mineral phases based on MINTEQ (described in chapter two) database (Postma, 2005) on four scenarios experiments were done using geochemical code PHREEQC-V3 (Parkhurst and Appelo, 2005) (Figure 12).

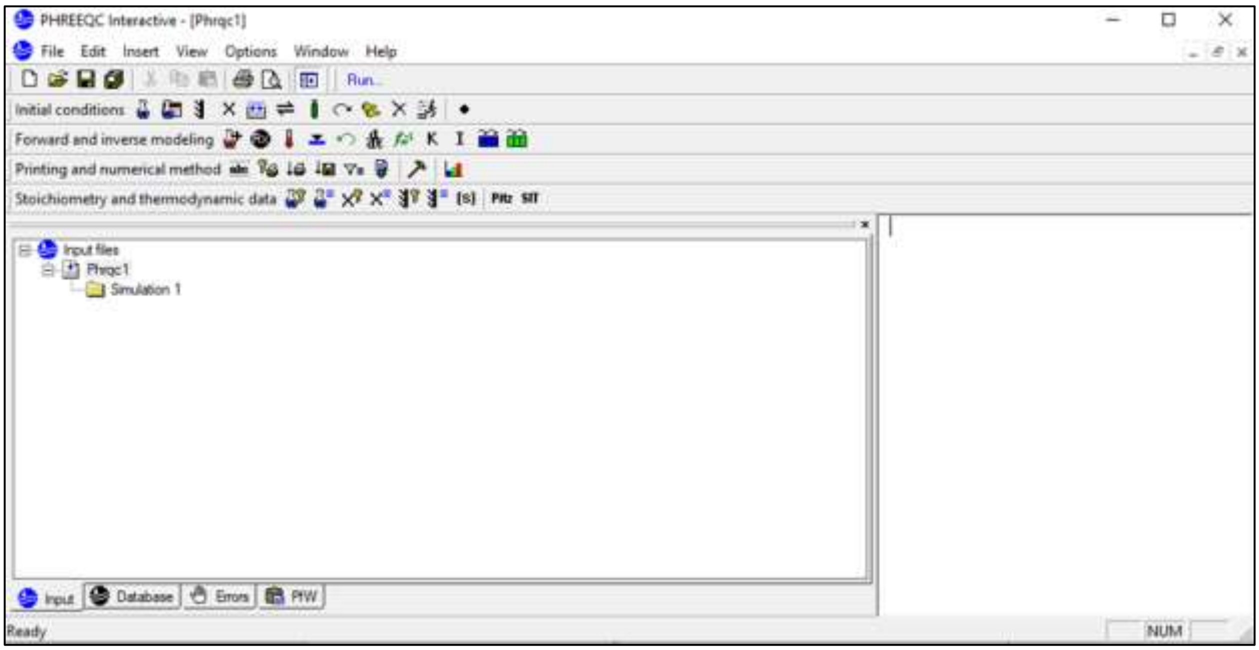

Figure 12: Represents the utilisation of the PHREEQC interactive interface for geochemical modelling and simulation, Lusaka, Zambia

These four experiments were conducted on samples from Uchi Tailing Dump. Thermodynamic data were taken from MINTEQ database (Postma, 2005). The following parameters were imported in the computer system of PHREEQC i.e. Eh (as pe), pH, Cu, Fe (total), Mn, Ca, Pb, Zn, Co and SO^{-2}. The pe (Eh) values employed in the PHREEQC tests were changed relative to those measured during sampling. The study employed four specific PHREEQC scenarios, including direct precipitation, evaporation, mixing with rainwater and mixing with stream water. These scenarios were used to investigate how the interaction between water accumulated on the surface of the tailings dumps and precipitation or dissolution of heavy metal-bearing phases affects the solubility of heavy metals. The results of the physiochemical and the PHREEQC tests employed were then used to provide a future scenarios and processes happening at Uchi Tailing Dump.

Tailing soil mixing with Stream water: In this scenario, PHREEQC was used to model the chemical reactions that occur when tailings' soil, which contains various minerals and contaminants from mining activities, mixes with stream water. This scenario defined the initial composition of the tailings' soil and the stream water and PHREEQC calculated the chemical changes that take place as they interact. This helped in understanding the potential release of dissolved species, metals and ions from the tailings' soil into the stream water and the resulting impact on water quality.

Tailing soil mixing with Rainwater: This case scenario involved simulating the interactions between tailings' soil and rainwater that infiltrates or percolates through the soil. By defining the initial compositions of both the tailings soil and rainwater, then used PHREEQC to predict how the rainwater's pH and chemical composition might have changed as it interacted with the soil. This helped in assessing the potential for acid generation, metal leaching and other geochemical reactions that could have occurred during rainwater-soil interactions.

Tailing soil undergoing Evaporation: In this scenario, PHREEQC was applied to model the evaporation of water from the surface of the tailing soil. As water evaporated, dissolved species and ions in the soil solution become more concentrated, potentially leading to the precipitation of certain minerals. By defining the initial composition of the tailings' soil and the environmental conditions, then used PHREEQC to understand how evaporation influences the geochemical processes and mineral transformations in the soil.

Tailing soil undergoing direct Precipitation: This case scenario involved studying the formation of minerals or solid phases directly from dissolved species within the soil solution. By defining the initial composition of the soil solution and the conditions under which precipitation occurred. PHREEQC then calculated the resulting speciation and distribution of aqueous species and solid phases formed as a consequence of direct precipitation. This allowed for insights into mineral formation and potential alterations to soil chemistry due to direct precipitation.

4.2.7 Statistical Analysis

In the analysis of 152 soil samples for characterisation, Excel 2016 was utilised as the primary tool. The data from the soil samples was inputted into an Excel worksheet, where each row represented a sample and each column represented different parameters such as pH, texture, elemental concentrations (Cu, Co, Fe, Pb, Zn), mineralogy and moisture content. To ensure accuracy and reliability, the data underwent a thorough cleaning process using Excel's data cleaning tools. This involved identifying and correcting errors, handling missing values and removing any outliers that could skew the analysis.

After the data cleaning process, basic descriptive statistics were calculated for each parameter. Excel functions such as AVERAGE, MEDIAN, STDEV, PERCENTILES and VAR.P were employed to compute essential statistical measures like mean, median, standard deviation and variance. These statistics provided a comprehensive overview of the central tendency, variability and distribution of the data. Scatter plots were used to explore relationships between variables, such as the correlation between elemental concentrations. Additionally, box plots were generated to illustrate the spread and variability of the data, particularly for parameters like mineralogy and texture.

4.3 Risk Assessment

To assess potential risks and evaluate the extent of heavy metal accumulation in the soil at Uchi Tailing Dump, an important soil index, the Geo-Accumulation Index (I-Geo) was utilised (Equation 3). This index helps determine whether the soil has been significantly impacted by anthropogenic activities such as mining and waste disposal, by comparing current heavy metal concentrations with pre-industrial levels. Firstly, the concentrations of elements of interest (Cu, Co, Fe, Ca, Mn, Zn) in the soil samples were determined using analytical methods AAS. Thereafter, reference values were set for the background concentrations of these elements in uncontaminated soils. In this case, the World Health Organization (WHO) standard limits were used as references. The Geo-Accumulation Index (I-Geo) was then calculated using Equation 3.

Geo-Accumulation Index (I-Geo):

$$\text{I-Geo} = \log_2 (C_e f / 1.5 \times B_e f) \qquad \text{Equation 3}$$

Where: I-Geo is the Geo-Accumulation Index, $C_e f$ is the concentration of the element of interest (e.g., heavy metal) in the soil sample, $B_e f$ is the background concentration of the same element, typically measured in the Earth's crust or uncontaminated soils (Saha et al., 2022)

The topsoil versus subsurface soil ratio was utilised to assess the extent and magnitude of contamination in the Uchi Tailing Dump area in Kitwe, Zambia. This method aimed to differentiate between natural (geogenic) and human-induced (anthropogenic) sources of element enrichment by comparing element concentrations in the topsoil (0-30 cm) to the deeper subsurface soil horizon (50-90 cm). To begin, thirty-two (32) soil samples were carefully collected from various points within the Uchi Tailing Dump area, targeting both the topsoil (0-30 cm depth) and the deeper subsurface soil (50-90 cm depth). This sampling strategy ensured a comprehensive representation of the dump's soil conditions. Upon collection, the soil samples underwent careful preparation. They were air-dried and sieved to remove any large debris or organic matter, ensuring uniformity in the samples and facilitating accurate analysis of element concentrations. Next, the concentrations of elements of interest (Cu, Co, Fe, Ca, Mn, and Zn) were determined in both the topsoil and subsurface soil samples by using AAS. This analytical process provided quantitative data on the presence and abundance of these elements in the soil samples. The last step in this method was the calculation of the top versus subsurface soil ratio for each sampling point. This calculation involved dividing the concentration of an element in the topsoil (0-30 cm) by the concentration of the same element in the deeper subsurface soil (50-90 cm). Each calculated ratio value represented the relative abundance of the element at different soil depths for every sampling point.

Lastly, the Coefficient of Industrial Contamination (Equation 4) (CIP) was computed for thirty-two soil samples to assess the areal extent of the surface soils contamination by elements arising from these tailings. The CIP was calculated by averaging the ratio of the concentrations of the elements (Cu, Co, Fe, Ca, Mn and Zn) measured to be more dominant at individual sampling sites, divided by the median value of the same elements in the whole Uchi Tailing Dump area. The six elements Cu, Co, Fe, Ca, Mn and Zn were selected for the computation of the CIP in the area using the formula from Kribek et al. (2010) (Equation 3).

$$\text{CIP} = \frac{1}{6}\left(\frac{Cu}{mCu} + \frac{Co}{mCo} + \frac{Fe}{mFe} + \frac{Ca}{mCa} + \frac{Mn}{mMn} + \frac{Zn}{mZn}\right) \ldots\ldots \text{Equation 4}$$

Where, mMe represents the median value of the individual element concentration.

CHAPTER FIVE: RESULTS, INTERPRETATION AND DISCUSSION

5.0 General Remarks

This chapter presents results, interpretation and discussions related to the three specific objectives outlined in chapter one.

5.1 The Chemical Characteristics of the Tailings at Uchi Tailing Dump, Kitwe, Zambia

This section presents and discusses the chemical characteristics of the tailings collected from Uchi Tailing Dump, Kitwe, Copperbelt Province. As mentioned in chapter four, the detailed results of all one hundred and fifty (152) samples analysed from Uchi Tailing Dump are presented in Appendices 1, 2, 3 and 4.

5.1.1 Abundance of Elements in the Tailings at Uchi Tailing Dump, Kitwe, Zambia

The study revealed that the elements Fe, Cu, Co, Mn and Ca are the most abundant in the topsoil of the Uchi Tailing Dump, Kitwe, Copperbelt Province. The abundance of these elements in topsoils is presented as box plots in Figures 13, 14 and 15. Detailed statistics including mean, median, percentiles, minimum and maximum values are presented in Tables 3, 4 and 5.

The presence of outliers in Iron (Fe) concentrations, ranging from 8193 to 13666 mg/kg, suggests potential anomalies or contamination in the soil (Figure 13). These elevated levels of Iron could pose environmental concerns, as excessive amounts of this element can affect soil health and ecosystem balance (Vítková et al., 2010). Additionally, the absence of outliers in copper (Cu), cobalt (Co), zinc (Zn), calcium (Ca) and manganese (Mn) indicates a more consistent distribution of these elements within the sampled soils. However, the lack of outliers does not necessarily indicate absence of environmental impact, as the median concentrations for copper (2418 mg/kg), cobalt (409 mg/kg) and zinc (15.10 mg/kg) are still notably high (Table 3).

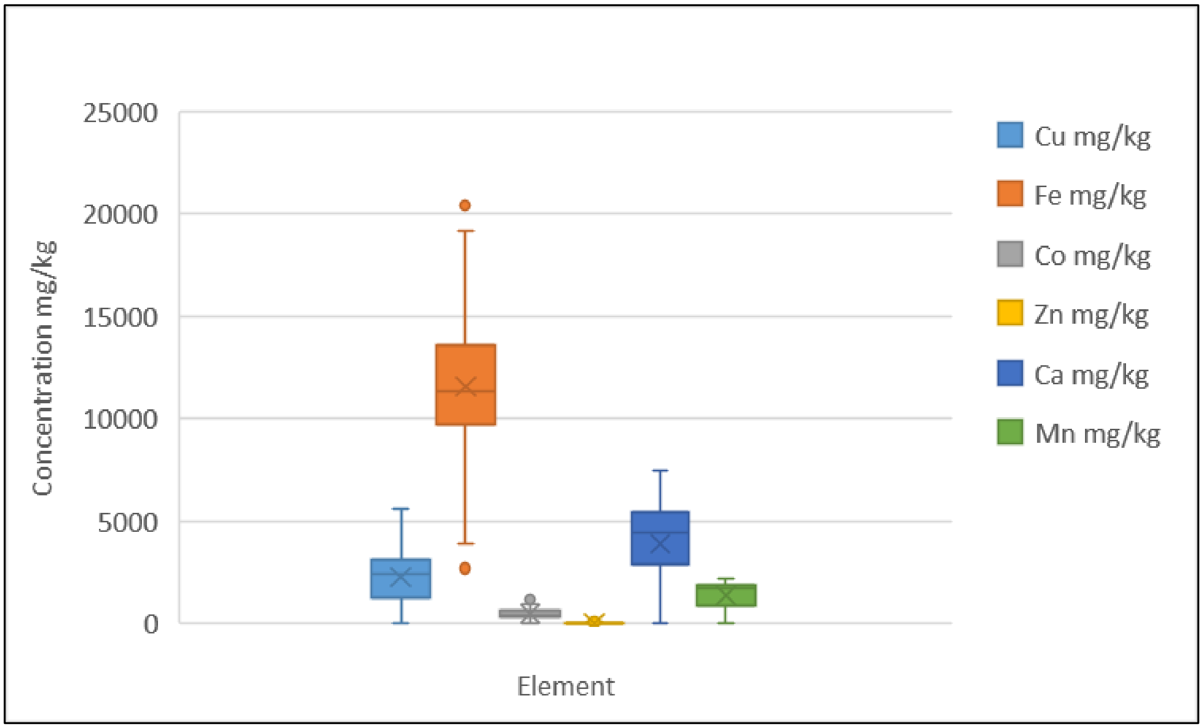

Figure 13: Abundance of elements showing the median and range of concentrations (mg/kg) in topsoils at Uchi Tailing Dump, Kitwe, Copperbelt Province during the dry season.

The analysis of soil samples from the Uchi Tailing Dump's vertical profile provides important insights into the concentrations of copper (Cu), cobalt (Co), iron (Fe), zinc (Zn), calcium (Ca) and manganese (Mn) (Figure 14). Copper shows a moderate concentration around 2692.93 mg/kg, with some samples exceeding 3835.97 mg/kg, indicating contamination (Wallingford, 2019). Similarly, cobalt has a median concentration of 487.95 mg/kg, with some samples going above 1034.42 mg/kg, suggesting potential localised contamination. The high concentration of iron at 10388.36 mg/kg, with samples reaching 16938.7 mg/kg, may be due to natural geological deposits or industrial sources. Zinc's median concentration is 13.38 mg/kg, but some samples go above 34.09 mg/kg, indicating localised higher levels. Calcium varies widely, with a median of 332.07 mg/kg and some samples reaching 8551.25 mg/kg, possibly due to geological factors. Lastly, manganese has a moderate median concentration of 1988.60 mg/kg, with localised areas showing higher levels. These elevated levels, particularly the outliers exceeding the median values, suggest localised contamination or natural variability. Such contamination could have adverse effects on soil health, ecosystem balance and possibly pose risks to human health and nearby water sources (Schnably and Virginia, 2003).

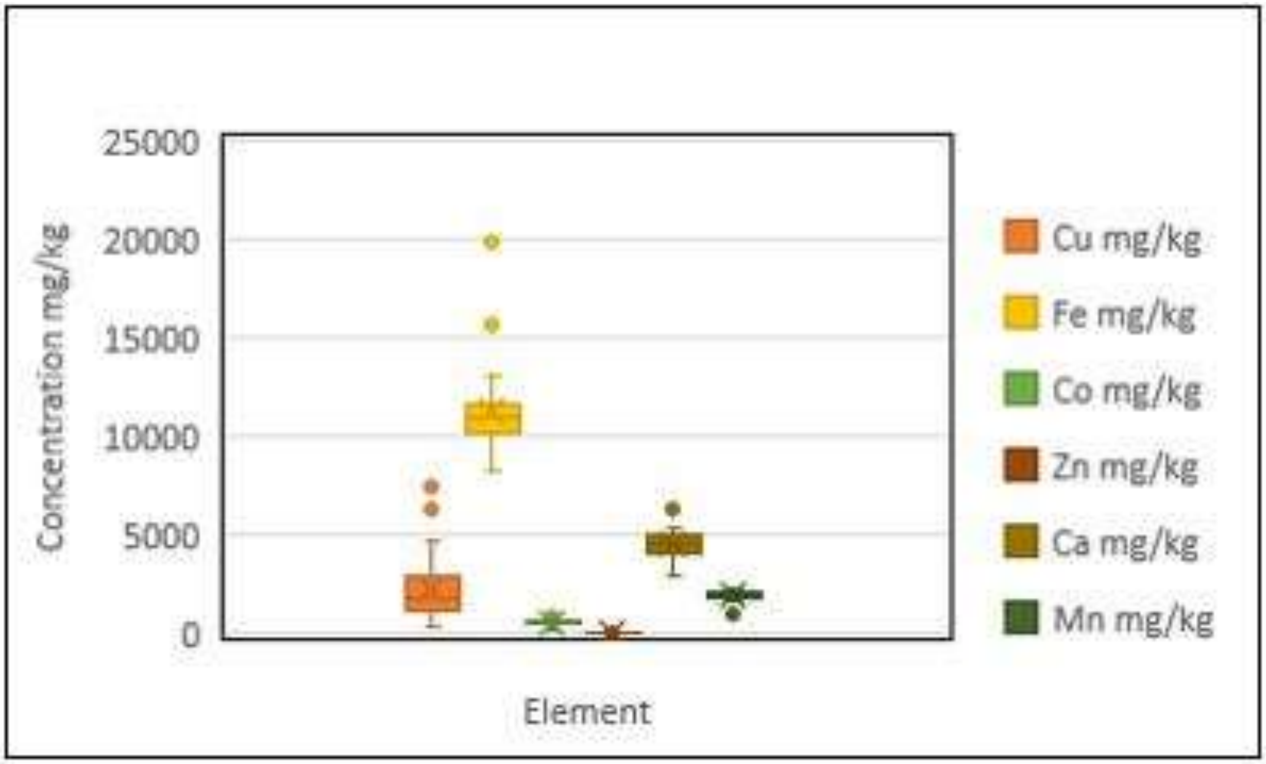

Figure 14: Abundance of elements showing the median and range of concentrations (mg/kg) in vertical profile soil at Uchi Tailing Dump, Kitwe, Copperbelt Province

The results of the concentrations of copper (Cu), cobalt (Co), iron (Fe), zinc (Zn), calcium (Ca), and manganese (Mn) from the Uchi Tailing Dump in the rainy season soil samples exhibited a broad range of values. Interpreting these data through a box and whisker plot revealed varying medians for each element where copper was approximately 1900 mg/kg, cobalt around 440 mg/kg, Iron at 9800 mg/kg, zinc near 10 mg/kg, calcium around 5200 mg/kg and manganese at about 2000 mg/kg (Figure 15). These medians show the central tendency of the dataset. Furthermore, the box plot illustrated the interquartile range (IQR) for each element, depicting the spread of the majority of data points. Notably, outliers are observed for elements such as iron, calcium and manganese, indicating potential localised areas of significantly higher concentration (Arunakumari et al., 2023). This visualization with the box and whisker plot effectively communicated the distribution and variability of these elements in the soil samples, indicating specific areas that require further remediation efforts.

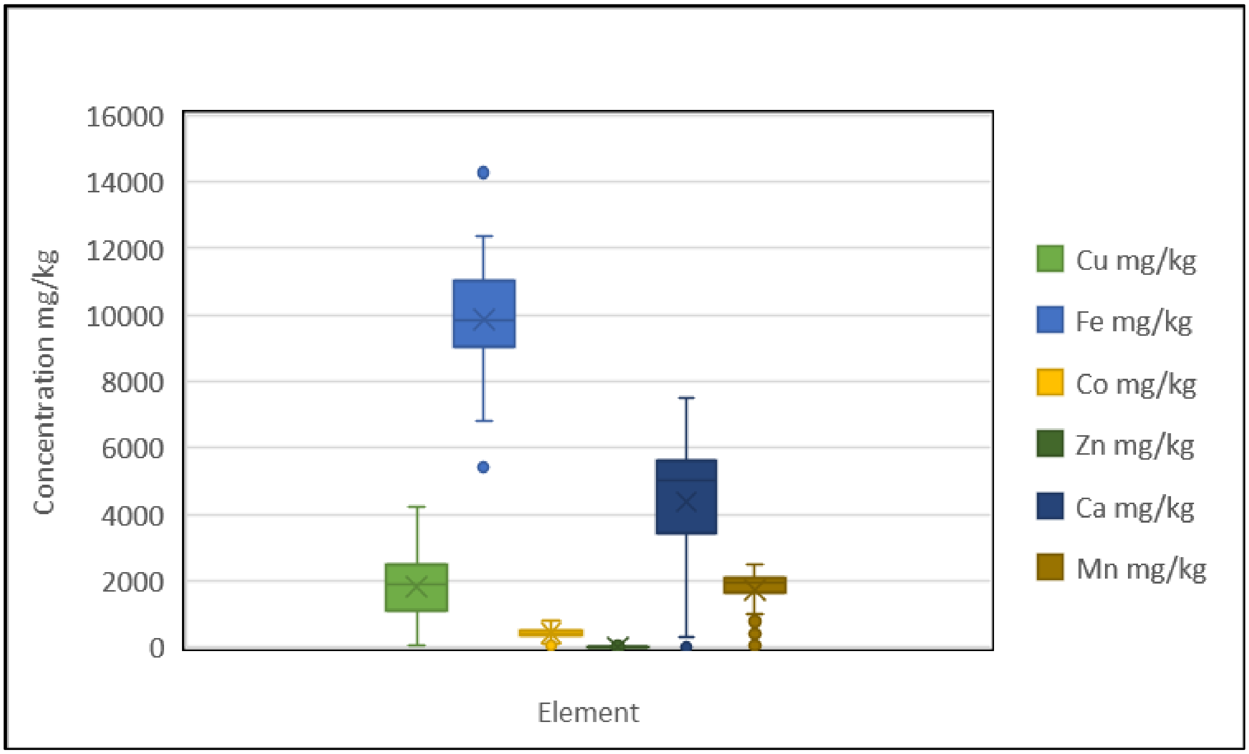

Figure 15: Abundance of elements showing the median and range of concentrations (mg/kg) in topsoils at Uchi Tailing Dump, Kitwe, Copperbelt Province during the rainy season

The presence of elevated levels of these elements, especially iron, calcium and manganese, indicate areas of contamination or natural geological deposits (Kříbek et al., 2011). These elevated concentrations have adverse effects on soil health, ecosystem balance and potentially pose risks to nearby water sources and human health (L. Norrgren et al., 2000). The outliers observed in the data also point to localised areas with significantly higher concentrations. The box and whisker plot allows for a comparison of the central tendency, variability and presence of outliers across the different sample points.

5.1.2 The Abundance of Elements in Tailings at Uchi Tailing Dump in the Dry Season (mid-August to mid-November)

The predominant elements in the topsoil of Uchi Tailing Dump were Fe, Cu, Co, Mn, Ca and Zn. Their median concentrations were 11300.85 mg/kg, 2418.61 mg/kg, 409.48 mg/kg, 1680.70 mg/kg, 4427.51 mg/kg and 21.16 mg/kg respectively (Table 3). These values represent the median concentrations, indicating the central tendency of the data. It is important to note that these values are specific to Uchi Tailing Dump during the mentioned dry season and may differ in other locations or time periods. For further information, such as specific sample numbers and data, as well as laboratory analytical detection limits for individual elements, they can be found in the Appendices. This dataset holds significance for a study or research project aimed at assessing the environmental impact of the tailing dump and its potential effects on the surrounding ecosystem.

The high median concentration of iron (Fe) at 11,300.85 mg/kg indicates a significant presence of this element. While iron is naturally occurring in soils, elevated levels suggest contamination from mining activities or the weathering of iron-bearing minerals (Bohdan et al., 2014). Similarly, the elevated median concentration of copper (Cu) at 2,418.61 mg/kg suggests a notable presence that could pose environmental concerns due to its toxicity to plants and animals at high levels (Ettler et al., 2022). In contrast, cobalt (Co) shows a relatively lower median concentration of 409.48 mg/kg compared to other elements. However, its presence could still be associated with certain mining activities, warranting attention depending on local regulations and environmental standards. The elevated median concentration of manganese (Mn) at 1,680.70 mg/kg indicates its significant presence. Manganese is essential for plant growth, but high levels can be toxic to both plants and animals (Sracek et al., 2010). Calcium (Ca) shows a high median concentration of 4,427.51 mg/kg, which is likely a natural occurrence (Kříbek et al., 2014). Calcium is a common element in soils and essential for plant nutrition (Schnably and Virginia, 2003). Finally, zinc (Zn) has a relatively low median concentration at 21.16 mg/kg compared to the other elements. Zinc is essential for plants, but high levels can be toxic, potentially affecting plant growth and ecosystem health (Dusengemungu et al., 2022). The interpretation of these results suggests soil composition at Uchi Tailing Dump are influenced by both natural factors and human activities. The presence of certain elements, particularly copper and manganese at elevated levels, raises concerns for potential environmental impacts.

The results of statistical distribution and abundance of elements in topsoil of the Uchi Tailing Dump, Kitwe, Copperbelt Province of Zambia during the dry season (Table 3). Table 3 displays the median, minimum, maximum and percentiles (25%, 50%, 75%, 90%, 95%, 99%). Percentiles shows a range from 1284.88 mg/kg (25th percentile) to 5392.85 mg/kg (99th percentile). In this case, copper concentrations differ significantly in the topsoil, with a median value indicating a notable presence. The range from minimum to maximum values suggests some areas have much higher copper levels, potentially posing environmental concerns (Ettler *et al.*, 2022). With cobalt Percentiles range from 295.62 mg/kg (25th percentile) to 1386.25 mg/kg (99th percentile). This shows that cobalt concentrations also vary, with the median value indicating a moderate presence. This range suggests different areas have varying levels, possibly influenced by localized factors.

Table 3: The statistical distribution and abundance of elements (mg/kg) in Topsoil of the Uchi Tailing Dump, Kitwe, Copperbelt Province Zambia during the Dry Season

Element	**Median**	**Minimum**	**Maximum**	**Percentiles (%)**					
				25	50	75	90	95	99
Cu	2418.61	14.23	5625.81	1284.88	2418.61	3063.80	3726.95	4084.73	5392.85
Co	409.48	6.05	1459.11	295.62	409.48	625.10	876.75	1217.79	1386.25
Fe	11300.85	2680.61	20421.76	9731.4	11300.8	13473.2	14832.7	16441.5	19369.0
Mn	1680.70	39.06	2218.62	897.08	1680.70	1875.84	2046.70	2117.16	2180.25
Ca	4427.51	2.09	7422.05	3041.13	4427.51	5437.53	5970.58	6313.89	7227.75
Zn	15.10	8.13	58.48	13.39	21.16	32.01	44.69	52.53	113.61

Iron with percentiles above shows a wide range of concentrations, with the median value indicating a significant presence. The variability suggests differing levels across the site which are influenced by natural geological formations or mining activities (Lweya et al., 2015). Manganese with above percentiles shows that concentrations vary, with the median value indicating a notable presence. This range suggests different areas within the dump may have varying manganese levels, potentially impacting plant and animal life (Dusengemungu et al., 2022).

The results from the element concentration analysis of the topsoil at Uchi Tailing Dump reveal significant implications for the environment and surrounding ecosystem. These elements, with copper showing a median concentration of 2418.61 mg/kg, iron at 11300.85 mg/kg, manganese at 1680.70 mg/kg and zinc at 15.10 mg/kg, could potentially disrupt soil ecosystems and affect plant growth and biodiversity (Vítková et al., 2011). High levels of copper and zinc, pose risks to human health if they leach into groundwater or contaminate crops grown in the area (Luo et al., 2006) The risk of water contamination is also a concern, as these elements might leach into nearby water bodies, affecting aquatic life and potentially impacting drinking water sources (Kříbek et al., 2011).

5.1.3 The Abundance of Elements in Tailings at Uchi Tailing Dump in the Rainy Season (mid-November to April)

The predominant elements Fe, Cu, Co, Mn, Ca and Zn in topsoil of Uchi Tailing Dump during the rainy season (mid-November to April) (Table 4). Their median concentrations were 9858.72 mg/kg, 1882.29 mg/kg, 423.34 mg/kg, 1941.83 mg/kg, 5013.80 mg/kg and 10.20 mg/kg respectively (Table 4). These concentrations provide an indication of the relative abundance of these elements in the topsoil of Uchi Tailing Dump during the specified rainy season. Among the predominant elements, iron shows high notable level although slightly lower than during the dry season, possibly due to increased leaching or dilution from higher moisture content (Wang, 2016). Copper remains notable at 1882.29 mg/kg, showing persistence from the dry season, raising concerns for environmental and human health (Mulenga, 2018). Cobalt maintains a median concentration of 423.34 mg/kg, suggesting ongoing sources of this element in the topsoil. Similarly, manganese exhibits a significant presence at 1941.83 mg/kg, with levels consistent with the dry season, indicating potential risks to soil and plant health (Baghdasaryan, 2016). Calcium remains abundant at 5013.80 mg/kg, although slightly lower than in the dry season, likely influenced by leaching or dilution (Sun et al., 2018). Zinc shows a relatively low median concentration of 10.20 mg/kg, consistent with the dry season, indicating a stable presence. Comparing these results to the dry season data, iron and calcium levels appear slightly lower during the rainy season, potentially due to increased leaching. However, copper, cobalt and manganese show similar or slightly higher concentrations, suggesting persistent contamination in the topsoil.

Table 4: The statistical distribution and abundance of elements (mg/kg) in Topsoil of the Uchi Tailing Dump, Kitwe, Copperbelt Province Zambia during the Rainy Season

Element	Median	Minimum	Maximum	Percentiles (%)					
				25	50	75	90	95	99
Cu	1882.29	55.08	4238.96	1144.75	1882.29	2391.21	3007.49	3118.81	3884.52
Co	423.34	71.10	779.12	346.30	423.34	507.79	567.09	593.90	714.31
Fe	9858.72	5401.21	14277.41	9088.47	9858.72	11032.44	11794.47	12274.91	13568.2
Mn	1941.83	69.37	2496.63	1671.62	1941.83	2085.65	2138.05	2195.03	2442.09
Ca	5013.80	23.56	7516.45	3708.31	5013.80	5610.73	6089.69	6958.11	7462.90
Zn	10.20	1.83	54.19	7.57	10.20	16.51	33.33	40.46	52.43

The table also shows several percentiles (25^{th}, 50^{th}, 75^{th}, 90^{th}, 95^{th} and 99^{th} percentiles). The analysis of percentiles in the concentrations of copper (Cu), cobalt (Co), iron (Fe), zinc (Zn), calcium (Ca) and manganese (Mn) from the Uchi Tailing Dump soil samples during the rainy season reveals how dataset was distributed. For the 25th percentile (Q1) indicates the lower range of concentrations, with copper (Cu) at 1144.75 mg/kg. The median (50th percentile Q2), for calcium (Ca) at 5610.73 mg/kg, signifies the middle value where 50% of the data points fall below and 50% above. Moving to the upper range, the 75th percentile (Q3) for iron (Fe) was at 11794.47 mg/kg, indicating concentrations above which 75% of the data points lie. Higher percentiles such as the 90th and 95th percentiles for cobalt (Co) revealed concentrations at 593.90 mg/kg and 714.31 mg/kg, respectively. These percentiles collectively aid in pinpointing areas requiring remediation efforts. Lower quartiles (Q1) highlight relatively less concerning areas, while upper quartiles (Q3) and higher percentiles point towards localized contamination hotspots

(Triantafyllidis, 2016). Particularly, the 99th percentile guides attention to outliers or exceptionally high concentrations that may pose environmental risks (Saha et al., 2022).

A line graph was used to compare the wet season (rainy season) with the dry season, showing how element concentrations changed across the seasons. The graph revealed that element concentrations were significantly higher during the dry season compared to the wet season (Figure 16).

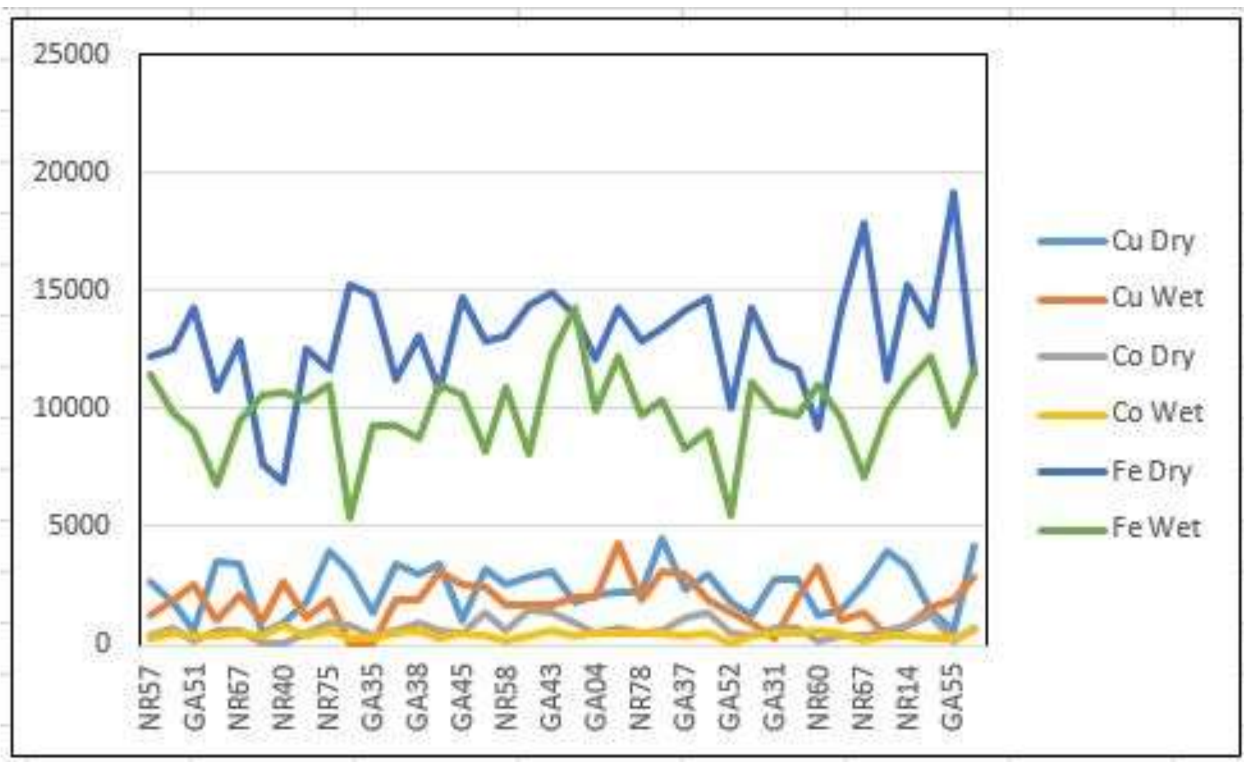

Figure 16: Comparison of elemental concentration by season, Uchi Tailing Dump, Kitwe, Zambia

5.1.4 The Elements Distribution in Tailings Soils at Uchi Tailing Dump on a Vertical Scale of One Meter

This section outlines the distribution of elements within a one-meter vertical profile of the tailings at Uchi Tailing Dump, Kitwe, Copperbelt Province, Zambia (Figure 17). The predominant elements observed in the subsurface soil of the dump were iron (Fe), copper (Cu), cobalt (Co), manganese (Mn), calcium (Ca) and zinc (Zn), with median concentrations of 11014.92 mg/kg, 1792.29 mg/kg, 542.83 mg/kg, 1949.33 mg/kg, 4540.26 mg/kg and 15.45 mg/kg, respectively (Table 5). These median concentrations represent the typical amounts of each element found at various depths within the one-meter profile of the tailings.

Figure 17: Vertical Profiling locations at Uchi Tailing Dump, Kitwe, Copperbelt Province, Zambia

Table 5: The statistical distribution and abundance of elements (mg/kg) in subsurface soil of the Uchi Tailing Dump, Kitwe, Copperbelt Province, Zambia

Element	**Median**	**Minimum**	**Maximum**	**Percentiles (%)**					
				25	50	75	90	95	99
Cu	1792.29	320.93	7492.32	1192.38	1792.29	2828.13	4416.16	5504.86	7150.33
Co	542.83	223.94	871.96	462.15	542.83	609.43	672.23	695.91	819.63

Fe	11014.92	8162.06	19876.03	10202.4	11014.9	11504.2	13099.7	15885.2	18735.9
Mn	1949.33	922.95	2260.07	1827.68	1949.33	2037.76	2148.94	2161.02	2239.29
Ca	4540.26	2888.35	6919.86	4180.66	4540.26	4930.13	5350.22	6327.18	6806.02
Zn	15.45	8.13	96.38	12.61	15.45	19.93	30.59	45.81	85.01

The high median concentrations of Iron and Calcium, exceeding 10,000 mg/kg and 4,500 mg/kg respectively, indicate their prevalence in the subsurface soil layers. Iron is a common element in soils and can be naturally occurring, but such elevated levels suggest contributions from mining activities or the weathering of iron-bearing minerals in the tailings (Sun *et al.*, 2018). Calcium, essential for plant nutrition and soil structure, is also abundant in the subsurface, which could have positive implications for plant growth (Ghose, 2004). On the other hand, copper and manganese also exhibit notable concentrations, with median values exceeding 1,700 mg/kg and 1,900 mg/kg respectively. These elements are essential micronutrients for plants, but at higher concentrations, they can pose risks to soil and ecosystem health (Ettler *et al.*, 2022). The moderate median concentration of Cobalt at 542.83 mg/kg suggests a presence that may be linked to mining activities, as cobalt can be associated with certain ores. In contrast, Zinc shows a relatively low median concentration of 15.45 mg/kg, indicating a lower presence compared to the other elements. While zinc is essential for plant growth, excessive levels can be harmful to soil organisms and aquatic life (Mwandira, 2015).

Table 5 above also shows several percentiles (25th, 50th, 75th, 90th, 95th and 99th percentiles) where Iron dominates the profile with a median concentration of 11014.92 mg/kg, indicating its prevalence in the subsurface layers. The wide range from 8162.06 mg/kg to 19876.03 mg/kg suggests variability, possibly from different depths or contamination sources. Copper (Cu) also shows significant presence with a median of 1792.29 mg/kg and a range from 320.93 mg/kg to 7492.32 mg/kg. Cobalt (Co) exhibits a moderate median of 542.83 mg/kg while manganese (Mn) shows a median of 1949.33 mg/kg, both with ranges reflecting variability across the profile. Calcium (Ca) stands out with a median of 4540.26 mg/kg, beneficial for soil fertility (Paramasivam and Anbazhagan, 2020) and Zinc (Zn) remains relatively low with a median of 15.45 mg/kg.

It was notably observed that the concentrations of most elements were higher in the subsurface levels compared to the topsoil at the Uchi Tailing Dump in Kitwe, Copperbelt Province, Zambia. This observation suggests that previous methods employed at the dump site were insufficient in removing all excess copper and vital elements, leading to their accumulation in the deeper layers of the tailings (Rs and Limited, 2012). The disparity in element concentrations between the subsurface and topsoil likely reflects the inefficiency of earlier technologies in adequately addressing the contamination.

The study of Uchi Tailing Dump, Kitwe, Copperbelt Province found peak element concentrations similar to those reported by Dusengemungu et al (2022). However, these concentrations exceeded the permissible limit set by the EPA, 2011. This signifies that the element levels in the area surpasses established environmental safety standards.

5.2 The Spatial Distribution of Metal Concentration in Tailings of Uchi Tailing Dump

The spatial distribution of elements within the tailings of the Uchi Tailing Dump were examined to understand how concentrations varied across the dump site. It was observed that certain elements were dispersed while others accumulated in specific areas within the tailings. Various sampling approaches can be employed to analyse the spatial distribution of elements; however, in this study, as outlined in Chapter 4, the interpolation technique was selected. Detailed descriptions of the distribution of the elements are provided.

5.2.1 Spatial Distribution of Heavy Metal Concentration for Cu and Co at Uchi Tailing Dump

Spatial distribution maps were generated for copper and cobalt concentrations across Uchi Tailing Dump, Kitwe, Copperbelt Province and are presented in Figure 18 and Figure 19, respectively.

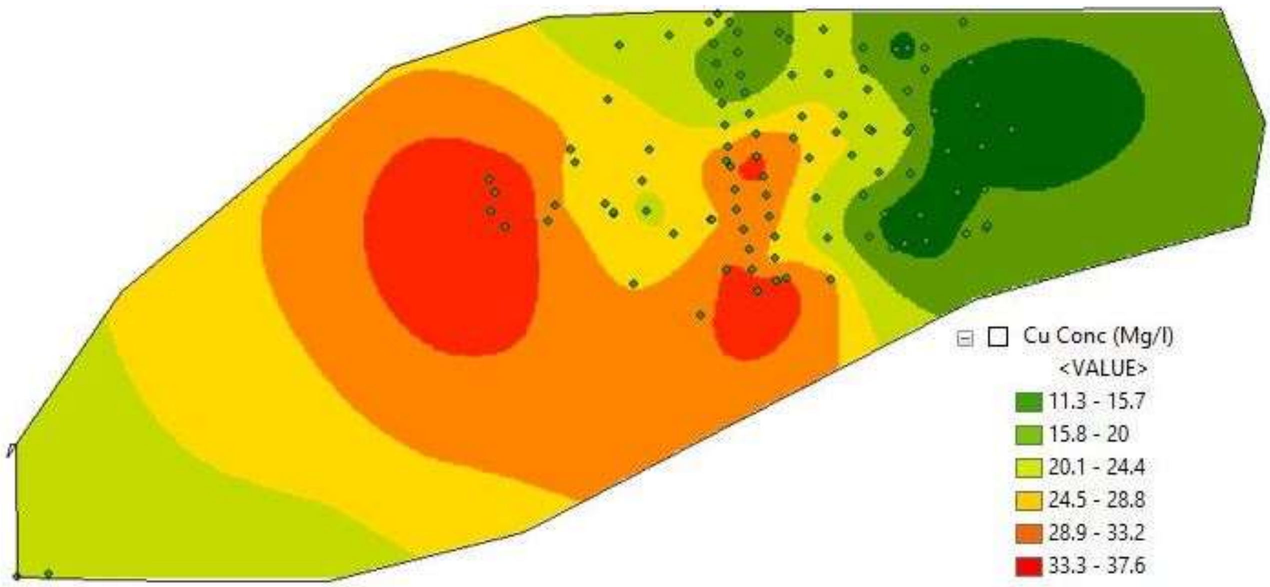

Figure 18: Spatial distribution of copper at Uchi Tailing Dump, Kitwe, Copperbelt Province

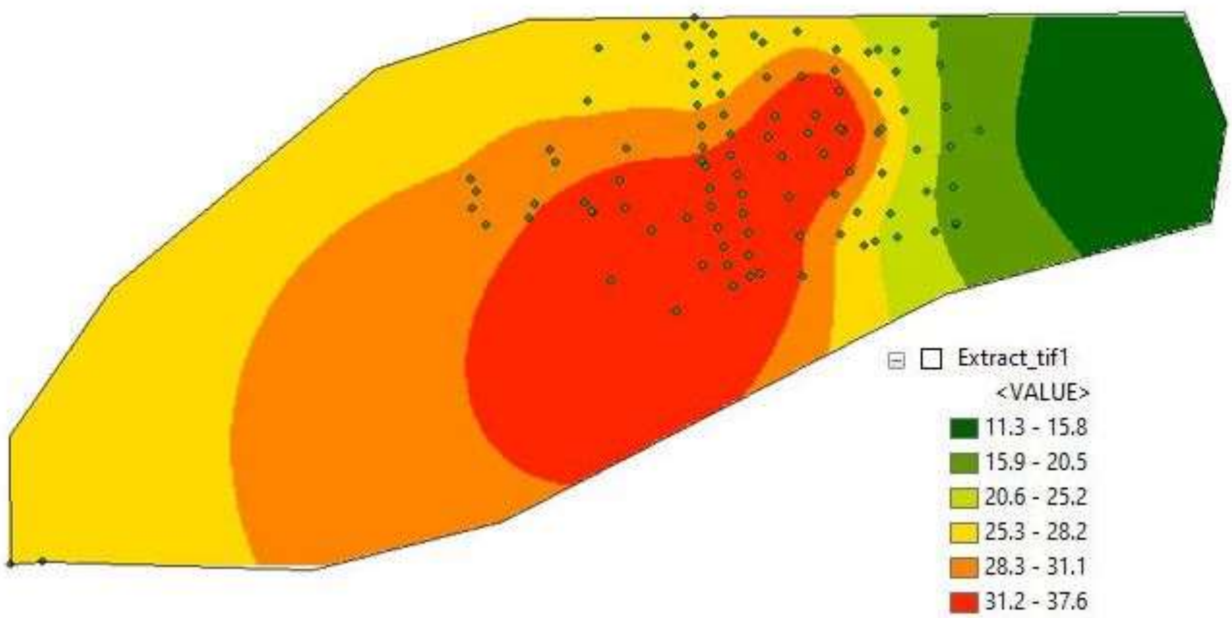

Figure 19: Spatial distribution of Cobalt at Uchi Tailing Dump, Kitwe, Copperbelt Province

The spatial distribution of copper (Cu) in the tailing soils of the surveyed Uchi Tailing Dump reveals a notable pattern of lower concentrations in the topsoils compared to the subsurface soils.

Specifically, during the dry season, Cu concentrations of about 1800 mg/kg were recorded in the topsoil samples, while in the rainy season, concentrations reached 2000 mg/kg. These findings are consistent with Trevor et al (2019), which investigated heavy metal distribution in soils near the Uchi Tailing Dump, including residential areas such as Nkana West and Wusakile and found significantly higher concentrations near active mining sites. However, this study focused specifically on the historical Uchi Tailing Dump, utilized by Nkana Mine in 2009 and identified unique features. These distinct patterns are attributed to the combined effects of water erosion and the dump's elevation (Banda et al., 2022). Water erosion is also responsible for the movement of heavy metals within the dump, influencing their distribution across the site (Gelena, 2018). Additionally, the dump's elevation could have contributed to the accumulation of certain elements in specific areas, thus explaining the observed spatial distribution of Cu within the tailings soils (Elaw, 2010). On the other hand, these differences could also be attributed to the use of improved metallurgical processes in the topsoil, which resulted in lower concentrations of copper and cobalt (Munanku et al., 2023). In contrast, the subsurface layers showed higher levels of these elements, due to the utilization of older, less efficient technologies. Furthermore, it is essential to consider the processes of dilution that the topsoil undergoes over time. This combination of dilution and erosion processes could explain the lower concentrations of copper and cobalt in the topsoil compared to the subsurface layers (Ngulube, 2016) further emphasizing the dynamic nature of elemental distribution in the tailings of Uchi Tailing Dump.

5.3 A Study to Characterise the Hydro-Geochemistry and Transport Patterns of Elements at Uchi Tailing Dump

The results of mineralogy and thin section analysis are as follows:

(a) Mineralogy

The mineralogy graphs present a visual representation showcasing the predominant minerals present in each sample (Figure 20 and Figure 21). The table also summarizes the XRD results for each sample, listing the phases detected along with their corresponding figures and descriptions from Appendix 1 (Table 6).

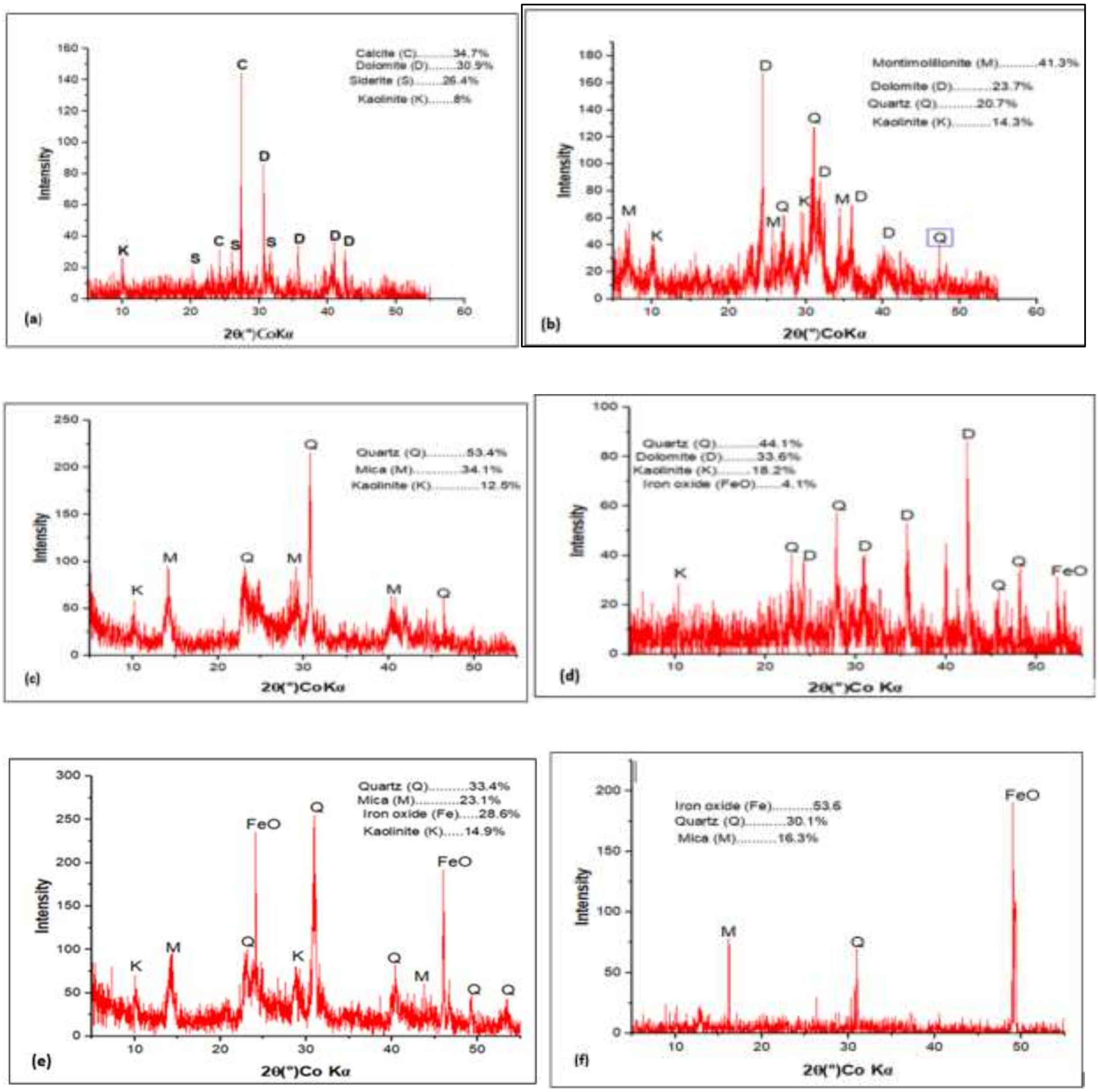

Figure 20: XRD graphs of sample: (a) GA31; (b) GA48; (c) GA55; (d) GA57; (e) NR60; and (f) NR63 at Uchi Tailing Dump, Kitwe, Copperbelt Province

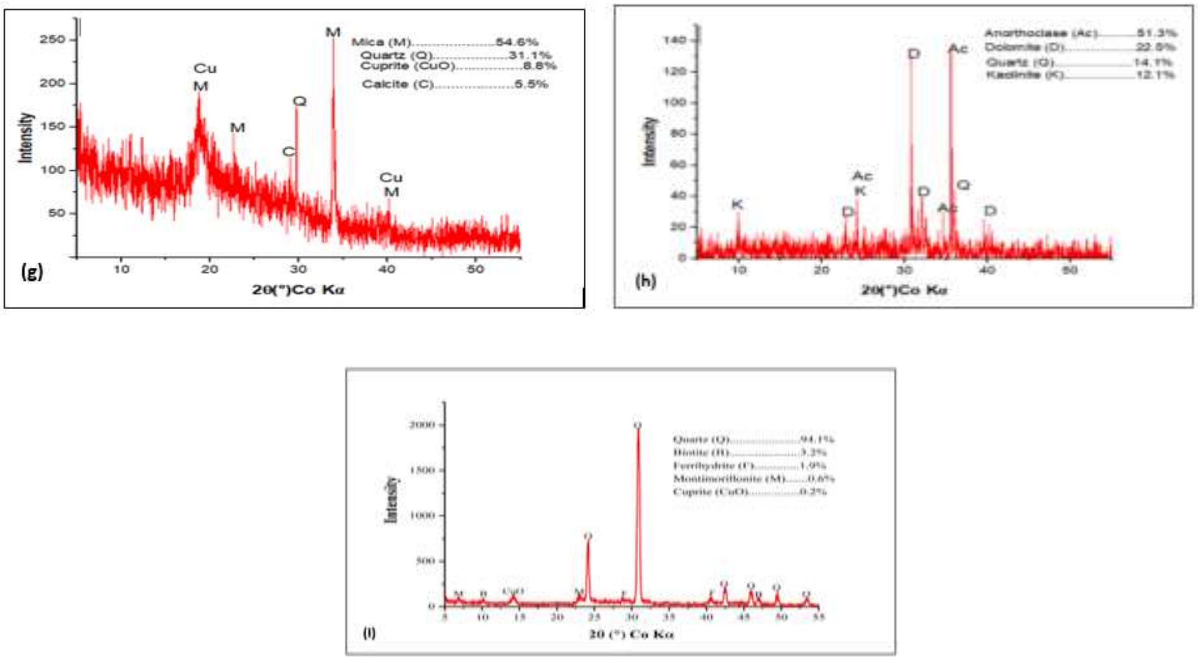

Figure 21: XRD graphs of sample: (g) OP20; (h) OP79; and (i) NR60 at Uchi Tailing Dump, Kitwe, Copperbelt Province

The XRD analysis of sample for mixing OP79 & NR60 to note the most dominant phases (Figure 22).

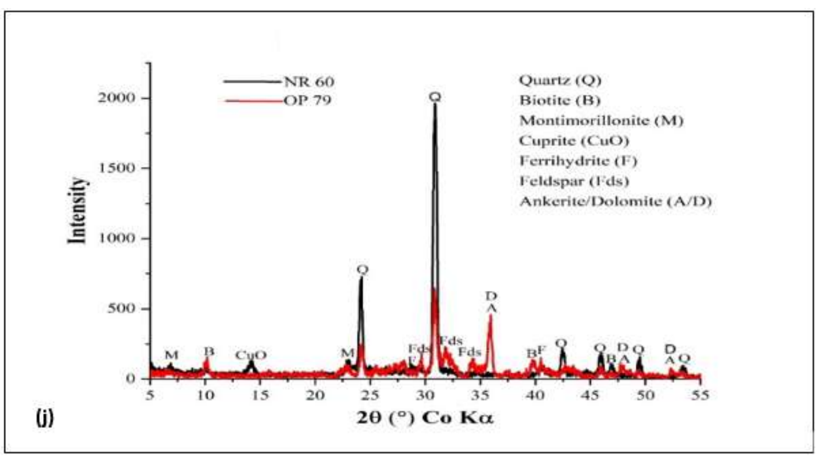

Figure 22: Mixing OP79 & NR60 to note the most dominant phases at Uchi Tailing Dump, Kitwe, Copperbelt Province

Table 6: Summarises the XRD results for each sample, listing the phases detected along with their corresponding figures and descriptions from Appendix 1 at Uchi Tailing Dump, Kitwe, Copperbelt Province

Sample	**Phases**	**Description**
NR60	Quartz, Biotite, Ferrihydrite, Montrimollinite, Cuprite	Appendix 1
OP79	Anorthoclase, Dolomite, Kaolinite, Quartz	Appendix 1
OP20	Mica, Quartz, Cuprite, Calcite	Appendix 1
NR63	Iron oxide, Quartz, Haematite	Appendix 1
NR64	Quartz, Mica, Iron oxide, Kaolinite	Appendix 1
NR57	Quartz, Dolomite, Kaolinite, Iron oxide	Appendix 1
GA55	Quartz, Mica, Kaolinite	Appendix 1
GA48	Montmorillonite, Quartz, Kaolinite, Dolomite	Appendix 1
GA31	Calcite, Dolomite, Siderite, Kaolinite	Appendix 1

A comprehensive mineralogical analysis of samples from Uchi Tailing Dump in Kitwe, Copperbelt Province, revealed the crystalline structure and material composition of the area. The mineralogy graphs present a visual representation showcasing the predominant minerals present in each sample. The results indicated a diverse range of minerals, including pyrite, chalcopyrite, quartz and calcite. Across various samples, the most predominant phases at the Uchi Tailing Dump were found to be quartz, kaolinite and dolomite, as revealed by XRD analysis. Pyrite and chalcopyrite are particularly notable, suggesting the presence of sulphide ores with potential economic significance (Haldar and Tišljar, 2013). Quartz and calcite are also prevalent, contributing to the overall mineralogical complexity of the site. The presence of pyrite and chalcopyrite, as evidenced by the mineralogy graphs, suggests the occurrence of sulphide ores within the dump (Aydinalp, 2020). These sulphide minerals are commonly associated with copper deposits, indicating the potential for significant copper mineralisation within the site (Nyambe et al., 2010). These finding aligns with the broader context of the Copperbelt Province, renowned for its copper-rich deposits. Moreover, the prevalence of quartz and calcite in the samples further enriches the mineralogical diversity of the site. Quartz is often associated with hydrothermal mineralisation, suggesting past hydrothermal activity in the region (Kříbek et al., 2010). Calcite, on the other hand, indicate post-depositional alteration processes, providing insights into the secondary mineralisation and alteration history of the site (Ettler et al., 2020).

From an economic standpoint, the identification of significant sulphide mineralisation, particularly pyrite and chalcopyrite, raises the possibility of economic mineral extraction. Chalcopyrite, in particular, is a primary copper ore mineral and its presence in the samples indicates the potential for copper recovery (Ettler et al., 2022). Pyrite, while not a direct source of copper, can be economically valuable for its sulphur content, which is essential in various industrial processes (Triantafyllidis et al., 2016).

(b) Thin Section Analysis

Thin sections were prepared from a selection of 25 samples out of the 152 samples at Uchi Tailing Dump. Microscopic analysis revealed that biotite, muscovite and quartz were dominant mineral phases identified (Figure 23).

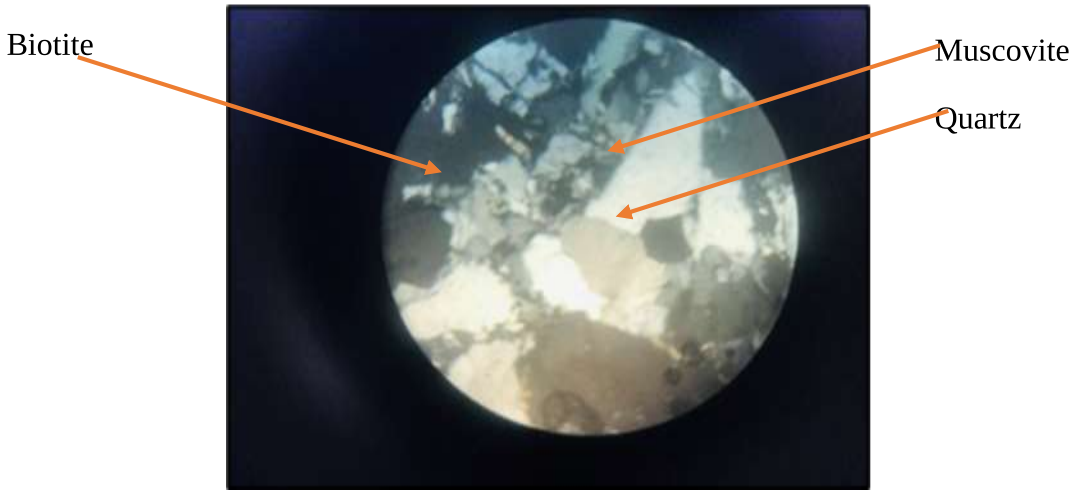

Figure 23: Thin section view of a soil showing biotite, muscovite and quartz at Uchi Tailing Dump, Kitwe, Copperbelt Province

The presence of minerals such as mica (biotite and muscovite) and quartz at the Uchi Tailing Dump does not indicate that metamorphism occurred at the site itself. Metamorphic processes typically take place at depths of 5–6 kilometres below the Earth's surface, far deeper than the shallow conditions at the dump (Kříbek et al., 2010). Instead, this mineralogical composition suggests that the source materials were likely extracted from underground environments where metamorphism had already occurred before mining. These materials were then transported and deposited at the Uchi Tailing Dump, reflecting their deeper origins rather than any metamorphic processes at the site (Peterson, 2022). The dominance of biotite, muscovite and quartz in the samples from Uchi Tailing Dump indicates several implications for the site. Firstly, the presence of these minerals suggests a metamorphic origin, hinting at the processes that have affected the rocks in the area (Arunakumari et al., 2023). Secondly, mica minerals like biotite and muscovite are known for their ability to retain metals such as copper, indicating the potential for mineralisation within the dump (Peterson, 2022). Quartz, being a common gangue mineral, suggests the presence of vein material or hydrothermal activity (Guimarães et al., 2011). Therefore, these results hint at the possibility of economic mineral deposits within the dump, making it an area of interest for further exploration and potential resource extraction.

5.4 Geochemical Modelling

Simulation results showing distinct saturation levels for mineral phases within the tailings, with cupric ferrite, cuprite and hematite indicating oversaturated conditions and high precipitation probabilities, while zincate and gypsum exhibit undersaturated conditions and low precipitation likelihood (Table 7).

Table 7: This table summarises the saturation values for various mineral phases within the tailings, Uchi Tailing Dump, Kitwe, Copperbelt Province

```
-----------------------------Saturation indices-----------------------------

  Phase               SI** log IAP   log K(298 K,   1 atm)

  Anhydrite          -4.82     -9.46   -4.64  CaSO4
  Antlerite          -1.57      6.72    8.29  Cu3(OH)4SO4
  Atacamite          -1.83      5.51    7.34  Cu2(OH)3Cl
  Bianchite          -8.34    -10.11   -1.76  ZnSO4:6H2O
  Brochantite        -1.10     14.24   15.34  Cu4(OH)6SO4
  Brucite           -10.77      6.02   16.79  Mg(OH)2
  Chalcanthite       -5.66     -8.30   -2.64  CuSO4:5H2O
  Cu(OH)2            -1.13      7.51    8.64  Cu(OH)2
  Cu2(OH)3NO3        -4.43      4.81    9.24  Cu2(OH)3NO3
  Cu2SO4            -12.34    -14.29   -1.95  Cu2SO4
  CuMetal             0.05     -8.71   -8.76  Cu
  CuOCuSO4          -12.32     -0.79   11.53  CuO:CuSO4
  CupricFerrite      10.72     16.60    5.88  CuFe2O4
  Cuprite             3.08      1.53   -1.55  Cu2O
  CuprousFerrite     14.23      5.31   -8.92  CuFeO2
  CuSO4             -11.31     -8.30    3.01  CuSO4
  Epsomite           -7.66     -9.80   -2.14  MgSO4:7H2O
  Fe(OH)2.7Cl0.3      4.73      1.69   -3.04  Fe(OH)2.7Cl0.3
  Fe2(SO4)3         -41.94    -38.36    3.58  Fe2(SO4)3
  Fe3(OH)8           -3.03     17.20   20.22  Fe3(OH)8
  Ferrihydrite       -0.35      4.54    4.89  Fe(OH)3
  Goethite            4.04      4.54    0.50  FeOOH
  Goslarite          -8.15    -10.11   -1.96  ZnSO4:7H2O
  Gypsum             -4.85     -9.46   -4.61  CaSO4:2H2O
  Halite             -9.71     -8.13    1.58  NaCl
  Hematite           13.10      9.09   -4.01  Fe2O3
  Jarosite-H         -5.90    -18.00  -12.10  (H3O)Fe3(SO4)2(OH)6
  Jarosite-Na        -5.41    -16.61  -11.20  NaFe3(SO4)2(OH)6
  Langite            -2.55     14.24   16.79  Cu4(OH)6SO4:H2O
```

Cont’ Table 7: This table summarises the saturation values for various mineral phases within the tailings, Uchi Tailing Dump, Kitwe, Copperbelt Province

Mirabilite	-11.93	-13.04	-1.11	Na2SO4:10H2O
Nantokite	-1.99	-8.75	-6.76	CuCl
O2(g)	-45.24	37.88	83.12	O2
Periclase	-15.49	6.02	21.51	MgO
Portlandite	-16.32	6.36	22.68	Ca(OH)2
Tenorite	-0.11	7.51	7.62	CuO
Thenardite	-12.86	-13.04	-0.18	Na2SO4
Zincite	-5.43	5.71	11.14	ZnO
Zincosite	-13.12	-10.11	3.01	ZnSO4
Zn(NO3)2:6H2O	-18.17	-14.73	3.44	Zn(NO3)2:6H2O
Zn(OH)2(A)	-6.74	5.71	12.45	Zn(OH)2
Zn(OH)2(B)	-6.04	5.71	11.75	Zn(OH)2
Zn(OH)2(C)	-6.49	5.71	12.20	Zn(OH)2
Zn(OH)2(E)	-5.79	5.71	11.50	Zn(OH)2
Zn(OH)2(G)	-6.00	5.71	11.71	Zn(OH)2
Zn2(OH)2SO4	-11.90	-4.40	7.50	Zn2(OH)2SO4
Zn2(OH)3Cl	-13.30	1.90	15.20	Zn2(OH)3Cl
Zn3O(SO4)2	-33.53	-14.51	19.02	Zn3O(SO4)2
Zn4(OH)6SO4	-21.38	7.02	28.40	Zn4(OH)6SO4
Zn5(OH)8Cl2	-28.99	9.51	38.50	Zn5(OH)8Cl2
ZnCl2	-20.35	-13.32	7.03	ZnCl2
ZnMetal	-38.99	-13.23	25.76	Zn
ZnO(Active)	-5.60	5.71	11.31	ZnO
ZnSO4:H2O	-9.54	-10.11	-0.57	ZnSO4:H2O

```
**For a gas, SI = log10(fugacity). Fugacity = pressure * phi / 1 atm.
  For ideal gases, phi = 1.

------------------
End of simulation.
```

The simulation results revealed distinct saturation levels for various mineral phases within the tailings. Cupric ferrite ($CuFe_2O_4$) exhibited a saturation of 10.72, indicating an oversaturated solution and a high probability of cupric ferrite precipitation. Cuprite (Cu_2O) was saturated at 3.08, suggesting a likelihood of cuprite formation due to oversaturation. In contrast, zincate ($ZnSO_4$: H_2O) showed a saturation of -9.54, indicating an undersaturated solution and a low probability of precipitation. Gypsum ($CaSO_4$:$_2H_2O$) displayed a saturation of -4.85, signifying an undersaturated condition and a low likelihood of gypsum precipitation. Hematite (Fe_2O_3) exhibited a high saturation value of 13.10, indicating an oversaturated solution and a significant likelihood of hematite precipitation. These findings provide valuable insights into the potential mineral phases and their precipitation behaviours, contributing to a better understanding of the geochemical processes within the tailings.

From the findings it was noted that Cupric ferrite aligns with research (Triantafyllidis et al., 2016) who also found similar saturation levels in their study of tailings from Kirki, Greece. The high levels of this implies that conditions within tailings are conducive for the formation of this phase. The other phase is the copper oxide which was found to be consistent with (Robbins, 2017) research on Gachsaran field. Copper oxide has implications for mobility of copper within the tailings and its potential to leach into the surrounding water sources (Trevor et al., 2019). Zincate had a negative value implying low probability of precipitation of Zinc. This contradicts with (Triantafyllidis et al., 2016) study work on similar tailings, where they found higher levels of zincate precipitation. The results suggest that zinc is unlikely to precipitate under the current conditions. However, simulations for cobalt could not be conducted due to limitations of the PHREEQC software, which lacks preloaded parameters for cobalt analysis.

The XRD analysis gave out mineralogical data into the solid phase composition of the tailings (Table 8 and 9). PHREEQC modelling complemented this by predicting chemical reactions and potential environmental impacts under various conditions (Table 8 and 9).

Table 8: XRD and PHREEQC results at Uchi Tailing Dump, Kitwe, Zambia

ID	XRD	PHREEQC
NR60	Quartz, Biotite, Ferrihydrite, Montrimollinite, Cuprite	Antlerite , Atacamite, Brochantite, Cuprite, CuprousFerrite, Ferrihydrite, Goethite, Hematite,Jarosite,Jarosite, Langite Lepidocrocite
OP79	Anorthoclase, Dolomite, Kaolinite, Quartz	Hematite, CuprousFerrite, Chalcopyrite
OP20	Mica, Quartz, Cuprite, Calcite	Mg-Ferrite, Gypsum, CuO
NR63	Iron oxide, Quartz, Haematite	goethite, quartz, siderite
NR64	Quartz, Mica, Iron oxide, Kaolinite	amorphous silica
NR57	Quartz, Dolomite, Kaolinite, Iron oxide	siderite,goethite, magnetite, gibbsite
GA55	Quartz, Mica, Kaolinite	Biotite, Muscovite, quartz, Kaolinite
GA48	Montmorillonite, Quartz, Kaolinite, Dolomite	Tenorite, Hematite, CuprousFerrite
GA31	Calcite, Dolomite, Siderite, Kaolinite	calcite, smectite, hematite, magnesite

Table 9: Summary of XRD and PHREEQC Results at Uchi Tailing Dump, Kitwe, Zambia

Method	Analysed Parameter	Key Findings
XRD Analysis	Mineralogical Composition	Identified minerals: Quartz, Dolomite, Kaolinite, Iron Oxides, Mica.
PHREEQC Modelling	Geochemical Processes and Stability	Predicted dissolution/precipitation reactions involving Calcite, Dolomite, Siderite, and Kaolinite.

5.5 Particle Size Distribution

The particle size distribution data (Table 10) reveals a gradation of particle sizes, with the finest particles passing through the smallest sieve openings (0.075 mm and Pan) and the largest particles retained on the largest sieve opening (4.75 mm) of the soil at the Uchi Tailing Dump. The majority of the soil mass consists of finer particles, as indicated by the higher mass percentages in the smaller sieve openings. The smallest sieve opening of 0.075 mm retained a significant portion of the soil mass at 76% followed by the 0.212 mm sieve with 8% of the mass. This dominance of finer particles, especially those passing through the 0.075 mm sieve, indicates a high potential for soil compaction and reduced permeability (Lemos et al., 2021). These fine particles contribute to soil compaction, making it less porous and more susceptible to waterlogging (Li et al., 2015). Additionally, the higher percentage of fine particles can affect the soil's nutrient and water holding capacity (Chileshe et al., 2020). While the majority of the soil mass consists of finer particles, the coarser particles retained on the larger sieves (4.75 mm) are also important. These coarser particles provide structural stability to the soil, preventing excessive compaction and aiding in drainage (Lemos et al., 2021). However, the relatively low percentage of these coarser particles suggests that their influence on soil stability may be limited.

Table 10: Showing particle size distribution calculation, Uchi Tailing Dump, Kitwe, Copperbelt Province

	Weight of Soil sample (grams)=	250					
ID: GA13	Sieve Opening (mm)	Mass of Sieve g	Total Mass g	Soil retained/each sieve g	% Mass Retained	Cummulative % mass retained	% Finer
	4.75	562.51	562.54	0.03	0.012003841	0.012003841	99.988
	2	422.37	426.02	3.65	1.46046735	1.472471191	98.52753
	1.18	546.45	548.71	2.26	0.904289373	2.376760563	97.62324
	0.43	494.14	496.68	2.54	1.016325224	3.393085787	96.60691
	0.212	308.1	327.99	19.89	7.958546735	11.35163252	88.64837
	0.075	349.11	540.11	191	76.42445583	87.77608835	12.22391
	Pan	412.62	443.17	30.55	12.22391165	100	0
Total				249.92	100		

The results showed the distribution of different particle sizes in the soil sample from Uchi Tailing Dump (Table 11). The majority of the soil consists of fine sand particles (0.075mm to 0.425mm), making up 84.38% of the sample. This was followed by fine material (<0.075mm) at 12.22%. Coarse sand (2mm to 4.75mm) and medium sand (0.425mm to 2mm) making up smaller portions at 1.46% and 1.92% respectively. Gravel (4.75mm to 75mm) was the least abundant, with only 0.01% of the sample. These results indicated that the soil was predominantly composed of fine sand, with smaller amounts of other particle sizes present.

Table 11: Particle Size Distribution analysis (using ASTM as described in chapter 2) at Uchi Tailing Dump, Kitwe, Copperbelt Province

Texture	**Sieve Size**	
Gravel	(4.75mm to 75mm)	0.012
Coarse sand	(2mm to 4.75mm)	1.460
Medium sand	(0.425mm to 2mm)	1.920
Fine sand	(0.075mm to 0.425mm)	84.380
Fine material	(<0.075mm)	12.220

The results of the particle size distribution analysis at Uchi Tailing Dump suggest a predominance of fine sand particles, comprising 84.38% of the sample. This indicates that the soil at the dump site is predominantly composed of fine-grained materials. This presence of fine sand have implications for the site's environmental characteristics, particularly in terms of permeability and water retention (Banahan and Byrne, 2019). Fine sand soils generally have good drainage properties but can also retain moisture, potentially influencing the movement of contaminants through the soil profile (Required and Karakurt, 2021). The relatively low percentages of coarse sand and gravel suggest limited porosity and permeability, which affect the leaching and movement of contaminants downwards (Wallingford, 2019). The presence of fine materials (<0.075mm) at 12.22% further adds to the potential for water retention and affect the mobility of contaminants in the soil.

In order to further analyse the soil at Uchi Tailing Dump, the particle diameter results were further graphically illustrated using semi-logarithmic plots known as particle distribution curves (Figure, 24 and Figure 25). In these plots, particle diameters were depicted on a logarithmic scale and the corresponding percent finer.

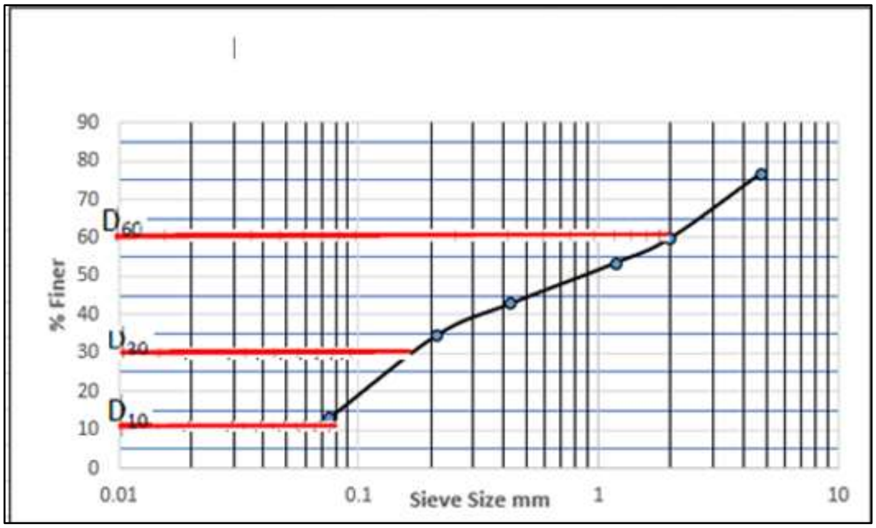

Figure 24: Particle size distribution curve showing D10, D30, and D60, Uchi Tailing Dump, Kitwe, Copperbelt Province

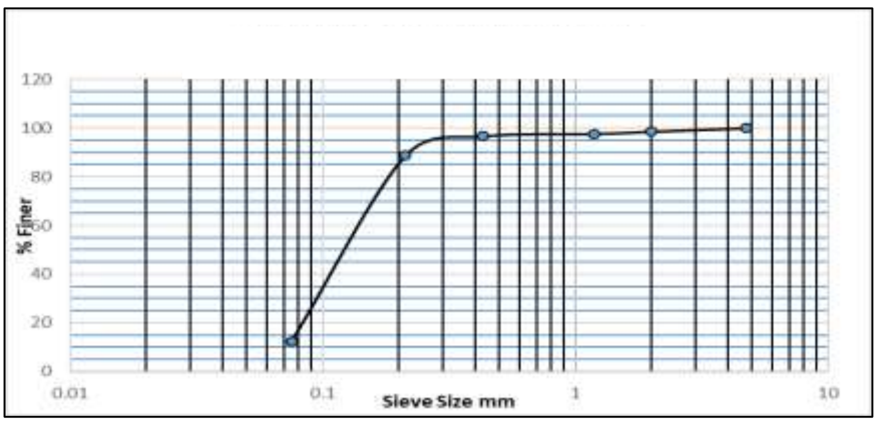

Figure 25: Particle size curve of finer vs sieve, Uchi Tailing Dump, Kitwe, Copperbelt Province

The particle size distribution at the Uchi Tailing Dump, as indicated by the samples, shows soil with a wide range of particle sizes. Each sample is characterized by its Coefficient of Uniformity (CU) and Coefficient of Curvature (CC) (Table 12).

Table 12: Showing the values of Coefficient of Curvature (CC) and Coefficient of Uniformity (CU) at Uchi Tailing Dump, Kitwe, Copperbelt Province

Sample	CC	CU
NR60	0.88	2.00
OP21	1.23	3.05
OP79	20.41	26.66
GA41	0.75	3.66
ER12	0.75	3.66

In this dataset, samples NR60, GA41 and ER12 exhibit CC values below 1.0, suggesting a poorly graded nature with varying particle sizes. Conversely, sample OP21 has a CC value of 1.23, indicating a relatively well-graded soil with a more even distribution of particle sizes. Sample OP79 stands out with a notably high CU value of 26.66, indicating a wide range of particle sizes and thus a poorly uniform soil composition. This suggests that the soil in sample OP79 has a significant difference in the sizes of particles present. These results shows that soils with a poorly graded nature may have reduced stability and compaction characteristics due to the varied sizes of particles (Required and Karakurt, 2021). Conversely, well-graded soils like sample OP21 offer better compaction properties and stability. The wide range of particle sizes in sample OP79, as indicated by the high CU value. This poses potential health risks, as fine particles in these soils can become airborne and pose respiratory hazards to individuals working or living nearby (Boss and Fredeen, 2000). This also raises concerns, particularly regarding soil erosion and runoff. Poorly uniform soils are more prone to erosion, potentially transporting pollutants and heavy metals into nearby water bodies, thus impacting aquatic ecosystems and water quality (Paramasivam and Anbazhagan, 2020). This uneven distribution of particle sizes also affects soil permeability, potentially leading to groundwater contamination.

5.6 Geo-Accumulation Index

The results for Geo-Accumulation are presented which also includes a summary statistics table for elements concentration alongside their permissible values according to the World Health Organization (WHO) (Table 13). These permissible values were utilised to calculate the Geo-Accumulation results (Figure 26). The Geo-Accumulation table provides a structured overview of the degree of element accumulation at the site, with the WHO standards to assess potential environmental impacts.

Table 13: Summary Statistics for Heavy Metal Concentration and Permissible values for Soils are according to the World Health Organization Kitwe, Copperbelt Province

Element	**No. of Samples**	**Mean (mg/Kg)**	**WHO Standards (mg/Kg)**
Iron Fe	152	11101.99	5000
Copper Cu	152	2112.44	30
Cobalt Co	152	443.75	50
Zinc Zn	152	22.23	50

These results are visually represented in the accompanying bar graph, where the height of each bar corresponds to the Igeo value and the labels indicate the classification of contamination for each metal (Figure 26).

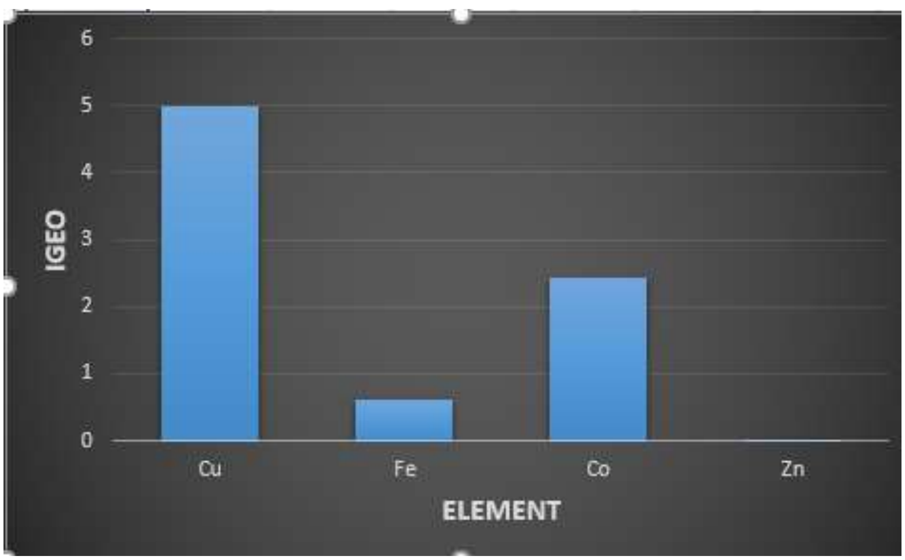

Figure 26: The bar graph visually represents the geo-accumulation results at the Uchi Tailing Dump, Kitwe, Copperbelt Province

The geo-accumulation results revealed significant differences in the contamination levels of copper (Cu), cobalt (Co), iron (Fe) and zinc (Zn) in the soil. Copper showed a high Igeo value of 5.00, classifying it as heavily contaminated (Guimarães et al., 2011). This indicated a substantial elevation in copper concentration above background levels, signifying a severe impact of copper pollution in the area. With such high levels of copper, pollution have detrimental effects on the ecosystem, including soil quality degradation and potential harm to plants and aquatic life in nearby water bodies (Saha et al., 2022). Cobalt, with an Igeo value of 2.44, was classified as moderately contaminated, suggesting an elevated but less severe contamination compared to copper (Dusengemungu et al., 2022). While moderately elevated cobalt levels are not as critical as copper, their presence does not raise immediate concerns. However, it is important to note that cobalt can have adverse effects on both human health and the environment if present in excessive amounts. Iron, on the other hand, showed an Igeo value of 0.6, indicating an uncontaminated status, where the concentration is similar to or slightly above background levels, posing no significant contamination concerns. Lastly, Zinc has an Igeo value of less than 1, indicating it is uncontaminated or "Practically No Accumulation." This suggests the zinc concentration is likely close to or below the background level, showing no significant contamination in the area.

The study reveals that the soil in the Uchi Tailing Dump area is contaminated with copper (Cu), iron (Fe) and cobalt (Co), as indicated by the geo-accumulation index. These findings align with previous studies by Dusengemungu et al. (2022) and Trevor et al. (2019), which also reported contamination of copper and cobalt in both the Uchi Tailing Dump and nearby residential areas. The presence of these pollutants, likely originating from natural processes such as rock weathering in the region, raises concern. Furthermore, the dumping of mine deposits from various mines around Zambia at the Uchi Tailing Dump, referred to as the site for mine waste materials, further contributed to the accumulation of these elements in the soil. This discussion highlights the persistent pollution in the area and emphasizes the need for mitigation measures to address the environmental impact of mining activities on soil quality and nearby communities.

CHAPTER SIX: CONCLUSION AND RECOMMENDATION

The conclusions derived from the study and recommendations are presented in this chapter in a summarised form.

6.1 Conclusion

The study conducted at the Uchi Tailing Dump in Kitwe, Copperbelt Province yielded several important conclusions. Firstly, it was found that the tailings at the dump contained elevated levels of copper (0.56%), cobalt (0.15%), iron (2.0%) and calcium (7.5%), with copper and cobalt being particularly high. Elevated copper levels in mined deposits is also attributed to the utilisation of outdated mining technologies. These methods lacked efficiency, which resulted in a higher concentration of copper within the extracted materials. The spatial distribution analysis revealed distinct patterns, with copper levels highest in the northwest and cobalt concentrations elevated in the northeast. Both the topsoil and subsurface samples taken from within the dump exhibited contamination, pointing towards anthropogenic influences. Further characterisation identified cuprite as a source of high copper content and iron oxide as the primary source of elevated iron levels. The most predominant phases at the Uchi Tailing Dump, as revealed by XRD analysis across various samples, include quartz, kaolinite and dolomite. The study also highlighted the role of montmorillonite minerals in maintaining pH stability and slowing element movement. Additionally, the high calcium content was attributed to calcite. The simulation results from PHREEQC revealed distinct saturation levels for various mineral phases within the tailings, with cupric ferrite ($CuFe_2O_4$) at 10.72, cuprite (Cu_2O) at 3.08, zincate ($ZnSO_4$: H2O) at -9.54, gypsum ($CaSO_4$: $2H_2O$) at -4.85 and hematite (Fe_2O_3) at 13.10. Particle size distribution analysis showed wide variations and a predominant fine sand texture (86%). The Geo-Accumulation Index (Igeo) and Coefficient of Industrial Pollution (CIP) confirmed contamination, particularly in copper (Igeo=5), cobalt (Igeo=2.5), iron (Igeo=0.5) and zinc (Igeo<0). Dust emissions, acid mine drainage, soil degradation and a reduction in biodiversity in the Uchi Stream are significant hazards associated with the Uchi Tailing Dump. In summary, the study underscores the significant pollution and environmental risks associated with the Uchi Tailing Dump, emphasizing the need for ongoing monitoring and remediation efforts to protect the ecosystem and community health in the area.

6.2 Recommendation

Based on the conclusions of this study, the following recommendations are made for Water experts in the Government, Private Sector, Non-Governmental Organization and academic and research institutions:

(i) There is a need for Zambia Environmental Management Agency (ZEMA) to set up an environmental monitoring system around the Uchi Tailing Dump and nearby areas. This will help to keep track of any changes in the environment over time. Monitoring regularly is important to ensure the safety of the environment and the people living nearby. By doing this, ZEMA can make sure that any potential risks from contamination are identified early, allowing for prompt action to protect the environment and the health of the local communities;

(ii) It's important for the Water Resources Management Authority (WARMA) to set up a continuous monitoring system for the groundwater near the Uchi Tailing Dump. This will help keep track of the quality of the water, especially with more activities happening in the area. Groundwater is essential for communities, so checking its quality regularly is important to make sure it's safe to use. By doing this, WARMA can quickly spot any problems with contamination and take action to protect the water and the people who rely on it;

(iii) The academic and research institutions such as the University of Zambia to consider conducting future research on:

- Sulphur concentration and total sulphur in the samples to gain a comprehensive understanding of the processes involved;
- Developing a sealing system specifically designed to prevent erosion and infiltration effects in tailings dumps and there should be a concentrated effort towards chemical improvements in tailings mud, aiming to limit the dissolution of pollutants. Continuous research and experimentation in these areas will contribute significantly to sustainable mining practices and environmental conservation efforts;
- How copper and cobalt minerals are deposited in the area. There is need to study this to understand the genetic model behind their formation; and

- Ecotoxicology assessments, may be warranted to understand how these metal concentrations affect local wildlife and ecosystems. Monitoring of plants, animals and aquatic life in the vicinity can provide insights into the direct impacts of these metals on various species.

(iv) The Government of Zambia should prioritise implementing restoration projects to rehabilitate Uchi Tailing Dump. These projects should involve reforestation efforts to restore vegetation cover, erosion control measures to prevent soil erosion and the establishment of containment areas to prevent pollution; and

(v) It is essential to communicate these findings to local communities to raise awareness about potential risks.

Based on the characterisation results, several restoration measures can be applied. Copper can be economically extracted using flotation followed by smelting, as the analysis confirms it exists in sulphide mineral form. Since copper is found in oxide form, heap leaching is also another suitable method, as indicated by the XRD and PHREEQC results. Additionally, bioleaching can be used, where bacteria like Acidithiobacillus Ferrooxidans oxidize copper sulphides, releasing soluble copper ions for recovery. These approaches ensure effective copper extraction based on its mineral form.

REFERENCES

Adebimpe, R. A., & Fatoye, A. O. (2021). Characterisation of Tailings from Itakpe Iron Ore Mine, Itakpe, Nigeria. 4, https://doi.org/10.18052/www.scipress.com/SGG.4.1, pp. 1-8.

Aluvihara, S. and Kalpage, C. S. (2020). 'Particle Size Analysis of Different Clay Types and Investigation of their Important Characteristics', Saudi Journal of Engineering and Technology, 05(04), pp. 163–172. https:doi.org/10.36348/sjet.2020.v05i04.006.

Arunakumari, K. et al. (2023). 'Persistence of heavy metals and human health risk assessment in the South Indian industrial area', Aqua, 72, pp. 1-15 https:doi.org/10.2166/aqua.2023.210.

Astm D6913-04R2009 (2004). 'Standard Test Methods for Particle-Size Distribution (Gradation) of Soils Using Sieve Analysis', ASTM International, West Conshohocken, PA, 04 (Reapproved 2009), pp. 1–35. https:doi.org/10.1520/D6913-17.1.6.

Bernhard W. (2010). Atomic Absorption Spectrophotometry, Theory and Technique. Handbook of Exploration Geochemistry, 1(C), pp. 109–138.

Aydinalp, C. (2021). 'An Introduction to Mineralogy', Africanza Report, pp. 78-96.

Baghdasaryan, T. (2016). Master ´ s thesis Assessment of the environmental impact of tailings in the Republic of Armenia Evaluation del impact Ambiental de sombreros de Tatevik Baghdasaryan. May, pp. 44-59.

Baieta, R., Mihaljevič, M., Ettler, V., Vaněk, A., Penížek, V., Trubač, J., Kříbek, B., Ježek, J., Svoboda, M., Sracek, O., & Nyambe, I. (2021). Depicting the historical pollution in a Pb–Zn mining/smelting site in Kabwe (Zambia) using tree rings. Journal of African Earth Sciences, (May). https://doi.org/10.1016/j.jafrearsci.2021.104246, pp. 150-181.

Bailey, M. (2021). Climate Profiles of Countries in Southern Africa: Zambia. 2021, Climate Centre, pp. 145-189.

Banahan, S. and Byrne, D. (2019). 'Methods of Particle Size Determination – A Review (2019)', Innopharma technology, pp. 1–25. Available at: https://www.innopharmatechnology.com/docs/default-source/eyecon2-whitepapers/methods-of-particle-size-determination.pdf.

Banda, A. M. et al. (2022). ‘Assessment of land use change in the wetland of Barotse Floodplain, Zambezi River Sub-Basin, Zambia’, Natural Hazards, (0123456789). https:doi.org/10.1007/s11069-022-05589-0.

Bohdan, K. et al. (2014). ‘Contamination of soils with dust fallout from the tailings dam at the Rosh Pinah area , Namibia : Regional assessment , dust dispersion modeling and environmental consequences’, 144, pp. 391–408.

Bohdan, K., Majer, V., & Nyambe, I. (2010). Discrimination of lithogenic and anthropogenic sources of metals and sulphur in soils of the central-northern part of the Zambian Copperbelt Mining District: A topsoil vs subsurface soil concept. https://doi.org/10.1016/j.gexplo.2009.12.005, pp. 104, 69–86.

Boss, C. B., & Fredeen, K. J. (2000). Concepts, Instrumentation and Techniques in Atomic Absorption Spectrophotometry. Journal of Analytical Sciences, pp. 2–12.

Câmara, G. et al. (2022). ‘Spatial Analysis and GIS : A Primer’, pp. 1–30.

Central Statistical Office. (2015). Zambia 2015 Living conditions monitoring survey key findings. Zambia Country Statistics, Government Republic of Zambia GRZ, pp. 14-22.

Chen, L., Jin, X., Chen, H., He, Z., & Qiu, L. (2020). Grain Size Distribution and Clay Mineral. Distinction of Rare Earth Ore through Different Methods, pp. 1–27.

Chileshe, M. N. et al. (2020). ‘Physico-chemical characteristics and heavy metal concentrations of copper mine wastes in Zambia: implications for pollution risk and restoration’, Journal of Forestry Research, 31(4), pp. 1283–1293. https:doi.org/10.1007/s11676-019-00921-0.

Coleman, A. Moustafa, E. (2022). Africa Report. African Export-Import Bank 72(B): research (Stellenbosch University), PP. 6-35.

Cook, N. J. (2000). ‘Mineral characterisation of industrial mineral deposits at the Geological Survey of Norway: a short introduction’, Ngu-Bull, 436, pp. 2000–189. Available at: http://www.ngu.no/filearchive/102/Bulletin436_19.pdf.

Daniels, W. L., & Galbraith, J. (2004). Mine soil morphology and properties in pre and post smcra coal mine soil morphology and properties in pre- and post-June 2004.

https://doi.org/10.21000/JASMR04010421, pp. 105-156.

Duarte, L. et al. (2020). 'A GIS open source application to perform the spatial distribution of prevention quality indicators (PQIs)', GISTAM 2020 - Proceedings of the 6th International Conference on Geographical Information Systems Theory, Applications and Management, (Gistam), pp. 129–134. https:doi.org/10.5220/0009805801290134.

Dusengemungu, L., Mubemba, B., & Gwanama, C. (2022). Evaluation of heavy metal contamination in copper mine tailing soils of Kitwe and Mufulira, Zambia, for reclamation prospects. Scientific Reports, 12(1). https://doi.org/10.1038/s41598-022-15458-2, pp. 1–16.

Elaw. (2010). Chapter 1: Overview of Mining and Its Impact. Guide for Evaluating Mining Projects EIAs. https://www.elaw.org/files/mining-eia-guidebook/Chapter1.pdf, pp. 122.

Ettler, V., Mihaljevič, M., Kříbek, B., Majer, V., & Šebek, O. (2011). Tracing the spatial distribution and mobility of metal/metalloid contaminants in Oxisols in the vicinity of the Nkana copper smelter, Copperbelt province, Zambia. Geoderma, pp. 164(1–2), 73–84.

Ettler, V. et al. (2012). 'Differences in the bioaccessibility of metals/metalloids in soils from mining and smelting areas (Copperbelt, Zambia)', Journal of Geochemical Exploration, 113, pp. 68–75. https:doi.org/10.1016/j.gexplo.2011.08.001.

Ettler, V., Konečný, L., Kovářová, L., Mihaljevič, M., Šebek, O., Kříbek, B., Majer, V., Veselovský, F., Penížek, V., Vaněk, A., & Nyambe, I. (2014). Surprisingly contrasting metal distribution and fractionation patterns in copper smelter-affected tropical soils in forested and grassland areas (Mufulira, Zambian Copperbelt). Science of the Total Environment, pp. 473–474, 117–124.

Ettler, V., Štěpánek, D., Mihaljevič, M., Drahota, P., Jedlicka, R., Kříbek, B., Vaněk, A., Penížek, V., Sracek, O., & Nyambe, I. (2020). Slag dusts from Kabwe (Zambia): Contaminant mineralogy and oral bio accessibility. Chemosphere, pp. 230-260.

Ettler, V. et al. (2022). 'Cobalt-bearing copper slags from Luanshya (Zambian Copperbelt): Mineralogy, geochemistry, and potential recovery of critical metals', Journal of Geochemical Exploration, 237(February). https:doi.org/10.1016/j.gexplo.2022.106987.

Fan, L., Zhao, W., Feng, W., Mo, P., Zhao, Y., Yang, G., & Xu, Z. (2021). Insight into the

Characteristics of Soil Microbial Diversity during the Ecological Restoration of Mines: A Case Study in Dabaoshan Mining Area, China, pp. 89-108.

Feng, Y. (2008). 'Soil mechanics', Of Earth Sciences Series, pp. 673-700.

Gelena, S. K. (2018). Acid Mine Drainage from Folldal Mine Tailings: Geochemical Characterisation and Simulation. Nmbu. Norwegian University of Life Sciences, Ås, pp. 75-96.

Ghose, M. K. (2004). 'Effect of opencast mining on soil fertility', 63(December), pp. 1006–1009.

Guimarães, G. M., Franklin, R. L., Figueiredo, A. M. G., Silva, P. S. C., & Fávaro, D. I. T. (2011). Enrichment Factor and Geoaccumulation Index Applied to Sediment Samples from the Guarapiranga Reservoir, Brazil, for Metal and Trace Element. 2011 International Nuclear Atlantic Conference, pp. 1–13.

Haldar, S. K. and Tišljar, J. (2013). Introduction to Mineralogy and Petrology, Introduction to Mineralogy and Petrology. https:doi.org/ 10.1016/C2012-0-03337-6.

Hart, R. J. W. J. J. B. D. J. and F. M. E. (2002). User's guide to PHREEQC (ver. 2) - A computer program for speciation, batch-reaction, one-dimensional transport and inverse geochemical calculations. USGS (gov), pp. 25-54 pp.

IMF. (2019). IMF Annual Report 2019: Our Connected World. Editorial and Publications Division of the IMF's Communications Department, pp. 10–12.

Ixchel, R. M., & Luz, P. M. De. (2021). Characterisation of mine tailings in their natural state and stabilized with cement, focused on construction Characterisation de residues minerals end estate natural y stabilized con cement, enforced a construction. Ciudad Universitario, pp. 2, 1–9.

Kemp, D., & Owen, J. R. (2014). The reality of remedy in mining and community relations: An anonymous case-study from Southeast Asia. Business and Human Rights in Southeast Asia: Risk and the Regulatory Turn, August, pp 239–257.

Kosgei, H., & Mukuwa, M. (2020). Environmental Effects of Tailing Damps in the Zambian Copperbelt Province, Zambia: Review Paper on Minerals of Zambia, April, pp. 8-10.

Kossoff, D., Dubbin, W. E., Alfredsson, M., Edwards, S. J., Macklin, M. G., & Hudson-Edwards, K. A. (2014). Mine tailings dams: Characteristics, failure, environmental impacts and remediation.

Applied Geochemistry, pp. 51, 229–245.

Kříbek, B., Majer, V., Veselovský, F., & Nyambe, I. (2010). Discrimination of lithogenic and anthropogenic sources of metals and sulphur in soils of the central-northern part of the Zambian Copperbelt Mining District: A topsoil vs. subsurface soil concept. Journal of Geochemical Exploration, pp. 104 (3), 69–86.

Kříbek, B. et al. (2011). 'The extent of arsenic and of metal uptake by aboveground tissues of Pteris vittata and Cyperus involucratus growing in copper- and cobalt-rich tailings of the Zambian Copperbelt', Archives of Environmental Contamination and Toxicology, 61(2), pp. 228–242. https:doi.org/ 10.1007/s00244-010-9604-4.

Kříbek, B. et al. (2014). 'Concentrations of arsenic, copper, cobalt, lead and zinc in cassava (Manihot esculenta Crantz) growing on uncontaminated and contaminated soils of the Zambian Copperbelt', Journal of African Earth Sciences, 99(PA2), pp. 713–723. https:doi.org/ 10.1016/j.jafrearsci.2014.02.009.

Lemos, M. et al. (2021). 'Mineralogical and geochemical characterization of gold mining tailings and their potential to generate acid mine drainage (Minas gerais, brazil)', Minerals, 11(1), pp. 1–16. https:doi.org/10.3390/min11010039.

Lindahl, J. (2014). Environmental Impacts of Mining in Zambia, towards better environmental management and sustainable exploitation of mineral resources. Geological Survey of Sweden, July, pp. 1–27.

Li, X. et al. (2015). 'Chemical partitioning of heavy metal contaminants in sediments of the Pearl River Estuary Chemical partitioning of heavy metal contaminants in sediments of the Pearl River Estuary', 2299, pp. 12-78. https:doi.org/10.3184/095422900782775607.

Lungu, J. (2008). Socio-economic change and natural resource exploitation: A case study of the Zambian copper mining industry. Development Southern Africa, 25(5), pp. 543–560.

Luo, X., Zhou, D., Liu, X., & Wang, Y. (2006). Solid / solution partitioning and speciation of heavy metals in the contaminated agricultural soils around a copper mine in eastern Nanjing city, China. 131, pp. 19–27.

Lweya, C., Jessen, S., Banda, K., Nyambe, I., Koch, C. B., & Larsen, F. (2015). Groundwater transport of Cu in laterites in Zambia. Applied Geochemistry, 56 (February 2019), pp. 94–102.

Maharana, J. K., & Patel, A. K. (2013). Physio-Chemical Characterisation and Mine Soil Genesis in Age Series Coal Mine Overburden Spoil in Chrono sequence in a Dry Tropical Environment. 1(1), pp. 1–7.

Månbro, C. and Parian, M. (2023). 'Chemical and Mineralogical Characterisation of Iron Ore Drillcore Using M-Xrf', pp. 159–174.

Mendelsohn. (2000). The Geology of the Northern Rhodesian Copperbelt. London (Macdonald & Co. Ltd.), pp.185a 32(255).

Minz, F. E. (2013). Mineralogical Characterisation of the Rockliden Antimony-Bearing Volcanic-Hosted Massive Sulphide Deposit, Sweden, Licentiate Thesis, pp. 36-78.

Mulenga, S. (2018). 'Dissertation Management of Mining Waste ; an exploration of both solid and non-solid waste in the mining industry , a case of lubambe mine in chililabombwe district on the copperbelt , pp. 45-89.

Munanku, T., Banda, K., Nyimbili, P. H., Mhlongo, S. E., & Masinja, J. (2023). Journal of African Earth Sciences Development of a multi-criteria decision analysis tool for the assessment of the potential pollution risk of tailings dumps to the environment – An approach validated using selected Zambian Mine tailings. Journal of African Earth Sciences, 200(February), pp. 12-18.

Mwandira, W. (2015). Development of bioremediation methods for soil and water contaminated with heavy metals in Kabwe Mine. Hokkaido University Collection of Scholarly and Academic Papers: HUSCAP, pp. 45-59.

Ngulube, R. (2016). A Review of Nchanga Tailings Dam Operations and Seasonal Assessment of Its Effluent Quality. American Journal of Environmental Protection, pp. 5(4), 90.

Norrgren, L Pettersson, U., Örn, S. and Bergqvist, P. A. (2000). 'Environmental monitoring of the Kafue River, located in the Copperbelt, Zambia', Archives of Environmental Contamination and Toxicology, 38 (3), pp. 334–341. https:doi.org/10.1007/s002449910044.

Nierwinski, H. P., Heidemann, M., Lavalle, L. A., & Sell, B. (2021). Study of mining tailings geotechnical parameters obtained from SCPTu tests carried on dry and saturated layers. EDP

Sciences, pp. 4-9.

Nyambe, I. A., & Kawamya, V. M. (2005). Approaches to sustainable minerals development in Zambia. Geological Society Special Publication, pp. 250, 73–86.

Pettersson, U. (2002). A geochemical study of the Kafue River, Zambia. Ph.D. (Ph.D. Thesis 2002), pp. 32-46.

Paramasivam, C. R. and Anbazhagan, S. (2020). 'Soil fertility analysis in and around magnesite mines , Salem , India', Geology, Ecology, and Landscapes, 4(2), pp. 140–150. https:doi.org/10.1080/24749508.2019.1608407.

Peterson, S. E. (2022). 'Thin-Section Petrography of Ceramic Materials', Thin-Section Petrography of Ceramic Materials, pp. 85-98 https:doi.org/10.2307/j.ctt3fgvbq.

Rahman, A. (2016). Bioremediation of Toxic Metals for Protecting Human Health and the Ecosystem. In (Doctoral dissertation, Orebro University), pp. 23-68.

Rainaud, C., Master, S., Armstrong, R., & Robb, L. (2005). Geochronology and nature of the Paleoproterozoic basement in the Central African Copperbelt (Zambia and the Democratic Republic of Congo), with regional implications. Journal of African Earth Sciences, pp. 42, 1–31.

Reforming Zambia's mines needs regional partners, improved domestic operating environment, (2022). the africa report, African Mining Indaba. Unpublished report. Retrieved from: https://www.theafricareport.com/205412/reforming-zambias-mines-needs-regional-partners-improved-domestic-operating-environment,pp 36-96 (Accessed 13 July 2023).

Required, E. and Karakurt, I. (2021). 'Determination of Particle Size Distribution By Sieving (Grain Size Analysis)', pp. 47-89.

Ribes, A. (2022). Extreme events and Climate Change: a statistical perspective Motivation, This talk. June, pp. 25-29.

Robbins, T., & Student, G. (2017). Geotechnical Evaluations of a Tailings Dam: Molybdenum and Copper Mine Project in Southern Idaho, pp. 1–13.

Rs, F., & Limited, M. (2012). Geochemical Characterisation of Mine Waste and Tailings Implications for Mine Waste Management, Flinders Mines Limited, pp.10-16.

Sandell, E. (2020). Post-Mining Restoration in Zambia: Faculty of Forest Science Southern Swedish Research Centre Alnarp, Doctoral thesis Swedish University of Agricultural Sciences, pp.30-69.

S. S. College, J. (2020). 'Spectroscopy - Atomic Absorption Spectroscopy', pp. 1–9.

Saha, A. et al. (2022). 'Spatial distribution and source identification of metal contaminants in the surface soil of Matehuala, Mexico based on positive matrix factorization model and GIS techniques', Frontiers in Soil Science, 2(December). pp. 15-17 https:doi.org/10.3389/fsoil.2022.1041377.

Satterfield, B. Z. (2020). 'Jar Testing' Soil Analysis testing, pp. 25-86.

Saussaye, L. et al. (2017). 'Geotechnical and mineralogical characterisations of marine-dredged sediments before and after stabilisation to optimise their use as a road material', Environmental Technology (United Kingdom), 38(23), pp. 3034–3046. https:doi.org/10.1080/09593330.2017.1287220.

Sheoran, V., Sheoran, A. S., & Poonia, P. (2010). Soil Reclamation of Abandoned Mine Land by Revegetation: A Review. January. International Journal of Soil, Sediment and Water, pp. 5-9.

Schlager, P. and Karlsruhe, D.- (2004). 'Sustainable Improvement in Safety of Tailings Facilities TAILSAFE A European Research and Technological Development Project Fifth European Community Framework Programme Energy , Environment and Sustainable Development (EESD) Contract Number : EVG1-CT-20', (May).

Schnably, J., & Virginia, W. (2003). Soil Characterisation, classification and Biomass Accumulation in the Otter Creek Wilderness Soil Characterisation, Classification and Biomass Accumulation in the Otter Creek Wilderness, Thesis for the degree of Master of Science in Division of Plant and Soil Sciences, pp.12-45.

Schro, T. J. (2005). Modelling of the Solid - Solution Partitioning of Heavy Metals and Arsenic in Embanked Flood Plain Soils of the Rivers Rhine and Meuse. National Library of Medicine (USA) (gov), pp. 39(18), 7176–7184.

Sikamo, J., Mwanza, A., & Mweemba, C. (2016). Copper mining in Zambia - History and future. Journal of the Southern African Institute of Mining and Metallurgy, pp. 116(6), 491–496.

Sivakugan, N. (2000). ‘Chapter 3 Soil classification’, Handbook of Income Distribution, 1, pp. 167–216.

Sillitoe, R., Perelló, J., Creaser, R., Wilton, J., & Dawborn, T. (2015). Two Ages of Copper Mineralization in the Mwombezhi Dome, Northwestern Zambia: Metallogenic Implications for the Central African Copperbelt. Economic Geology, pp. 110, 1917–1923.

Sracek, O. et al. (2010). ‘Geochemistry and mineralogy of Cu and Co in mine tailings at the Copperbelt, Zambia’, Journal of African Earth Sciences, 57(1–2), pp. 14–30. https:doi.org/ 10.1016/j.jafrearsci.2009.07.008.

Sracek, O. et al. (2012).‘Mining-related contamination of surface water and sediments of the Kafue River drainage system in the Copperbelt district, Zambia: An example of a high neutralization capacity system’, Journal of Geochemical Exploration, 112, pp. 174–188. doi: 10.1016/j.gexplo.2011.08.007.

Sun, W. et al. (2018). ‘An extensive review on restoration technologies for mining tailings’,pp. 12-19.

Thomas, O., Labat, S., Cornelius, T., & Richard, M. I. (2022). X-ray Diffraction Imaging of Deformations in Thin Films and Nano-Objects. Nanomaterials, pp. 12(8), 1–25.

Trevor, M. et al. (2019). ‘Statistical and Spatial Analysis of Heavy Metals in Soils of Residential Areas Surrounding the Nkana Copper Mine Site in Kitwe District, Zambia’, American Journal of Environment and Sustainable Development, 4(1), p. 27. Available at: http://www.aiscience.org/journal/ajesdhttp://creativecommons.org/licenses/by/4.0/.

Triantafyllidis, S., Loupasakis, C., & Tsangaratos, P. (2016). Geochemical modelling-based rehabilitation proposal for abandoned sulfidic flotation mill tailings, Kirki, Thrace, NE Greece. Environmental Earth Sciences, pp. 75(21).

USGS. (2015). U. S. Environmental Protection Agency FY 2013. Annual Performance Report FY 2015 Annual Plan, pp. 4-8.

Vítková, M., Ettler, V., Johan, Z., Kříbek, B., Šebek, O., & Mihaljevič, M. (2010). Primary and secondary phases in copper-cobalt smelting slags from the Copperbelt Province, Zambia. Mineralogical Magazine, pp. 74(4), 581–600.

Vítková, M., Ettler, V., Johan, Z., Křībek, B., Šebek, O., Mihaljevič, M., Šebek, O., Hyks, J., Astrup, T., Křībek, B., Sracek, O., Křībek, B., Mihaljevič, M., Majer, V., Veselovský, F., Vencelides, Z., Nyambe, I. A., Křībek, B., Majer, V., … Nyambe, I. A. (2011). Response of Enchytraeus crypticus worms to high metal levels in tropical soils polluted by copper smelting. Journal of Geochemical Exploration, pp. 144(1–4), 427–432.

Wallingford. HR (2019). A review of the risks posed by the failure of tailings dams. January. Minimising the risk of tailing dams through the use of remote sensing data Report, UK Space Agency & Global challenge Research Fund, pp. 24-30.

Wang, Y. (2016). Analysis of Soil Samples from Polluted Mining Areas. Thesis presented for the degree of Doctor of Philosophy. October. pp. 52-76.

WRB, I. (2014). World Reference Base for soil resources 2014: international soil classification system for naming soils and creating legends for soil maps. World Soil Resources Reports No. 106. FAO, Rome, pp. 42-72.

Yantambwe, M. I., & Cailteux, J. L. H. (2019). Geological observations in the five-klippes area, North-Western Katanga Copperbelt (Democratic Republic of the Congo). Geological Belgica, pp. 22(3–4), 111–119.

Zambia Climatology Dept, (2023). Climate Zambia, Rainfall pattern Impacts in Zambia Report. Retrieved from: https://weather-and-climate.com/average-monthly-precipitation-Rainfall,kitwe-zm,Zambia (Accessed 25 May 2023).

Zambia Meteorological Department (ZMD), (2013). Annual Report. Ministry of Works and Supply, Lusaka, Zambia, pp 15-23.

APPENDICES

Appendix 1: Database of Topsoil Samples collected from Uchi Tailing Dump, Kitwe, Copperbelt Province, Zambia during Dry Season (24th September to 6th October 2022) showing sample identification, site description and coordinates where samples were collected from

Sample Identity (ID)	Coordinates		Site Description
	Longitude	Latitude	
NR57	28° 13.983'E	12° 49.615'S	Sample collected near stream/river of New Uchi Tailing Dump
GA02	28° 13.718'E	12° 49.609'S	Sample collected in the grass area of New Uchi Tailing Dump
GA51	28° 13.985'E	12° 49.855'S	Sample collected in the grass area of New Uchi Tailing Dump
NR74	28° 13.735'E	12° 49.891'S	Sample collected near stream/river of New Uchi Tailing Dump
NR67	28° 13.813'E	12° 49.604'S	Sample collected near stream/river of New Uchi Tailing Dump
NR68	28° 13.947'E	12° 49.617'S	Sample collected near stream/river of New Uchi Tailing Dump
NR40	28° 13.906'E	12° 49.614'S	Sample collected near stream/river of New Uchi Tailing Dump
NR77	28° 13.957'E	12° 49.860'S	Sample collected near stream/river of New Uchi Tailing Dump
NR66	28° 13.738'E	12° 49.583'S	Sample collected near stream/river of New Uchi Tailing Dump
GA35	28° 13.905'E	12° 49.799'S	Sample collected in the grass area of New Uchi Tailing Dump
GA73	28° 13.734'E	12° 49.756'S	Sample collected in the grass area of New Uchi Tailing Dump

GA38	28° 13.863'E	12° 49.647'S	Sample collected in the grass area of New Uchi Tailing Dump
Sample Identity (ID)	**Coordinates**		**Site Description**
	Longitude	**Latitude**	
OP20	28° 13.780'E	12° 49.775'S	Sample collected from an open space/bare of New Uchi Tailing Dump
GA45	28° 13.942'E	12° 49.865'S	Sample collected in the grass area of New Uchi Tailing Dump
OP41	28° 13.911'E	12° 49.667'S	Sample collected from an open space/bare of New Uchi Tailing Dump
NR58	28° 14.040'E	12° 49.633'S	Sample collected near stream/river of New Uchi Tailing Dump
GA69	28° 13.964'E	12° 49.715'S	Sample collected in the grass area of New Uchi Tailing Dump
GA43	28° 13.925'E	12° 49.771'S	Sample collected in the grass area of New Uchi Tailing Dump
GA71	28° 13.872'E	12° 49.720'S	Sample collected in the grass area of New Uchi Tailing Dump
GA04	28° 13.725'E	12° 49.659'S	Sample collected in the grass area of New Uchi Tailing Dump
GA56	28° 13.983'E	12° 49.642'S	Sample collected in the grass area of New Uchi Tailing Dump
NR78	28° 14.060'E	12° 49.837'S	Sample collected near stream/river of New Uchi Tailing Dump
NR76	28° 13.864'E	12° 49.904'S	Sample collected near stream/river of New Uchi Tailing Dump
GA37	28° 13.880'E	12° 49.698'S	Sample collected in the grass area of New Uchi Tailing Dump
GA48	28° 13.961'E	12° 49.721'S	Sample collected in the grass area of New Uchi Tailing Dump
GA52	28° 14.034'E	12° 49.847'S	Sample collected in the grass area of New Uchi Tailing Dump

GA33	28° 13.861'E	12° 49.853'S	Sample collected in the grass area of New Uchi Tailing Dump
GA31	28° 13.837'E	12° 49.752'S	Sample collected in the grass area of New Uchi Tailing Dump
Sample Identity (ID)	**Coordinates**		**Site Description**
	Longitude	**Latitude**	
GA17	28° 13.795'E	12° 49.850'S	Sample collected in the grass area of New Uchi Tailing Dump
NR60	28° 14.048'E	12° 49.687'S	Sample collected near stream/river of New Uchi Tailing Dump
NR64	28° 13.601'E	12° 49.612'S	Sample collected near stream/river of New Uchi Tailing Dump
NR67	28° 13.813'E	12° 49.604'S	Sample collected near stream/river of New Uchi Tailing Dump
OP21	28° 13.772'E	12° 49.750'S	Sample collected from an open space/bare land of Uchi Tailing Dump
NR14	28° 13.774'E	12° 49.918'S	Sample collected near stream/river of New Uchi Tailing Dump
GA40.5	28° 13.905'E	12° 49.641'S	Sample collected in the grass area of New Uchi Tailing Dump
GA55	28° 13.995'E	12° 49.693'S	Sample collected in the grass area of New Uchi Tailing Dump
GA15	28° 13.796'E	12° 49.905'S	Sample collected in the grass area of New Uchi Tailing Dump
OP23	28° 13.763'E	12° 49.697'S	Sample collected from an open space/bare land of Uchi Tailing Dump
GA32	28° 13.846'E	12° 49.803'S	Sample collected in the grass area of New Uchi Tailing Dump
NR01	28° 13.713'E	12° 49.583'S	Sample collected near stream/river of New Uchi Tailing Dump
OP79	28° 13.715'E	12° 49.829'S	Sample collected from an open space/bare land of an Old Uchi Tailing Dump

GA13	28° 13.767'E	12° 49.891'S	Sample collected in the grass area of New Uchi Tailing Dump
GA08	28° 13.739'E	12° 49.763'S	Sample collected in the grass area of New Uchi Tailing Dump
GA16	28° 13.795'E	12° 49.878'S	Sample collected in the grass area of New Uchi Tailing Dump
Sample Identity (ID)	**Coordinates**		**Site Description**
	Longitude	**Latitude**	
GA24	28° 13.758'E	12° 49.671'S	Sample collected in the grass area of New Uchi Tailing Dump
GA27	28° 13.748'E	12° 49.595'S	Sample collected in the grass area of New Uchi Tailing Dump
FG03	28° 13.721'E	12° 49.634'S	Sample collected near playground/football area of Uchi Tailing Dump
GA07	28° 13.736'E	12° 49.738'S	Sample collected in the grass area of New Uchi Tailing Dump
GA30	28° 13.828'E	12° 49.700'S	Sample collected in the grass area of New Uchi Tailing Dump
GA29	28° 13.817'E	12° 49.649'S	Sample collected in the grass area of New Uchi Tailing Dump
GA49	28° 13.965'E	12° 49.772'S	Sample collected in the grass area of New Uchi Tailing Dump
GA47	28° 13.961'E	12° 49.669'S	Sample collected in the grass area of New Uchi Tailing Dump
GA44	28° 13.933'E	12° 49.822'S	Sample collected in the grass area of New Uchi Tailing Dump
GA50	28° 13.977'E	12° 49.824'S	Sample collected in the grass area of New Uchi Tailing Dump
GA36	28° 13.891'E	12° 49.748'S	Sample collected in the grass area of New Uchi Tailing Dump
GA34	28° 13.913'E	12° 49.851'S	Sample collected in the grass area of New Uchi Tailing Dump

OP12	28° 13.762'E	12° 49.867'S	Sample collected from an open space/bare land of Uchi Tailing Dump
OP19	28° 13.785'E	12° 49.799'S	Sample collected from an open space/bare land of Uchi Tailing Dump
OP18	28° 13.788'E	12° 49.825'S	Sample collected from an open space/bare land of Uchi Tailing Dump
OP09	28° 13.745'E	12° 49.792'S	Sample collected from an open space/bare land of Uchi Tailing Dump
Sample Identity (ID)	**Coordinates**		**Site Description**
	Longitude	**Latitude**	
OP06	28° 13.733'E	12° 49.712'S	Sample collected from an open space/bare land of Uchi Tailing Dump
OP10	28° 13.747'E	12° 49.816'S	Sample collected from an open space/bare land of Uchi Tailing Dump
OP11	28° 13.755'E	12° 49.842'S	Sample collected from an open space/bare land of Uchi Tailing Dump
OP05	28° 13.729'E	12° 49.685'S	Sample collected from an open space/bare land of Uchi Tailing Dump
NR63	28° 14.060'E	12° 49.839'S	Sample collected near stream/river of New Uchi Tailing Dump
NR62	28° 14.057'E	12° 49.791'S	Sample collected near stream/river of New Uchi Tailing Dump
NR61	28° 14.053'E	12° 49.738'S	Sample collected near stream/river of New Uchi Tailing Dump
NR46	28° 13.961'E	12° 49.614'S	Sample collected near stream/river of New Uchi Tailing Dump
NR59	28° 14.040'E	12° 49.633'S	Sample collected near stream/river of New Uchi Tailing Dump
OP82	28° 13.445'E	12° 49.795'S	Sample collected from an open space/bare of Old Uchi Tailing Dump
OP80	28° 13.520'E	12° 49.812'S	Sample collected from an open space/bare of Old Uchi Tailing Dump

OP70	28° 13.913'E	12° 49.716'S	Sample collected from an open space/bare of Old Uchi Tailing Dump
OP72	28° 13.819'E	12° 49.727'S	Sample collected from an open space/bare of Old Uchi Tailing Dump
OP26	28° 13.749'E	12° 49.620'S	Sample collected from an open space/bare land of Uchi Tailing Dump
OP42	28° 13.916'E	12° 49.718'S	Sample collected from an open space/bare land of Uchi Tailing Dump
GA28	28° 13.801'E	12° 49.596'S	Sample collected in the grass area of New Uchi Tailing Dump
Sample Identity (ID)	**Coordinates**		**Site Description**
	Longitude	**Latitude**	
GA54	28° 14.011'E	12° 49.743'S	Sample collected in the grass area of New Uchi Tailing Dump
GA53	28° 14.023'E	12° 49.795'S	Sample collected in the grass area of New Uchi Tailing Dump
OP25	28° 13.753'E	12° 49.648'S	Sample collected from an open space/bare land of Uchi Tailing Dump
NR39	28° 13.856'E	12° 49.591'S	Sample collected near stream/river of New Uchi Tailing Dump
OP22	28° 13.771'E	12° 49.722'S	Sample collected from an open space/bare land of Uchi Tailing Dump
OP81	28° 13.440'E	12° 49.818'S	Sample collected from an open space/bare of Old Uchi Tailing Dump

Appendix 2: Database of Subsurface Soil Samples collected from Uchi Tailing Dump, Kitwe, Copperbelt Province, Zambia (24th September to 6th October 2022) showing sample identification, site location and coordinates where samples were collected

Sample Identity (ID)	**Coordinates**		**Site Description**
	Longitude	**Latitude**	
GA2VF2-3L	28° 13.752'E	12° 49.627'S	Sample collected from vertical profile of the GA of Uchi Tailing Dump 3rd layer
VP1ER-1L	28° 13.770'E	12° 49.906'S	Sample collected from vertical profile of edge of Uchi Tailing Dump 1st Layer
OP3VF3-1L	28° 13.778'E	12° 49.727'S	Sample collected from vertical profile of OP of Uchi Tailing Dump 1st layer
GA2VF2-2L	28° 13.752'E	12° 49.627'S	Sample collected from vertical profile of GA of Uchi Tailing Dump 2nd layer
OP3VF3-4L	28° 13.778'E	12° 49.727'S	Sample collected from vertical profile of OP of Uchi Tailing Dump 4th layer
VP1ER-2L	28° 13.770'E	12° 49.906'S	Sample collected from vertical profile of edge of Uchi Tailing Dump 2nd layer
VF1NR1 -3RD	28° 13.720'E	12° 49.582'S	Sample collected from vertical profile of NR1 of Uchi Tailing Dump 3rd layer
GA4VF4 -3RD	28° 13.983'E	12° 49.643'S	Sample collected from vertical profile of GA of Uchi Tailing Dump 3rd layer
GA4VF4 -1ST	28° 13.983'E	12° 49.643'S	Sample collected from vertical profile of GA of Uchi Tailing Dump 1st layer
VF1NR1-1ST	28° 13.720'E	12° 49.582'S	Sample collected from vertical profile of NR1 of Uchi Tailing Dump 1st layer
VF1NR1-2ND	28° 13.720'E	12° 49.582'S	Sample collected from vertical profile of NR1 of Uchi Tailing Dump 2nd layer
VP1ER-3L	28° 13.770'E	12° 49.906'S	Sample collected from vertical profile of edge of Uchi Tailing Dump 3rd layer

GA4VF4-2L	28° 13.983'E	12° 49.643'S	Sample collected from vertical profile of GA of Uchi Tailing Dump 2^{nd} layer
Sample Identity (ID)	**Coordinates**		**Site Description**
	Longitude	**Latitude**	
OP3VF3-3RD	28° 13.778'E	12° 49.727'S	Sample collected from vertical profile of OP of Uchi Tailing Dump 3^{rd} layer
VFINR1-BL	28° 13.720'E	12° 49.582'S	Sample collected from vertical profile of NR1 of Uchi Tailing Dump Bottom layer
GA2VF2-1ST	28° 13.752'E	12° 49.627'S	Sample collected from vertical profile of GA of Uchi Tailing Dump 1^{st} layer
OP3VF3-2ND	28° 13.778'E	12° 49.727'S	Sample collected from vertical profile of OP of Uchi Tailing Dump 2^{nd} layer
VP1/0/4	28° 13.635'E	12° 49.818'S	Sample collected from vertical profiling of Old Uchi Tailing Dump 4^{th} layer
VP1/0/2	28° 13.635'E	12° 49.818'S	Sample collected from vertical profiling of Old Uchi Tailing Dump 2^{nd}layer
VP1/0/5	28° 13.635'E	12° 49.818'S	Sample collected from vertical profiling of Old Uchi Tailing Dump 5^{th} layer
VP2/0/3	28° 13.593'E	12° 49.821'S	Sample collected from vertical profiling 2 of Old Uchi Tailing Dump 3^{rd} layer
VP1/0/8	28° 13.635'E	12° 49.818'S	Sample collected from vertical profiling of Old Uchi Tailing Dump 8^{th} layer
VP2/0/7	28° 13.593'E	12° 49.821'S	Sample collected from vertical profiling of Old Uchi Tailing Dump 7^{th} layer
VP2/0/1	28° 13.593'E	12° 49.821'S	Sample collected from vertical profiling 2 of Old Uchi Tailing Dump 4^{th} layer
VP2/0/4	28° 13.593'E	12° 49.821'S	Sample collected from vertical profiling 2 of Old Uchi Tailing Dump 4^{th} layer
VP1/0/3	28° 13.635'E	12° 49.818'S	Sample collected from vertical profiling of Old Uchi Tailing Dump 4^{th} layer
VP2/0/6	28° 13.593'E	12° 49.821'S	Sample collected from vertical profiling of Old Uchi Tailing Dump 4^{th} layer
VP2/0/5	28° 13.593'E	12° 49.821'S	Sample collected from vertical profiling of Old Uchi Tailing Dump 4^{th} layer

VP1/0/1	28° 13.635'E	12° 49.818'S	Sample collected from vertical profiling of Old Uchi Tailing Dump 4th layer
VPI/0/6	28° 13.635'E	12° 49.818'S	Sample collected from vertical profiling of Old Uchi Tailing Dump 4th layer
VP2/0/2	28° 13.593'E	12° 49.821'S	Sample collected from vertical profiling of Old Uchi Tailing Dump 4th layer

Appendix 3: Database of Topsoil Samples collected from Uchi Tailing Dump, Kitwe, Copperbelt Province, Zambia during wet season (20th March to 16th April 2023) showing sample identification, site location and coordinates where samples were collected from

Sample Identity (ID)	**Coordinates**		**Site Description**
	Longitude	**Latitude**	
S3	28° 14.843'E	12° 49.624'S	Stream sediment sample collected from Uchi Stream near Uchi Tailing Dump
10/O	28° 13.594'E	12° 49.822'S	Sample collected from top of hill of Old Uchi Tailing Dump
S2	28° 14.211'E	12° 49.707'S	Stream sediment sample collected from Uchi Stream near Uchi Tailing Dump
3/O	28° 13.438'E	12° 49.779'S	Sample collected from top of hill of Old Uchi Tailing Dump
8/O	28° 13.618'E	12° 49.910'S	Sample collected from top of hill of Old Uchi Tailing Dump
1/N	28° 14.055'E	12° 49.834'S	Sample collected from New Uchi Tailing Dump
12/N	28° 13.863'E	12° 49.903'S	Sample collected from New Uchi Tailing Dump
19/N/6	28° 13.833'E	12° 49.577'S	Sample collected from New Uchi Tailing Dump
1/O	28° 13.716'E	12° 49.829'S	Sample collected from top of hill of Old Uchi Tailing Dump
S1	28° 14.092'E	12° 49.713'S	Stream sediment sample collected from Uchi Stream near Uchi Tailing Dump
4/N	28° 13.918'E	12° 49.847'S	Sample collected from bare land of New Uchi Tailing Dump
S9/N	28° 13.768'E	12° 49.912'S	Stream sediment sample collected from Uchi Stream near Uchi Tailing Dump
2/O	28° 13.583'E	12° 49.810'S	Sample collected from top of hill of Old Uchi Tailing Dump
5/O	28° 13.587'E	12° 49.679'S	Sample collected from top of hill of Old Uchi Tailing Dump

4/O	28° 13.457'E	12° 49.838'S	Sample collected from top of hill of Old Uchi Tailing Dump
11/O	28° 13.512'E	12° 49.830'S	Sample collected from top of hill of Old Uchi Tailing Dump
2/N	28° 14.045'E	12° 49.714'S	Sample collected from near Uchi Stream of New Uchi Tailing Dump
Sample Identity (ID)	**Coordinates**		**Site Description**
	Longitude	**Latitude**	
7/N	28° 13.774'E	12° 49.906'S	Sample collected from bare land of New Uchi Tailing Dump
S7	28° 13.702'E	12° 49.949'S	Stream sediment sample collected from Uchi Stream near Uchi Tailing Dump
S8	28° 13.724'E	12° 49.572'S	Stream sediment sample collected from Uchi Stream near Uchi Tailing Dump
8/N	28° 13.758'E	12° 49.735'S	Sample collected from bare land of New Uchi Tailing Dump
S6BIN	28° 12.887'E	12° 50.271'S	Stream sediment sample collected from Uchi Stream near Uchi Tailing Dump
9/O	28° 13.669'E	12° 49.846'S	Sample collected from top of hill of Old Uchi Tailing Dump
6/O	28° 13.539'E	12° 49.742'S	Sample collected from top of hill of Old Uchi Tailing Dump
S5BM	28° 12.847'E	12° 50.275'S	Stream sediment sample collected from Uchi Stream near Uchi Tailing Dump
12/O	28° 13.629'E	12° 49.781'S	Sample collected from top of hill of Old Uchi Tailing Dump
S4	28° 14.958'E	12° 49.657'S	Stream sediment sample collected from Uchi Stream near Uchi Tailing Dump
9/N	28° 13.712'E	12° 49.579'S	Sample collected from bare land of New Uchi Tailing Dump
17/N/5	28° 13.909'E	12° 49.716'S	Sample collected from grass area of New Uchi Tailing Dump
13/O	28° 13.546'E	12° 49.758'S	Sample collected from top of hill of Old Uchi Tailing Dump
7/O	28° 13.638'E	12° 49.741'S	Sample collected from top of hill of Old Uchi Tailing Dump
11/N	28° 13.789'E	12° 49.826'S	Sample collected from grass area of New Uchi Tailing Dump

15/N	28° 14.068'E	12° 49.771'S	Sample collected from bare land of New Uchi Tailing Dump
18/N	28° 13.787'E	12° 49.625'S	Sample collected from near Uchi Stream of New Uchi Tailing Dump
16/N	28° 13.979'E	12° 49.676'S	Sample collected from grass area of New Uchi Tailing Dump
13/N	28° 14.001'E	12° 49.780'S	Sample collected from near Uchi Stream of New Uchi Tailing Dump
10/N	28° 13.735'E	12° 49.632'S	Sample collected from grass area of New Uchi Tailing Dump
Sample Identity (ID)	**Coordinates**		**Site Description**
	Longitude	**Latitude**	
14/N	28° 14.051'E	12° 49.650'S	Sample collected from bare land of New Uchi Tailing Dump

Appendix 4: Database of Heavy Metal concentrations from Uchi Tailing Dump, Kitwe, Copperbelt Province, Zambia

Sample ID	**Cu %**	**Co %**	**Fe %**	**Zn**
NR57	0.262	0.041	1.224	0.011
GA02	0.183	0.066	1.252	0.005
GA51	0.062	0.012	1.423	0.003
NR74	0.351	0.055	1.077	0.002
NR67	0.347	0.062	1.282	0.003
NR68	0.045	0.007	0.768	0.003
NR40	0.095	0.011	0.688	0.004
NR77	0.174	0.049	1.258	0.003
NR75	0.396	0.094	1.165	0.003
NR66	0.314	0.083	1.528	0.004
GA35	0.137	0.040	1.486	0.003
GA73	0.338	0.057	1.124	0.002
GA38	0.302	0.088	1.308	0.003
OP20	0.338	0.063	1.084	0.005
GA45	0.100	0.045	1.473	0.003
OP41	0.325	0.136	1.281	0.004
NR58	0.250	0.065	1.305	0.003
GA69	0.291	0.146	1.438	0.004
GA43	0.309	0.137	1.491	0.003

GA71	0.182	0.095	1.392	0.003
Sample ID	**Cu %**	**Co %**	**Fe %**	**Zn**
GA04	0.216	0.048	1.214	0.002
GA56	0.219	0.071	1.424	0.002
NR78	0.222	0.054	1.291	0.003
NR76	0.452	0.065	1.338	0.004
GA37	0.235	0.115	1.420	0.003
GA48	0.301	0.131	1.470	0.005
GA52	0.184	0.044	1.008	0.008
GA33	0.128	0.036	1.431	0.002
GA31	0.279	0.073	1.207	0.002
GA17	0.276	0.074	1.169	0.002
NR60	0.126	0.017	0.913	0.004
NR64	0.146	0.043	1.413	0.001
NR67	0.258	0.041	1.788	0.003
OP21	0.391	0.061	1.124	0.001
NR14	0.329	0.086	1.523	0.012
GA40.5	0.149	0.123	1.356	0.004
GA55	0.062	0.014	1.914	0.001
GA15	0.419	0.076	1.144	0.002

OP23	0.116	0.025	0.392	0.000
GA32	0.194	0.080	1.278	0.002
NR01	0.378	0.060	1.375	0.003
Sample ID	**Cu %**	**Co %**	**Fe %**	**Zn**
OP79	0.264	0.085	1.254	0.002
GA13	0.310	0.057	1.054	0.003
GA08	0.299	0.029	0.766	0.001
GA16	0.007	0.001	0.659	0.000
GA24	0.148	0.026	0.924	0.002
GA27	0.001	0.002	0.268	0.000
FG03	0.129	0.030	0.856	0.001
GA07	0.233	0.040	0.983	0.009
GA30	0.288	0.041	1.056	0.002
GA29	0.162	0.037	1.130	0.002
GA49	0.186	0.046	1.657	0.003
GA47	0.100	0.011	2.042	0.003
GA44	0.086	0.020	1.080	0.002
GA50	0.041	0.018	1.087	0.004
GA36	0.264	0.031	1.286	0.001
GA34	0.096	0.012	0.915	0.003

OP12	0.329	0.035	0.970	0.001
OP19	0.304	0.032	0.854	0.001
OP18	0.325	0.034	0.820	0.001
OP09	0.295	0.031	0.832	0.001
OP06	0.281	0.030	0.795	0.002
Sample ID	**Cu %**	**Co %**	**Fe %**	**Zn**
OP10	0.292	0.035	0.987	0.001
OP11	0.285	0.032	1.058	0.001
OP05	0.084	0.035	0.970	0.001
NR63	0.242	0.034	0.990	0.002
NR62	0.270	0.033	1.042	0.001
NR61	0.150	0.022	0.976	0.004
NR46	0.017	0.005	0.913	0.004
NR59	0.131	0.015	1.061	0.001
OP82	0.563	0.032	0.939	0.002
OP80	0.201	0.055	1.036	0.002
OP70	0.283	0.042	1.183	0.002
OP72	0.309	0.049	1.129	0.001
OP26	0.112	0.034	0.886	0.004
OP42	0.291	0.039	1.301	0.001

GA28	0.012	0.005	1.452	0.001
GA54	0.026	0.006	1.874	0.001
GA53	0.007	0.002	0.792	0.001
OP25	0.083	0.021	0.855	0.002
NR39	0.410	0.052	1.137	0.001
OP22	0.390	0.045	1.012	0.001
OP81	0.534	0.042	1.013	0.002
Sample ID	**Cu %**	**Co %**	**Fe %**	**Zn**
GA2VF2-3L	0.269	0.049	1.039	0.001
VP1ER-1L	0.328	0.036	0.949	0.001
OP3VF3-1L	0.378	0.022	0.816	0.001
GA2VF2-2L	0.281	0.031	1.022	0.002
OP3VF3-4L	0.112	0.045	1.137	0.002
VP1ER-2L	0.749	0.061	1.988	0.006
VF1NR1 -3RD	0.198	0.067	1.061	0.002
GA4VF4 -3RD	0.075	0.065	1.310	0.003
GA4VF4 -1ST	0.276	0.048	1.103	0.001
VF1NR1-1ST	0.285	0.060	1.158	0.001
VF1NR1-2ND	0.330	0.087	1.608	0.003
VP1ER-3L	0.635	0.050	1.569	0.002

GA4VF4-2L	0.090	0.041	1.142	0.002
OP3VF3-3RD	0.139	0.050	1.143	0.002
VFINR1-BL	0.239	0.057	1.070	0.002
GA2VF2-1ST	0.193	0.070	1.186	0.002
OP3VF3-2ND	0.126	0.050	1.248	0.001
VP1/0/4	0.179	0.044	0.959	0.001
VP1/0/2	0.127	0.057	1.018	0.002
VP1/0/5	0.169	0.058	0.918	0.001
VP2/0/3	0.095	0.061	0.994	0.010
Sample ID	**Cu %**	**Co %**	**Fe %**	**Zn**
VP1/0/8	0.110	0.048	1.090	0.002
VP2/0/7	0.176	0.058	1.140	0.002
VP2/0/1	0.143	0.057	1.122	0.001
VP2/0/4	0.108	0.042	0.921	0.001
VP1/0/3	0.165	0.066	1.057	0.001
VP2/0/6	0.466	0.054	1.101	0.001
VP2/0/5	0.225	0.069	1.112	0.001
VP1/0/1	0.032	0.051	1.100	0.001
VPI/0/6	0.111	0.061	1.202	0.002
VP2/0/2	0.442	0.030	0.830	0.001

GA2VF2-3L	0.269	0.049	1.039	0.001
VP1ER-1L	0.328	0.036	0.949	0.001
OP3VF3-1L	0.378	0.022	0.816	0.001
GA2VF2-2L	0.281	0.031	1.022	0.002
OP3VF3-4L	0.112	0.045	1.137	0.002
VP1ER-2L	0.749	0.061	1.988	0.006
VF1NR1 -3RD	0.198	0.067	1.061	0.002
GA4VF4 -3RD	0.075	0.065	1.310	0.003
GA4VF4 -1ST	0.276	0.048	1.103	0.001
VF1NR1-1ST	0.285	0.060	1.158	0.001
VF1NR1-2ND	0.330	0.087	1.608	0.003
Sample ID	**Cu %**	**Co %**	**Fe %**	**Zn**
VP1ER-3L	0.635	0.050	1.569	0.002
GA4VF4-2L	0.090	0.041	1.142	0.002
OP3VF3-3RD	0.139	0.050	1.143	0.002
VFINR1-BL	0.239	0.057	1.070	0.002
GA2VF2-1ST	0.193	0.070	1.186	0.002
OP3VF3-2ND	0.126	0.050	1.248	0.001
VP1/0/4	0.179	0.044	0.959	0.001
VP1/0/2	0.127	0.057	1.018	0.002

VP1/0/5	0.169	0.058	0.918	0.001
VP2/0/3	0.095	0.061	0.994	0.010
VP1/0/8	0.110	0.048	1.090	0.002
VP2/0/7	0.176	0.058	1.140	0.002
VP2/0/1	0.143	0.057	1.122	0.001
VP2/0/4	0.108	0.042	0.921	0.001
VP1/0/3	0.165	0.066	1.057	0.001
VP2/0/6	0.466	0.054	1.101	0.001
VP2/0/5	0.225	0.069	1.112	0.001
VP1/0/1	0.032	0.051	1.100	0.001
VPI/0/6	0.111	0.061	1.202	0.002
VP2/0/2	0.442	0.030	0.830	0.001
S3	0.122	0.031	1.146	0.005
Sample ID	**Cu %**	**Co %**	**Fe %**	**Zn**
10/O	0.186	0.044	0.982	0.002
S2	0.256	0.039	0.901	0.002
3/O	0.104	0.036	0.679	0.001
8/O	0.216	0.055	0.955	0.001
1/N	0.101	0.040	1.056	0.001
12/N	0.266	0.078	1.067	0.003

19/N/6	0.112	0.037	1.032	0.002
1/O	0.190	0.060	1.105	0.002
S1	0.006	0.025	0.540	0.001
4/N	0.006	0.028	0.929	0.001
S9/N	0.187	0.047	0.928	0.001
2/O	0.189	0.057	0.877	0.001
5/O	0.308	0.024	1.104	0.001
4/O	0.252	0.053	1.055	0.001
11/O	0.247	0.040	0.819	0.000
2/N	0.169	0.022	1.087	0.001
7/N	0.171	0.041	0.811	0.000
S7	0.173	0.055	1.236	0.004
S8	0.203	0.034	1.428	0.004
8/N	0.205	0.049	0.989	0.001
S6BIN	0.424	0.051	1.217	0.002
Sample ID	**Cu %**	**Co %**	**Fe %**	**Zn**
9/O	0.190	0.047	0.975	0.001
6/O	0.309	0.052	1.034	0.001
S5BM	0.298	0.042	0.829	0.001
12/O	0.193	0.045	0.903	0.001

S4	0.137	0.007	0.544	0.001
9/N	0.090	0.042	1.117	0.001
17/N/5	0.030	0.047	0.994	0.001
13/O	0.199	0.049	0.973	0.001
7/O	0.328	0.056	1.101	0.001
11/N	0.107	0.044	0.965	0.000
15/N	0.141	0.012	0.711	0.002
18/N	0.035	0.040	0.983	0.001
16/N	0.086	0.042	1.111	0.002
13/N	0.159	0.025	1.226	0.005
10/N	0.190	0.033	0.927	0.002
14/N	0.293	0.059	1.163	0.002